

Genetic circuits for the control of multi-strain bacterial populations

Thesis by
Reed Dillard McCardell

In Partial Fulfillment of the Requirements for the
Degree of
Doctor of Philosophy

The logo for the California Institute of Technology (Caltech), featuring the word "Caltech" in a bold, orange, sans-serif font.

CALIFORNIA INSTITUTE OF TECHNOLOGY
Pasadena, California

2021
Defended April 26, 2021

© 2021

Reed Dillard McCardell
ORCID: 0000-0002-0955-3133

All rights reserved

ACKNOWLEDGEMENTS

I am able to complete this thesis with the life-long support I have received from my family, friends, universities and community—and also a good deal of luck. I am privileged to occupy the position I do in my country and community, and I am lucky that circumstances have led me to where I am today. During this 2020-2021 academic year, marked by frightening health and economic crises due to the COVID-19 pandemic, and sociopolitical unrest surrounding increasingly visible systemic inequalities in the USA, I am more aware and thankful for the privileges I enjoy than I have ever been. My mission for the future is to create for others opportunities and support akin to what I have received.

Sometimes it can be hard to remember all the important people that have aided one's life and work over a long period of time. I will make it look easy now by condensing all the nostalgia—and fear of leaving anyone out—into neat paragraphs that I hope will honor everyone who deserves it.

My parents, Ryan and Jill McCardell, joke that they knew I would end up doing something like science since they watched me play with Hot Wheels cars as a kid. Instead of *vroom*-ing them around like cars, I apparently sat spinning the wheels with one finger, watching the little axel assemblies turn. I remember my fascination with the workings of systems and I owe my current ability to fascinate myself professionally to their superb parenting, education and encouragement. Without them, none of this would be possible.

My brother, Tad is rapidly transforming himself from my little brother into a mentor and best friend to me. He is uncompromising in his efforts to find his personal brand of success—and to do so righteously and fairly. Tad's commitment to his own happiness and the happiness of others makes him the most wonderful kind of person to be around. It is a great honor to be part of his life; I am elevated by association with him and hope to live up to his example of kindness, humility and effort.

The Spicy Bois (56 gang) are as much a part of this thesis as I am. Devin, Keshin, Alden, Nico and Eric are exceedingly fine examples of human beings; I am guided by them every day. It has been my great pleasure to enjoy the amazing graduate student lifestyle by surfing, camping, hiking, eating, drinking, reading—sometimes wallowing—and growing together with my best friends. Somehow, writing this

thesis probably started at a childhood birthday party, or at the beach, or in an elementary school classroom, together with the Spicy Bois. Thank you for your commitment to our friendship and for making my life rich.

My fiancée, Lauren, is such an important person in my personal and professional growth that I divide my life into pre- and post-Lauren. From her I have learned emotional intelligence, personal strength and social awareness that add beautiful context to the actions I take as a scientist, health care provider and person. The support and joy she has given my life in the process of my PhD is impossible to overstate. I feel like a superhero when I'm with Lauren; I look forward to a long life of excitement and adventure together with her.

When I first met **my advisor, Richard Murray**, he asked me "what do you want to do?", in reference to my research interests and goals. I was awed; I had expected to learn how I might mold myself into his laboratory, but it turned out he wanted to know if his laboratory could help me. That question conveys Richard's peerless dedication to the ideals of academic service. Richard is a model academic, championing openness, honesty and selflessness in science. Everything he does supports scientific advancement and student education. He taught me to pursue science without ego, to teach, and to keep the broader context—solid principles, my life and the lives of others—in sight. My styles of science and mentorship are bettered immensely by what I have learned from Richard. It has been an honor watching and learning from his conduct as a mentor, scientist and person.

The students and staff of the Murray laboratory have shown me excellence in many forms. I've tried to learn as much as I can from them so I might be as excellent myself. **Andrey Shur** is ingenious and unstoppable; his commitment to getting things done motivated me through the difficult, inevitable doldrums in the scientific process. Andrey is the inspiration behind everything I've learned about 3D printing and "making" to solve problems. **Andy Halleran** showed me what elegance, grace and style look like in science; he is my internal benchmark for how "great" science is done and communicated. **Victoria Hsiao** helped me find my feet when I joined the lab and was the model of productivity and balance I held throughout my PhD. **Cindy Ren, Ayush Pandey, and William Poole** showed me the power of mathematics and computing in biology—in science as a whole, really. Their patient, rigorous communication of their work taught me the language of quantitative science and inspired a fascination with quantitation that improves every part of my work—and some parts of my life. **Vipul Singhal** showed me how deep the rabbit hole of science

goes. In our regular Thursday deep-dives into *things*, I discovered how philosophy, math, ethics, biology—basically everything—are related, and how each can inform another. **John Marken** and **Sam Clamons** have a knack for identifying open questions, overlooked assumptions and untapped directions in projects. I remind myself frequently to be principled, methodical and deeply informed like Sam and John, to ensure I do the most valuable, rigorous science. **Rory Williams'** goofy demeanor masks a powerful dedication to improvement. Watching him grow from a good graduate student into a stellar one keeps me motivated to chase excellence always. I also credit Rory with building the term "big dog" into the popular and amusing epithet it is today. **Leo Green** is a humble superstar. He radiates friendship, calm and betterment onto his constantly growing circle of friends and colleagues. He is relentless in his pursuit of professional advancement, yet maintains amazing balance between his work, life and family. He teaches with empathy and is truly dedicated to lifelong learning. In nearly all situations, personal and professional, I try to act by Leo's example. **Mark Prator** is more than a labmate, he is a life-long friend. He is an invaluable laboratory force in support of any project he does, but most importantly, he keeps research human. The hours we spent throwing suction cups at windows, making up insane fantasy universes, shooting NERF darts at cups etc. etc. are the most memorable hours of my time at Caltech. With Mark, I learned to play D&D, played some great board games, broke myself against punishing track workouts. A lot of the creativity I enjoy exercising and hobbies I love, I developed with Mark. It will be my great pleasure to continue "yes and"-ing on to infinity with him. Thanks for everything big dog.

Justin Bois paid me a compliment I will not forget. After one of his many many lectures, Justin told me he thought I was a "brave person" doing something valuable by learning the things he was teaching, despite my lack of experience and background. I think about that compliment all the time. Channeling the "bravery" he bestowed on me, I am a more confident, curious student of everything I pursue. Compliments to my ego aside, Justin is **the** model educator; he is single-handedly responsible for teaching Caltech-style biology (and beyond) to a majority of Caltech students (and also beyond). He deserves recognition for this everywhere it can be given. In my future teaching opportunities, I hope I can provide the superb clarity, precision, breadth and rigor Justin brings to all his many students.

The **USC Keck MD/PhD program and Caltech** materially, logistically, and culturally created the opportunity for me to participate in all the rigorous and exciting

training I've had so far. I had just entered the Los Angeles airport for a flight to an interview at another MD/PhD institution when I got the email informing me I had been accepted by USC/Caltech MD/PhD. Right then, it was clear I would attend USC/Caltech. I haven't regretted that decision yet. It is the honor of my life to learn medicine from the educators and caregivers at USC; and the art of scientific research from the peerless faculty at Caltech.

My **committee members Niles Pierce, Victoria Orphan and Rustem Ismagilov** deserve the first clause of Bilbo Baggins' party quote: "*I don't know half of you half as well as I should like...*" Looking back, I met with them half as much as I would have liked, but I do rather like them, hopefully as much as they deserve. Working through reports for funding sources with Niles and his lab members; finding my passion for microbiology—and a common hometown—with Victoria; these experiences were rich sources of learning and connection to the Caltech community. My advisory committee gave me valuable outside perspectives on the content of my research, but also boosted my confidence by supporting the work and helping me improve it. I take every chance I get to tell younger students to meet with their team of advisors **more**, that it will make their work better and life easier. Going forward, I will work to know these advisors—and any others—as much as I ought, so I can learn from them as much as I can.

Though you all may not have wanted a thesis dedication as a gift; this thesis is for all of you.

ABSTRACT

Microbial species rarely exist alone. Nearly everywhere you could think to look, microorganisms of various species live together in harmony. Microbes together in their communities are incredibly powerful actors wherever they are found; they perform small miracles—the conversion of milk into yogurt—and large ones—production of most of the planet’s oxygen and organic carbon. Our burgeoning knowledge of microbial life combined with modern technologies to manipulate it create a critical, exciting opportunity to harness microbial power for the betterment of technology, people, and the planet. This thesis presents a body of work which explores the manipulation of microbial communities using the intersectional bio-engineering approach of synthetic biology. We demonstrate how molecular tools evolved by bacteria can be repurposed to create rationally designed systems for controlling features of bacterial populations.

We begin by examining a genetic circuit that caps the size of a bacterial population by coordinating the deaths of population members—the **population capping** or "**pop cap**" circuit. Briefly, *E. coli* cells in the *pop cap* circuit are engineered to synthesize a chemical—a quorum sensing (QS) signal—that reports the density of the population, sense this chemical, and produce the *ccdB* toxin to destroy themselves in response. The molecular tools that make up this circuit are drawn from organisms across the spectrum of bacterial diversity. Brought together, they create a feedback control circuit that controls population size by causing member cells to die when a target population size has been reached. To improve the performance of this population controller and reduce the influence of the environment on the circuit, we add the *aiiA* quorum sensing signal degradase to allow the experimenter control over the degradation rate of the QS density signal. Additionally, we explore RNA and protein mechanisms to sequester the death-causing toxin—inactivating it—allowing us to release a population cap. The resulting "**cap and release**" circuit is a flexible motif that can be scaled to control multi-strain populations, expanding the scope of control beyond the single-strain populations regulated by the base *pop cap* circuit.

Using the scalable *cap and release* motif, we design a genetic circuit to regulate a multi-strain community. Two different cell strains expressing symmetric, interconnected *cap and release* systems form the "**A=B**" circuit, so named for its ability to control the composition of the community to a target ratio of A cells to B cells, or $A_{population} = \alpha B_{population}$. Through dynamical system models of the system, we

explore the effects of active QS signal degradation on composition control performance and perform a parameter sensitivity analysis of the system to help determine the best method for building a functioning $A=B$ system in the laboratory. We use a high throughput construction and screening protocol to create variants of the $A=B$ system with identical architectures, but slightly differing component production rates. We crown the most successful variant with a series of experiments to determine if it indeed recapitulates our model's predictions for its performance. Our implementation of the $A=B$ circuit can successfully regulate the composition of a community, with interesting additional effects on total population density.

The *cap and release* and $A=B$ circuits need parts that can do three things: 1) send a signal between cells to communicate information, 2) compare two signals, 3) regulate cell growth or death. We highlight bacteriocins, bacterial protein exotoxins that are released from a producer cell to kill other cells of similar species, as attractive tools for bacterial community engineering both for their multi-functionality and modular protein structure. By themselves, bacteriocins can perform all the functions needed for population control: they transmit themselves between cells, have unique high-affinity sequestering antitoxin proteins, and are toxins to receiver cells. We begin the process of their characterization and usage as synthetic biological "parts" by creating non-native expression systems that match native expression strengths. Using these experimenter-controlled systems we design preliminarily test a bacteriocin-based bacterial community control circuit. Additionally, given the *E. coli* colicin bacteriocins' unique, nearly plug-and-play modular domain structure, we explore possibilities for engineering colicin proteins themselves for increased functional diversity or uses outside of growth regulation.

PUBLISHED CONTENT AND CONTRIBUTIONS

A version of Chapter 2 originally appeared as:

Control of bacterial population density with population feedback and molecular sequestration

Reed D. McCardell, Shan Huang, Leopold N. Green, Richard M. Murray

bioRxiv. doi: <https://doi.org/10.1101/225045>

RDM conceived the research idea with advice and guidance from RMM. RDM, SH and LNG designed and performed the presented experiments. RDM created the mathematical models and performed the presented simulations. RDM wrote the manuscript with input from RMM.

A version of Chapter 3 originally appeared as:

Control of density and composition in an engineered two-member bacterial community. Reed D. McCardell, Ayush Pandey, Richard M. Murray *bioRxiv*; doi: <https://doi.org/10.1101/632174>

RDM conceived the research idea with advice and guidance from RMM. RDM designed and performed the presented experiments. AP created the mathematical models and performed the computational and theoretical analysis with input from RDM. RDM wrote the manuscript with input from RMM.

TABLE OF CONTENTS

Acknowledgements	iii
Abstract	vii
Table of Contents	ix
Chapter I: Introduction	1
Chapter II: Population density control in synthetic bacterial communities . . .	9
2.1 Introduction	9
2.2 Results	12
2.3 Discussion	33
2.4 Materials and Methods	34
2.5 Supplementary Material	38
Chapter III: Composition control in an engineered multi-member community	39
3.1 Introduction	39
3.2 Results	42
3.3 Discussion	59
3.4 Materials and Methods	60
3.5 Supplementary Material	64
Chapter IV: Colicin toxins as multi-functional tools for bacterial population control	69
4.1 Introduction	69
4.2 Results	73
4.3 Future Work	80
4.4 Discussion	82
4.5 Materials and Methods	82
Chapter V: Concluding remarks and lessons learned	85
5.1 Working with burdensome genetic circuits	85
5.2 Choosing appropriate measurements	87
Bibliography	89

Chapter 1

INTRODUCTION

The work presented in this thesis sits at the intersection of microbiology: studying life too small to see (bacteria, archaea, viruses, fungi, prions, protozoa, algae etc.); and bioengineering: using engineering tools to understand and build biological systems. The approach taken in this work is sometimes called *synthetic* biology for its emphasis on "rebuilding" biology into easily analyzed, well-understood systems with new functions.

Bacterial synthetic biology is particularly exciting due to a powerful synergy between the current states of microbiology, biotechnology and engineering. A long history of microbiology research has taught us the kinds of things bacteria can do and what tools they use to do them; a growing repository of biotechnology allows us to edit, shuffle or otherwise play with the DNA that encodes such tools; and engineering disciplines contain tried-and-true analytical frameworks to understand changes we make to complex systems, allowing us to design new biological systems or better understand ones we study.

Specifically, we are interested in using DNA editing technology and the mathematical framework of dynamical systems to design new systems to control heterogeneous *communities* of bacteria.

The social life of bacteria

Even before the microscope made microbes visible, scientists speculated that life of some unseen sort was responsible for things like food spoilage, disease, or the transformation of grain juice into alcohol. As technology marched forward, so too did our understanding of the very real microbial world. We now know a great deal about where microbes live, what they look like, what they eat, how they grow, etc. These discoveries have provoked revolutionary advancements in medicine, chemistry, manufacturing, environmental science—it is hard to overstate the impact microbiology has had on human society and our understanding of our planet.

Current microbiology research drills into the molecular sub-cellular workings of microorganisms, but also examines the larger roles they play in environments like human bodies, soils, or the planet as a whole. While the concept is not new to the

field, the last few decades have seen an explosion in studies acknowledging microbial populations as pseudo-multicellular organisms comprised of highly interconnected, interdependent—*social*—communities.

These social communities rarely contain only one member species; rather, tens to hundreds to thousands of species coexist alongside each other in most environments [1]. We can describe a community by its *composition*, the relative abundances of each species in the population. A community's composition may be termed *rich* when many different species are present or *even* when the relative abundance of the member species is more equal. Many metrics of diversity attempt to combine richness and evenness into a single numerical quantity, usually increasing with both.

Among communities of macro-scale organisms, higher community diversity is associated with greater community stability and productivity (referring to the community's ability to stably maintain size, diversity, and important ecosystem functions) [2]. On the micro-scale, the same principle holds. Decomposition of organic matter—a critical process for whole ecosystems—is reduced as soil microbial diversity falls [3]. Human gut microbiome composition is correlated with, or even causative of significant medical conditions like diabetes and autoimmune disease [4–6]. The relationship between commensal microbes and the physiology of their hosts raises interesting new ideas about community "productivity" or "function" (does digestion count as "productivity"? Is human health a "function" of microbes?). Whatever role microbes play in their environment, it is clear that **microbial community composition is important** and deserves continued attention from biologists and engineers who wish to understand how it is and why.

Because microbes are such powerful forces in their environments, when environmental change disrupts a community's composition, compromising its sometimes critical function, environmental degradation and microbial community collapse feed back on each other out of control. An engineer thinking about this problem will recognize that stable, diverse community compositions are clearly desirable states and wonder "how can I cause a microbial community to establish a target composition? And how do I make it stay there?".

Genetic engineering

We are only able to attempt microbial community engineering thanks to the proliferation of reliable, easy to use genetic engineering technology. Biochemists discovered, studied and optimized enzymes that act on DNA, transforming them

into the common hammers and nails that allow us to build DNA essentially at will. This transformative technology allows researchers to configure the small pieces of biology we know a lot about into large systems for desired purposes.

The DNA technology used for genetic engineering was itself mined from the DNA of bacteria, viruses, and other microbes. Engineers adapted microbial technology with appropriate DNA-related functions to new roles as human technologies. Polymerase chain reaction (PCR) [7], Gibson assembly [8], GoldenGate assembly [9], Sanger sequencing [10] and bacterial transformation [11] are the basic techniques that enable all the work we present (see 3G assembly for the full protocol [12]). They are clever, powerful things that deserve their own attention, but are considered basic technology in the field and go without detailed explanation.

To build systems that enable control of bacterial communities, the process is the same; we need to know what tools bacteria use to regulate themselves and their communities...then steal those tools for our own purposes. The classic process in synthetic biology is "part-ification" of such tools, the full characterization of a complex biological tool and subsequent transformation into a well-understood "part" (like a capacitor or an I-beam) that can be used to build new biological systems.

The process of characterizing engineered parts is difficult in any discipline without equally well-understood, standardized testbeds in which a part under study can be precisely manipulated and measured. Biology is an especially interesting discipline for how little we understand it—despite all we know today, there is still so much to learn before any biologist can claim what they study is "fully understood". This sets up a unique challenge for bioengineers trying to make precise, predictable systems in a platform that is inherently complex and unpredictable. To get the best of both worlds, our work is carried out using the world's most well-studied microbe (maybe the world's most well-studied *organism*): the bacterium *Escherichia coli*. *E. coli* is easy to grow, has a completely sequenced genome and has been the testbed for nearly every piece of DNA technology ever developed. Laboratory-optimized strains of *E. coli* provide an ideal balance of a controlled biological system (as "under control" as any biology can be) and relevance to the "real-life" biology that patterns our bodies and our planet.

Synthetic biology and microbial communities

In the early 2000's, "synthetic biology" was born. Bioengineers used DNA technologies to create cell-powered "genetic circuits" that imparted complex behaviors

to the cellular host. These early investigators paired an intuitive dynamical systems modeling approach, based in ordinary differential equations, with precise laboratory work to design circuits that bestowed new behaviors on bacteria [13, 14]. They demonstrated that human-designed genetic programs could be reliably coded into populations of bacteria, whose resulting behavior recapitulated the predictions made by the designer's model.

Synthetic biology has grown to encompass a great variety of topics, from our work in microbial community control to the effort to build a functioning bacterial cell from the ground up, supported by advanced quantitative disciplines like engineering, physics, statistics and control theory. In general, synthetic biologists work like engineers, using standardized tools and techniques to create new things with biological parts.

In the case of microbial community control the synthetic biology framework uses mathematical tools from control and dynamical systems engineering to transform our microbiology knowledge and DNA editing technology into biological designs. However, we want to build systems to control microbes—living things—rather than more standard control targets like temperature in a refrigerator or liquid level in a water tank. To do this, we need biological equivalents of the parts used to make a thermostat or level controller: a sensor to detect the state of the system, a controller to turn system state into a decision about what to do next, and an actuator to affect the system and keep it under control.

Control systems are often modeled as sets of differential equations whose analysis with mathematical and computational tools give lots of insight into the properties of the system. Analytically solving the equations reveals system steady states and the stability of those steady states. Computer simulations can numerically compute the expected behavior of the system from different start states, or identify parameters in the system critical to its performance. Data collected from experiments help uncover the likely values of parameters in the equations, which makes model predictions even more accurate. We rely on a number of these techniques to aid our design process and streamline the process of building our population control systems in the laboratory.

Unlike a refrigerator, an engineered microbial community does not have a central computer that handles all sensing, processing and actuation. The control functions are distributed among all the individual bacteria in the community, meaning the goal is to design a DNA-based system for each bacterium that allows the community to synthesize and sense the community state, then coordinate decision making and

actuation to maintain control. The genetic parts required must:

1. Send information between cells in the community
2. Process and respond to information signals from the community (or environment/experimenter)
3. Regulate the number of cells of any type in the community

These functions knit a group of individual bacteria into a true *community* that acts together to actively change its own characteristics (e.g. total size or composition) in support of a desired ecological/biochemical/medical goal.

Bacteria have a staggering variety of molecular tools to do exactly these things, the great majority of which are likely unknown and unused—except by the bacteria that invented them. Using DNA editing technology, we can take microbial tools for communication, information processing and community regulation and configure them into a population control system whose behavior we can predict using control system modeling tools.

1. Communication is key

Much of bacterial communication is done by exchanging metabolites, enabling different members to grow at different rates, determining composition. This communication is convoluted, arising as a consequence of metabolism—intimately tied to just about every process in a cell. Engineering community control by manipulating metabolism is certainly powerful, but runs the risk of destabilizing the entire biological system if not planned very carefully. This is not meant to undermine the importance of metabolic interactions; they underlie much of native community structure and can be useful tools in microbial community engineering [15].

Some bacteria are more explicit about communication, decoupling it from the basic mechanisms of growth. Acyl-homoserine lactones (AHLs) are chemicals that allow bacteria to communicate specific messages beyond "grow at this rate due to the availability of nutrient x", giving them a more active, precise role in community determination. AHLs are used in nature to ensure community coordination and increase fitness [16, 17]. They can also be parasitized by invaders to destroy coordination and establish new community compositions [18, 19].

Metabolism-independent cell-to-cell communications modules are extremely valuable to microbial community engineers; these AHL systems have already been adapted into the synthetic biology toolbox to great effect [20–23].

In AHL systems we find simple, genetically encoded modules for creating communication among our engineered community members. There are many different AHL systems available for use in synthetic biology [24–26]; we primarily use the Lux (3-oxo-C6-HSL) [27] and Cin (3-hydroxy-C14-HSL) [28] systems.

2. Control of gene expression

Already in the toolbox of synthetic biologists are various transcription factors, protein tools bacteria natively use to ensure efficient regulation of their repertoire of genes. Combining a transcription factor (TF), a DNA element that regulates gene expression in response to that TF, and a gene of choice, a synthetic biologist can set up experimenter-controlled expression of that chosen gene in a bacterium. Controlling expression of genes via TFs is the foundational technique in most synthetic biology work; regulating the expression of transcription factors with other transcription factors allows gene expression networks to perform complex, useful functions [29–32].

Most engineered DNA is input into bacteria as a plasmid, a circular piece of DNA that replicates independently from the main genome. However, there is a limit on the total amount of plasmid DNA a bacterium can accept. When a synthetic biologist wants to use a TF to regulate a gene in their system, they need to include it on a plasmid, using up space that may be required for other critical components. To keep design space open, TF expression is usually integrated into the main bacterial genome. Easy to use integration technologies enable researchers to create their own genome-integrated *E. coli* strains [33]; even more elaborate integrated strains are made as chassis for synthetic biology, enabling plug-and-play gene regulation with known parameters [34]. We both create our own custom genome-integrated *E. coli* and use the versatile Marionette *E. coli* strains to create our engineered bacteria.

3. Regulating life and death

In native bacterial communities, there are 4 ways for the population of a member to change: emigration, immigration, reproduction and death. A human gut microbiome regularly receives new input that can contain additional bacteria, likewise it is purged by gut motility. Nutrients are regularly available, but growth is far slower than in optimal conditions. Death is, of course, inevitable at some rate. Controlling a

bacterial community means controlling one or more of these activities. Here again, we can turn to bacteria themselves to find useful tools to meet our needs.

Some bacteria have evolved tools to actively regulate life and death within their communities. These are frequently genetically encoded protein toxins, produced by a cell to kill itself on command. In some cases, the toxin is paired with a specifically matched anti-toxin that spares a producer from the toxin. Toxins and anti-toxins (TA systems) play roles we are only still discovering in modifying bacterial populations. A "selfish gene" explanation might contend that the genes encoding TA systems use their functions to ensure their survival or dominance in the collective genome of a bacterial population (many TA systems cause bacteria to become "addicted" to their presence and create fitness repercussions if the TA system is jettisoned). On the other hand, bacterial populations may retain TA systems as tools to improve their fitness in particular situations [35, 36]. Whether the TA systems selfishly manipulate bacteria or the bacteria have found utility in the TA systems, TA systems absolutely regulate life and death to modify population composition.

With our understanding of bacterial physiology and our ability to manipulate it, there are endless opportunities to create bacteria whose growth or death are controlled by an experimenter—set up outside control of ribosome synthesis [37], control expression of a critical metabolic protein [38], even simply regulating the metabolic load on a cell can alter growth rate [39]. Many toxins and antitoxins affect the rate of *death* in a community; others, like the T7 phage *gp2* protein modify the *growth rate* of cells by interfering with critical growth processes—in this case RNA synthesis by RNA polymerase [40]. Every growth (or death) regulatory tool has a mode of action, potency, strength and weakness that makes it unique and may suggest a particular use case in population regulation. A particularly interesting set of TA systems, the bacteriocins, work *between* cells rather than inside individual cells. Their structure and multi-functionality make them attractive for microbial community engineering and will be discussed in Chapter 3.

Toxins, antitoxins, growth inhibitors, engineered physiology—growth regulators in general—are fascinating, both for their ecological roles and their potential in bioengineering. Many of these tools are receiving renewed interest due to the expansion of synthetic biology; hopefully their "part-ification" can be useful to the field and reveal new complexity in microbial ecology.

Putting it together

With the explosion of interest in microbial communities in soil, the ocean, human guts, scientists are applying research approaches from every discipline of science to shed light on the complex, influential, social lives of microbes. Using insights from microbiome researchers and experience from pioneering microbial community engineers, we have designed genetic circuits we hope will be useful in building and manipulating the powerful microbial life that shapes our planet.

*Chapter 2***POPULATION DENSITY CONTROL IN SYNTHETIC BACTERIAL COMMUNITIES****2.1 Introduction**

Microbial communities are everywhere and perform critical functions for the health of ecosystems at every scale. When environments change, community species compositions change, but we cannot predict changes or prevent them without greater knowledge of microbial communities and community control technology.

Bioengineers in various fields recognize the importance of microbial community control for different reasons. Synthetic biologists run into limits on the complexity of genetic circuits that are tolerated by homogeneous populations of microbes; increasing the complexity of genetic circuits requires the distribution of circuit burden across a heterogeneous community of microbes [41, 42]. Additionally, genetic circuits designed without provisions for coordination of circuit-containing cells lose precision in their function due to cell-to-cell variability [43, 44]. Control of community composition and gene expression dynamics are required to create a stable platform for reliable circuit function.

Bioprocess engineers recognize the efficiency and yield gains to be made by distributing production processes across a community of organisms [45, 46]. Literature detailing the benefits of polyculture production emphasizes that this process is optimized at specific community compositions, necessitating precise, stable control of community composition [47–49].

Ecologists and microbiologists recognize the potential of microbial community control to enable greater understanding of biological diversity through community control experiments mimicking and investigating natural ecology. Those seeking to remediate and preserve natural microbial diversity see the value of genetic circuits for community control in efforts to understand and beneficially alter natural microbial communities [50, 51].

At its core, control of community composition is really the control of population density for many coexisting microbes at the same time. The basic unit of multi-member composition control is control of an individual homogeneous population's

density. The population density control circuit published by You *et al* [52] is one of the foundational genetic circuits in the population control space; it has served as template, springboard and inspiration for studies building alternative or more complex population control circuits.

Despite the clear utility of genetic circuits that explicitly control population sizes, a relatively small number of circuits tackling this challenge have been published in the space of community synthetic biology.

In You *et al* [52], the authors create a genetic circuit closely mimicking the architecture of native autoinducing quorum sensing circuits, but replace the induced downstream gene with the *ccdB* toxin (Fig 1B in [52]). Instead of coordinating expression of a bioluminescent protein with the quorum sensing chemical (as in *Aliivibrio fischeri* [53]), this circuit coordinates cell death throughout a population of *E. coli*, capping normal population growth at a specific density. The components of the circuit are the LuxI AHL synthase, LuxR activatory transcription factor, pLux inducible promoter and *ccdB* toxin.

With rare exceptions, other genetic circuits designed for population control are similarly designed, using quorum sensing mediated autoactivation of toxins or growth inhibitors to affect bacterial population growth.

In Scott *et al*'s multi-strain community circuit [54], culture dominance by one strain is avoided by the expression of a very similar quorum sensing autoactivation circuit in each strain. The Lux or Rpa systems (in the two community member strains) coordinate expression of the $\phi X174$ lysis protein, causing each strain's population to grow up to a threshold density, at which point the quorum sensing signal activates lysis throughout the population, dramatically reducing strain density. Oscillatory cycles of growth and lysis of the two strains in coculture allow cocultures that would ordinarily become dominated by one strain to maintain a mixed composition over long culture times. Where the You *et al* population control circuit sets steady state population densities, the Scott *et al* circuit produces oscillatory population dynamics (although a steady state is possible in specific parameter ranges). This difference in circuit behavior is not likely to be caused by the difference in toxic protein (*ccdB* vs $\phi X174$), but rather due to the positive feedback regulation of AHL production in Scott *et al*, compared to the externally-inducible, but stable rate of AHL production in You *et al*.

With a similar goal of maintaining coculture diversity, Dinh *et al* created a feedback

AHL regulated circuit for control of bacterial *growth* rather than *death* [55]. In this circuit, growth rate of one strain in coculture is regulated by the degradation of phosphofructokinase A (*pfkA*) in response to Lux AHL. In this way, even when this strain dominates a coculture at inoculation, over time its growth rate decreases and allows a second uncontrolled strain to grow, maintaining a mixed population. The growth control circuit is structured identically to the You *et al* circuit but uses a growth inhibitory mechanism rather than a death activatory toxin. Despite stable AHL production rates in this circuit, the choice to inhibit *growth* with AHL feedback does not produce a steady population density, presumably because *pfkA* is never completely degraded away and cells may continue to grow even at high population densities. Contrast this with the expression of a toxin, which can theoretically increase the death rate in a population to match the growth rate, thereby allowing a steady state population to be achieved.

Quorum sensing and growth or death regulation are not the only components that can be used to regulate population densities. Kerner *et al* created a coculture of auxotrophic *E. coli* whose growth rate and composition can be precisely tuned by the expression of metabolite export proteins [15]. In this case, metabolites play the dual role of intercellular signal and growth regulator, where AHLs and toxins are used together in other circuits. The sub-populations in this community cannot be separated from each other; their genetic circuits cannot perform monoculture population density control because by nature, auxotrophs are dependent on partners or external supplementation for survival.

Other chemicals and proteins can be used as combined signals and growth regulators. Antibiotics and their resistance genes can regulate growth and death in genetic circuit designs, as can secreted intercellular bacteriocin toxins like nisin or lactococcin A [56, 57].

Returning to AHL and toxin-based genetic circuits, more complexity is possible in genetic circuit function. Balagaddé *et al* used the *ccdA* antotoxin in conjunction with *ccdB* to create a genetic circuit capable of downregulating population density with the *ccdB* toxin *and* inhibiting that downregulation with *ccdA* (rescuing a population from growth inhibition). Using this new circuit function, they designed a synthetic predator-prey ecology capable of recapitulating the out of phase oscillations characteristic of that relationship [58].

These different circuits illustrate the various ways population regulation can be approached using genetic circuit parts appropriated from bacterial physiology. There

remains design space to be filled in *stable* monoculture population density control by the combination of the technologies reviewed above. By adding the *ccdA* antitoxin to the population capping architecture published by You *et al.*, we create a genetic circuit capable of stable population control with the additional functionality afforded by antitoxins. This circuit allows the stable capping of population density using feedback toxin expression, but also the progressive release of a population density cap with independently regulated antitoxin expression, allowing two-input upward and downward control of population density.

Using a functional screening process, we build an implementation of the *cap and release* circuit. Then, by adding quorum sensing signal degradation, we give experimenters control over AHL degradation, a critical parameter in circuit function. The resulting signal degradation-capable *cap and release* circuit is an environment-independent controller of population density as well as a scalable motif for single and multiple strain community control.

2.2 Results

Examining a feedback population control circuit

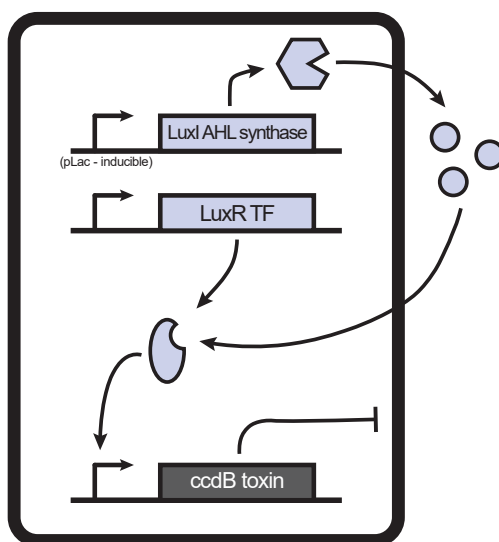


Figure 2.1: Architecture of *pop cap* Schematic representation of the population capping circuit published in [52]. Secreted AHL signals implements negative feedback control of population density.

We started by reexamining the design of the You *et al.* (2004) population control circuit (Fig. 2.1). The *pop cap* design is based on the production, sensing and response to secreted acyl-homoserine lactone (AHL) quorum sensing molecules that

broadcast population density throughout the community. Cells respond to AHL by expressing a toxin, killing themselves when AHL and toxin levels get too high. This negative feedback causes the artificial capping of the population's density below normal limits (normal e.g. nutrient limitation or maximum physiologic density causing stationary phase). For its population capping function, we call this the *pop cap* circuit

The specific components that make up the You *et al.* *pop cap* implementation (and much of our later circuit designs) are as follows:

- **pLac inducible promoter:** An inducible promoter repurposed from its native role in the *Lac* operon. Transcription from this promoter is activated by the unbinding of the LacI repressor when LacI is complexed with lactose, or in this case, the modified inducer chemical IPTG (isopropyl β -D-1-thiogalactopyranoside). In this circuit, pLac drives LuxI expression.
- **LuxI AHL synthase:** An enzyme that synthesizes Lux-type AHL chemicals (3-oxohexanoyl-homoserine lactone, 3-O-C6-HSL) from S-adenosylmethionine (SAM) (amino donor) and an appropriate acyl–acyl carrier protein (acyl-ACP) (acyl donor) [59]. Lux AHL chemicals can freely diffuse through bacterial membranes, meaning their concentration in a mixed culture environment is equal both inside and outside cells.
- **LuxR transcription factor:** A transcription factor that binds Lux AHL molecules, dimerizes, then binds as a dimer-AHL complex to the pLux promoter, *activating* transcription of downstream genes.
- **ccdB toxin:** A small 101 amino acid toxin protein expressed natively from the *E. coli* F plasmid *ccd* operon. In this circuit, its transcription is driven by the pLux inducible promoter. ccdB covalently traps DNA gyrase in an unstable DNA strand-cleaved conformation [60, 61]. Stuck in this state during replication, the genome fragments and the cell dies

Stripping away the minutiae of the circuit's implementation in You *et al.* (exact plasmid origins of replication, promoter types, plasmid design) we can write a set of differential equations that describe the major kinetic events that underlie the circuit's activity. The dynamics of C , cell population size (ml^{-1}); T , average intracellular ccdB toxin concentration (nM); and A , AHL chemical concentration (nM) are described by the following:

$$\frac{dC}{dt} = k_C C \left(1 - \frac{C}{C_{max}}\right) - d_C C T, \quad (2.1)$$

$$\frac{dT}{dt} = k_T A - d_T T, \quad (2.2)$$

$$\frac{dA}{dt} = k_A C - d_A A. \quad (2.3)$$

We assume in eq. (2.1) that population (C) growth unconstrained by circuit action follows a logistic model with a growth rate of k_C (h^{-1}), a carrying capacity of C_{max} (ml^{-1}), and an intrinsic death rate of D (h^{-1}). During circuit-regulated growth, we assume the cell death rate is proportional to the intracellular concentration of the toxin protein (T) with a rate constant of d_C ($nM^{-1}h^{-1}$). In eq. (2.2) we assume the production rate of toxin T is proportional to an activatory Hill function of AHL concentration (A , assumed to be the same inside and outside the cells due to free transmembrane diffusion) with a rate constant of k_T (h^{-1}), equilibrium constant of k (nM), and Hill coefficient β (assumed to be 2). Toxin is produced from a promoter activated by a complex of AHL chemical and dimerized AHL transcription factor, commonly expressed as a Hill function, as we do here. In eq. (2.3) we assume AHL signal synthesis rate is proportional to C with a rate constant of k_A ($nMmlh^{-1}$); in the laboratory implementation of this circuit, k_A is modifiable by the experimenter by changing the concentration of the IPTG inducer of pLac. We also assume degradation of toxin and AHL follows first-order kinetics with rate constants of d_T (h^{-1}) and d_A (h^{-1}).

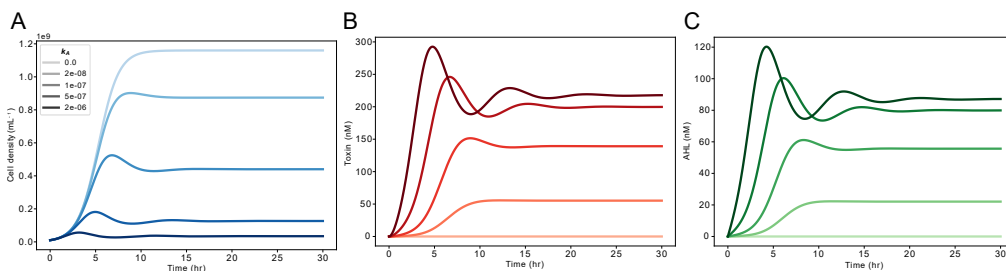


Figure 2.2: Simulation of *pop cap* system Dynamics of each species in the model of *pop cap* are simulated in response to increasing AHL production rate, k_A . (A) Total population density (B) Average intracellular toxin concentration in the population. (C) Environmental concentration of AHL, assumed to be equal inside and outside cells due to free diffusion.

Simulations of the model demonstrate the expected behavior of the system (see materials and methods for parameters and initial conditions) (Fig. 2.2). In each

panel, we have simulated the dynamics of each species using five different values for k_A (simulating response to IPTG inducer). With k_A at 0, the circuit is "OFF" and the model predicts normal logistic growth of the cell population to C_{max} . With increasing k_A , population growth overlaps normal logistic growth, but eventually deviates, overshoots its final steady state, then finally settles at steady state at a density below C_{max} . This is the population capping function of the circuit. Population capping is mediated by the ccdB toxin, induced by AHL signal produced by the population. The ccdB toxin and AHL signal accumulate to higher and higher steady state concentrations with increasing k_A , depressing the population density steady state with increasing ccdB concentration (Fig. 2.2, B-C).

Demonstrating population control

The You *et al.* implementation of *pop cap* uses secreted Lux-type (3-oxohexanoyl-homoserine lactone, 3-O-C6-HSL) quorum sensing molecules to broadcast population density and the ccdB toxin to kill cells. The LuxI AHL synthase is expressed by the inducible pLac promoter, responsive to IPTG. The plasmids that carry the circuit are structured as follows:

- **Plasmid 1:** ColE1 origin (high copy ~300-500/cell [62, 63]), pLac promoter drives the *co-transcriptional* expression of both the LuxR TF and LuxI synthase.
- **Plasmid 2:** p15a origin (low copy ~10-15/cell), pLux promoter drives expression of ccdB toxin fused to lacZ α fragment.

Notably, the ccdB expressing Plasmid 2 has copy number ~200-400x lower than that of Plasmid 1. All genetic constructs "leak" a small amount of protein even without induction of transcription; it is possible that, due to the potency of ccdB, using anything other than a low copy plasmid may amplify ccdB leak to lethal levels, even in the absence of Lux AHL chemical. Plasmid 1 (pLuxRI2 from You *et al.*) transcribes the coding sequences of LuxI and LuxR together, meaning an experimenter increases the amount of transcription factor in a cell while they increase Lux AHL synthesis rate. This produces protein dynamics not captured in the mathematical model; it is possible that the Hill equation assumptions made about ccdB toxin expression in response to Lux AHL, via LuxR, are not always accurate if the LuxR concentration changes along with AHL concentrations.

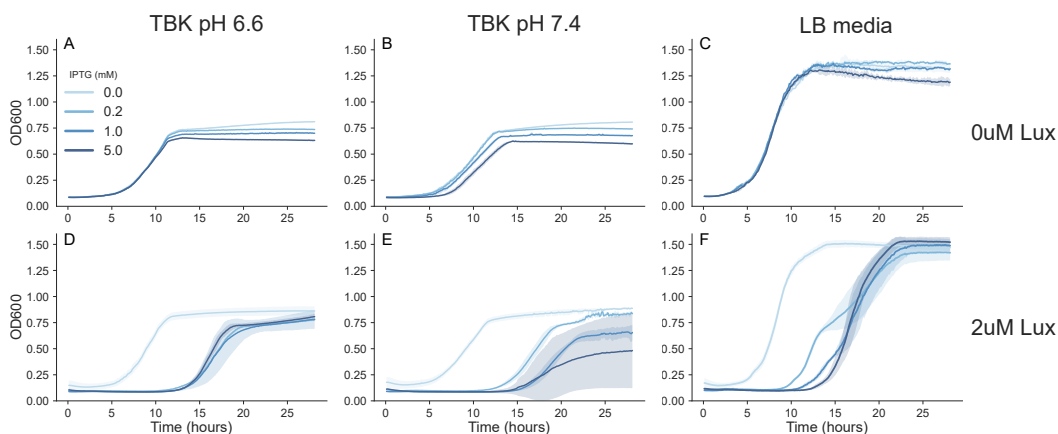


Figure 2.3: Recapitulating population capping. Cells containing the *pop cap* circuit were grown in the indicated media and inducer concentrations. Curves are the mean of 3 replicates, shaded areas represent standard deviation.

We tested the *pop cap* circuit using the original plasmids (*plasmid 1*: pLuxRI2 and *plasmid 2*: *pluxccdB3*) in DH5 α *E. coli*. Cultures were grown in 4 concentrations of IPTG (mimicking 4 increasing k_A values) in three different growth media: the buffered defined TBK medium from the You *et al* publication at two pHs and standard LB medium.

Pop cap - TBK pH 6.6	OD600 - endpoint	σ
Uninduced maximum density	0.8106	0.0035
5 mM IPTG - cap	0.6316 (77% uncapped)	0.0058
Pop cap - TBK pH 7.4		
Uninduced maximum density	0.807	0.001
5 mM IPTG - cap	0.599 (74% uncapped)	0.0075
Pop cap - LB		
Uninduced maximum density	1.319	0.039
5 mM IPTG - cap	1.19 (90% uncapped)	0.038

In the TBK media (Fig. 2.3, panels A-B), our experiments consistently recapitulated the qualitative function of the circuit, but never matched the published magnitude of the circuit's effect. You *et al.* demonstrated population density capping to 10% the density of a control population (hereafter referred to as "max density") with 1 mM IPTG induction, while our experiments only produced a cap to ~75% of max density at 5 mM IPTG. Between the two TBK media at different pH values, the circuit had very similar population capping performance, but growth dynamics were significantly different. In TBK at pH 6.6, growth rate in each IPTG concentration was nearly identical until 10 hours, at which point each culture abruptly stopped

growing at its population cap.

Similar abrupt halts in growth were observed in TBK pH 7.4, but each culture's growth rate was different, producing non-overlapping curves. Growth at pH 6.6 more closely recapitulated the model's prediction that capped populations would grow similarly to the uncapped population until an abrupt decrease in growth rate; at pH 7.4, IPTG induction produced a noticeable difference in growth rate between the capped cultures.

In LB medium (Fig. 2.3, panel C), circuit induction had an even smaller effect on population density; no difference in density between the IPTG concentrations was apparent until after 11 hours, when the culture in 5 mM IPTG slightly decreased in density until it settled only 10% lower by the end of the experiment.

While these data suggested the dynamic range of the circuit was limited, we demonstrated the full potential dynamic range of the circuit by progressively inducing circuit components with IPTG in the presence of 2 μ M Lux AHL. In all media, induction of circuit components with IPTG combined with manual addition of Lux AHL (rather than relying on LuxI AHL synthesis) produced dramatic population caps (Fig. 2.3, panels D-F). The intensity of these caps was such that no growth was observed in any condition except the uninduced 0 mM IPTG condition, in which the cells would not be expected to respond to the high concentration of Lux AHL.

These heavily capped cultures did not grow from their seeding densities until 10-12 hours after the start of the experiment. At that time, each heavily capped culture began to overgrow its cap until it reached the vessel's capacity. In TBK pH 6.6, all heavily capped cultures all began to grow after 12 hours, following approximately normal logistic growth to maximum density by the end of the experiment. In TBK pH 7.4 and LB medium, the time at which the capped culture began to grow was related to the IPTG inducer concentration. With increasing IPTG induction, the capped culture remained dormant at its seeded density for longer times.

These results suggested that this implementation of the circuit was not optimized for maximum response, especially not in LB medium. An improperly low Lux AHL production rate seems a probable cause of this poor dynamic range given how drastic an effect exogenous AHL could produce when the circuit response elements were induced with IPTG. Additionally, we found that heavily capped cultures were not stable; rather, they would eventually overgrow their very low population cap and continue growing to maximum density. This suggests either an evolutionary escape

from population control [64], or unforeseen dynamics in circuit components (e.g. unexpected decrease in AHL signal concentrations or *ccdB* production). We believe this phenomenon is caused by the growth of cheater bacteria who have evolved away from circuit function. Sequencing the plasmids of the overgrown cultures may reveal inactivating changes in plasmid sequence.

It is important to note that our data were taken using optical density (OD600) absorbance measurements, while the original authors measured viable colony forming units (CFU). Our results may have been identical in magnitude to those published, but were obscured by the different measurement technique. The toxic mechanism of *ccdB* may affect these measurement types differently. We address this in the following section.

Toxin sequestration allows population cap release—the *cap and release* motif

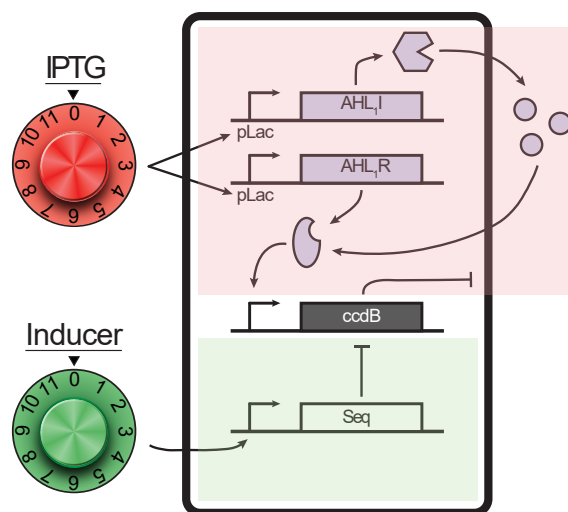


Figure 2.4: The *cap and release* circuit motif. Red shaded area indicates the feedback populating *capping* arm of the circuit. Green shaded are indicates the *cap release* arm. Seq is either the *ccdA* antitoxin that sequesters *ccdB* at the protein level, or RNA-OUT, which binds the RNA-IN sequence on *ccdB* mRNA, sequestering it at the mRNA level.

The *ccdB* toxin has a naturally occurring peptide antitoxin, *ccdA*, that is involved in regulating the *ccd* operon, from which both *ccdB* and *ccdA* are expressed [65, 66]. By creating a third *ccdA* expressing plasmid to accompany the 2 *pop cap* plasmids, we modified the *pop cap* system to include experimenter-controlled *ccdB* toxin sequestration. This sequestration mechanism acts at the *protein level*; *ccdB* and *ccdA* are both proteins that sequester each other.

- ***ccdA* antitoxin:** When present together with *ccdB*, *ccdA* binds *ccdB* with

picomolar affinity [67], sequestering it and blocking its toxic activity. *ccdA* can bind and inactivate both free *ccdB* and *ccdB* already complexed with DNA gyrase; *ccdA* reverses *ccdB*/gyrase binding and restores gyrase to normal function.

We also designed an alternate version of the *pop cap* architecture containing a different *ccdB* sequestration device, this one using the Rhl AHL system [68] and an mRNA level sequestration system called RNA-IN/RNA-OUT [69] to regulate expression of the *ccdB* toxin. This mechanism acts at the mRNA level:

- **RNA-IN:** An RNA sequence containing a ribosome binding site (RBS) that initiates translation of the downstream encoded protein. The RBS is normally accessible to ribosomes (i.e. it is not hidden from ribosomes by any secondary RNA structure). RNA-IN is built into genetic circuits as a DNA sequence between a promoter and protein coding sequence; it becomes functional when transcribed into RNA.
- **RNA-OUT:** The sequestration device for the RNA-IN containing mRNA. It is also built into circuits as a DNA sequence that becomes a functional mRNA sequence when transcribed from a promoter. RNA-OUT binds to a section of RNA-IN via RNA base pairing, causing a conformation change in the IN/OUT complex that hides the RBS in RNA-IN from ribosomes, blocking translation of the gene downstream of RNA-IN.

By adding a *ccdB* sequestration device (either *ccdA* or RNA-OUT) to the *pop cap* circuit under regulation by a second external inducer, we turned the *pop cap* circuit into a new circuit motif with two inputs. As demonstrated above, feedback control of *ccdB* expression via AHL signals sets a steady state population cap. Inducible *ccdB* sequestration allows the progressive release of that population cap. We call this motif the ***cap and release*** circuit (Fig. 2.4). We add a new equation to the *pop cap* model to reflect the new circuit components.

$$\frac{dC}{dt} = k_C C \left(1 - \frac{C}{C_{max}}\right) - d_C C T, \quad (2.4)$$

$$\frac{dT}{dt} = k_T A - k_{on} T R - d_T T, \quad (2.5)$$

$$\frac{dR}{dt} = g_R - k_{on} T R - d_R R, \quad (2.6)$$

$$\frac{dA}{dt} = k_A C - d_A A. \quad (2.7)$$

Where R (nM) represents the average concentration of sequestration device in the population.

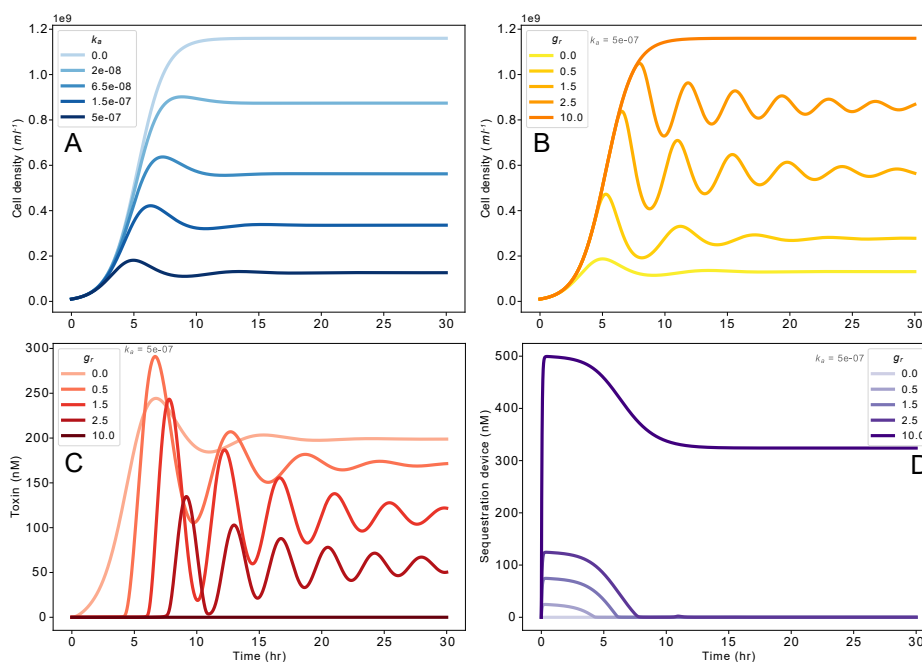


Figure 2.5: Simulation of *cap* and *release* system Population dynamics of *cap* and *release* are simulated in response to (A) increasing AHL production rate, k_A , (B) increasing *Seq* production rate, g_R , against a background of high k_A . (C) Toxin dynamics during *cap* release with increasing g_R . (D) *Seq* dynamics during *cap* release with increasing g_R .

Equations (2.4) and (2.7) are unchanged from the *pop cap* model (eqs. (2.1) and (2.3)). We have added eq. (2.6) that models the production of the toxin sequestration device (*Seq*). We lump all terms related to *Seq* production into g_R (nMh^{-1}), as this term is arbitrarily modifiable by the experimenter by changing *Seq* inducer concentration. Toxin/*Seq* binding is assumed to be proportional to their

concentrations with constant k_{on} ($nM^{-1}hr^{-1}$). We omit an unbinding term since the affinity between toxin and *Seq* is incredibly strong for both systems used. *Seq* degradation is first-order with rate d_R (hr^{-1}). The same toxin/*Seq* binding term is added to eq. (2.2) to form eq. (2.5). Now, cell death is modified only by *free* toxin, since the sequestration complex is inert.

Simulating the responses of this system to increasing k_A (simulating increasing IPTG inducer concentration) (Fig. 2.5, A) and g_R (increasing *Seq* inducer concentration) (Fig. 2.5, B-D), demonstrates both population control behaviors of this circuit. As in *pop cap*, increasing k_A alters normal logistic growth to produce population density steady states lower than maximal. Increasing g_R against a background of high k_A increases the amount of *Seq* present in each cell, which sequesters an approximately equal concentration of ccdB toxin, releasing population capping pressure and producing higher steady state population density. We see this clearly in (Fig. 2.5, D) in which increasing amounts of *Seq* are produced in the population, but as ccdB toxin is produced, free *Seq* concentration decreases to zero if more ccdB is produced than *Seq*, or to a positive steady state value if more *Seq* is produced than ccdB. When excess *Seq* is produced due to very high g_R , growth is normal because no free toxin exists to limit growth.

Scanning the parameters associated with *Seq*: g_R , k_{on} , and d_R , we find that g_R must be large (100-1000x larger than k_T) to make significant changes to population density; that k_{on} must also be large to allow toxin sequestration to occur at a useful rate; and that d_R should also be large relative to d_T to avoid extremely oscillatory toxin and population dynamics during cap release that may preclude establishment of a population steady state in a normal experiment duration (10-24 hours). By design or by nature, all of these parameter values are captured in our circuit design. *Seq* is expressed from a promoter-RBS combination much stronger than that expressing ccdB toxin *and* this stronger *Seq* expression unit is contained on a plasmid with copy number $\sim 100x$ larger than the ccdB expression plasmid. These two factors satisfy the need for larger g_R than k_T . By nature, both ccdA and RNA-OUT *Seq* devices have extremely high affinity for ccdB (or its mRNA) and significantly faster d_R relative to d_T , satisfying the requirements for useful and timely *Seq* activity. It is a well-known feature of the native ccdA/ccdB system that ccdA is degraded much faster than ccdB [70]. The half-life of mRNA is also significantly shorter than that of protein [71].

Circuit component sequestration is a tool used for a number of reasons in recent

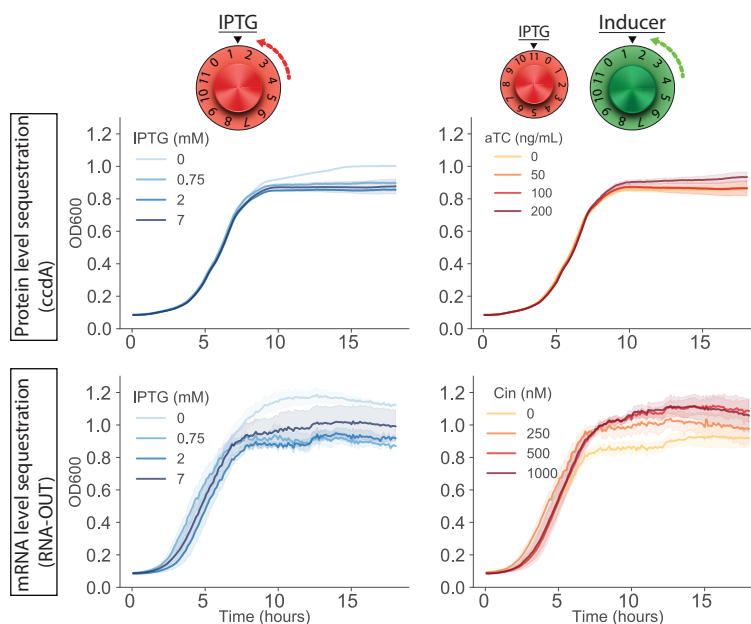


Figure 2.6: Testing toxin sequestration. Both mRNA and protein-level *ccdB* sequestration modules were tested in two different *cap and release* circuit implementations. (LEFT column) - Population capping with IPTG. (RIGHT column) - Release from population capping at 7 mM IPTG. Rows correspond to the two circuit implementations with different sequestration modules.

synthetic biology literature. Circuits with two functional sequestering elements allow the closest biological approximation of an integral controller [72, 73]. While circuits built using the *cap and release* motif do not work around the hurdle of species dilution and degradation [74], *ccdB* sequestration does allow for improved control accuracy if either species or the complex is used to regulate controller output, as we do in this circuit with unbound *ccdB*. Sequestration in the *cap and release* system gives an experimenter both downward and upward control over a community's population density with independent inputs, creating opportunities to translate information from two signals into complex density regulation. The two-input motif can also be configured to link different strains together to form a controlled multi-membered community.

We grew cultures expressing both *cap and release* circuit variants (employing either *ccdB/A* protein sequestration or RNA-IN/RNA-OUT mRNA sequestration) in TBK medium pH 6.6.

In the *ccdB/ccdA* variant (Fig. 2.6, TOP row), population capping was again only modest, to 83% the density of uninduced culture. Similar to our test of *pop cap*, cultures at all IPTG concentrations grew identically until around 8 hours, at which

point they abruptly ceased growth and remained stable at their population cap. The growth rate of *uninduced* culture slowed at this time, but did not stop, continuing slowly until it reached its maximum by the end of the experiment. Population capped at 7 mM IPTG, the *ccdB/ccdA* variant was very slightly released from its population cap by *ccdA* induction with aTC; maximal *ccdA* induction did not fully release the population cap to the density achieved by uninduced culture.

Cap and release - <i>ccdB/ccdA</i>	OD600 - endpoint	σ
Uninduced maximum density	1.001	0.001
7 mM IPTG - cap	0.836	0.041
200 ng/mL aTC - release	0.934	0.031

The variant employing mRNA sequestration (Fig. 2.6, BOTTOM row) demonstrated similar population capping in response to IPTG. Interestingly, the maximal 7 mM IPTG condition produced *less* of a population cap than did lower concentrations. The strongest population cap was produced by 0.75 mM IPTG to 77.5% of uninduced density. Induction of mRNA sequestration with Cin AHL against 7 mM IPTG produced intermediate amounts of population cap release, culminating in nearly complete cap release with 1mM Cin.

Cap and release - RNA-IN/RNA-OUT	OD600 - endpoint	σ
Uninduced maximum density	1.121	0.009
0.75 mM IPTG - cap	0.869	0.0015
7 mM IPTG - cap (less effective)	0.904	0.03
1 mM Cin - release (from 7 mM IPTG)	1.058	0.1

Comparing the two circuit variants, approximately similar population capping (to about 80% of max density) was achieved by both, *but* more complete cap release was observed in the variant employing RNA-level toxin sequestration (RNA-OUT) (Fig. 2.6). Induction of *ccdA* only released the population cap back to 93% maximum density, while RNA-OUT completely removed the cap.

The growth dynamics of each population may be affected by the sequestration device used to modify *ccdB* levels. In the variant with protein-level sequestration (*ccdA*, Fig. 2.6 TOP row), growth of each population is smooth and consistent across replicates. In the variant employing RNA-level sequestration (RNA-IN/OUT, Fig. 2.6 BOTTOM row), growth of each population is jerky and noisy across replicates. We hypothesize that the molecular level (DNA, RNA, protein) of *ccdB* sequestration is responsible for these effects; at lower mRNA copy numbers compared to protein

copy numbers, stochasticity in sequestration may play a larger role in regulating *ccdB* activity, producing the observed noise and variability in cell growth.

In a similar experiment testing the *ccdB/ccdA* sequestration *cap and release* variant, we were able to compare methods of population density measurement. In this experiment, 5 mM IPTG and 100 ng/mL aTC were the highest concentration of population cap and release inducer used, respectively. At the end of the experiment presented in Fig. 2.12, we removed samples of protein-level sequestration (*ccdB/ccdA*) circuit cultures and used two different methods to determine the number of viable cells present: traditional petri plate CFU counting or a small volume culture spotting technique (see materials and methods). We clearly find that absorbance-based optical density measurements overestimate the number of viable cells present in culture compared to CFU counts (Fig. 2.7). OD600 measurements normalized to the uninduced growth condition indicate population capping to 84% uninduced density with 5 mM IPTG. Maximal *ccdA* induction at 100 ng/mL aTC produced an apparent complete recovery of population density with OD600 measurement.

Both methods of viable cell counting reveal significantly stronger population capping to normalized values between 25-50% of uninduced population density with maximal 5 mM IPTG induction. 100 ng/mL aTC induction of *ccdA* is revealed to release these strong population caps only about halfway back to maximum density rather than the complete recovery reported by OD measurement. The viable cell counts from these populations tell us that our experiments approximate the originally published population capping magnitude more closely than optical density measurements report, but we still have not replicated capping to $\leq 10\%$ of max population density.

The specific mechanism of action of *ccdB* may be responsible for the inflation of

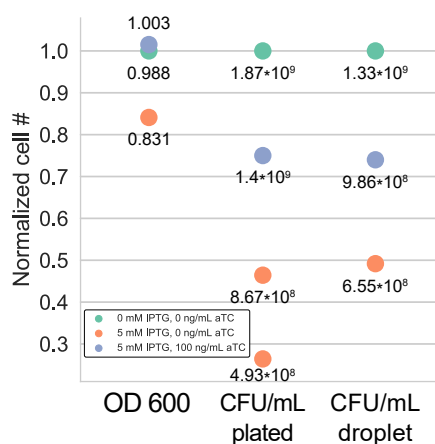


Figure 2.7: Comparing absorbance and viable cell counting methods. Values for each column are normalized to the uncapped condition. Densities are those after 18 hours of growth. Absorbance based optical density clearly overestimates the viable cell count in a culture undergoing capping with the *ccdB* protein.

absorbance-based measurement compared to viable cell counts. It traps DNA gyrase in an unstable DNA strand-cleaved conformation [60, 61]. Stuck in this state during replication, the genome fragments and the cell dies. A cell without a genome may still look alive to an absorbance-based measuring device when it is more or less a husk of a cell that will not *act* alive when checked for viability.

Experimenter-controlled signal degradation and an optimized *cap and release* motif

In their characterization of *pop cap* the authors modified passive degradation rates of the Lux AHL signal by varying experiment pH, showing that higher degradation rates at higher pH result in lower steady state AHL concentrations and thus, higher steady state population density [52]. While increasing pH will increase the passive degradation of AHL signals, not every environment—especially inaccessible field environments—may support appropriate AHL degradation parameters. To make the circuit environment-independent, we added inducible expression of the *aiiA* lactonase, a promiscuous degradase of AHL signals (Fig. 2.8).

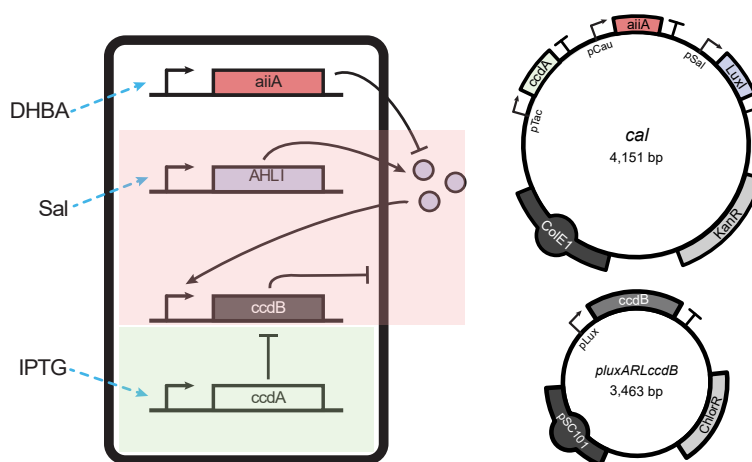


Figure 2.8: The "cap and release" population control motif. (A) Diagram of circuit components. Sal = sodium salicylate, DHBA = 3,4-dihydroxybenzoic acid, IPTG = isopropyl β -D-1-thiogalactopyranoside. AHL₁ is Lux (3-O-C6-HSL) AHL. (B) Plasmid design. *ccdB* is expressed from a separate very low copy plasmid (pSC101 approx. 5 per cell). All other plasmids expressed together from a high copy plasmid (ColE1 approx. 300-500 per cell). Cell line used expresses all TFs including LuxR from genome [34].

- ***aiiA* lactonase:** A protein originally discovered in *Bacillus thuringiensis*. It is a metalloenzyme capable of hydrolyzing the lactone ring of AHL molecules. Its expression by *B. thuringiensis* in various environments has been shown

to attenuate virulence of pathogenic bacteria that rely on AHL signals for community coordination. [18, 75, 76]

$$\frac{dC}{dt} = k_C C \left(1 - \frac{C}{C_{max}}\right) - d_C C T, \quad (2.8)$$

$$\frac{dT}{dt} = k_T A - k_{on} T R - d_T T, \quad (2.9)$$

$$\frac{dR}{dt} = g_R - k_{on} T R - d_R R, \quad (2.10)$$

$$\frac{dA}{dt} = k_A C - d_{ac} C A - d_A A. \quad (2.11)$$

Despite adding components for AHL degradation, the model of the system's major events does not change significantly. Eq. (2.7) becomes (2.11) with the addition of one term reflecting the new per cell AHL degradation rate caused by the expression of *aiiA* in each cell in the system. d_{ac} ($mL \cdot hr^{-1}$) is arbitrarily modifiable by the experimenter by changing the concentration of the *aiiA* inducer DHBA. The first order AHL degradation term does not go away. AHL will passively degrade in every environment; we have just added enzymatic degradation on top of that breakdown rate.

Our model of *cap and release* indicates that degradation of every species in the circuit: cell-internal proteins, nucleic acids and cell-external AHL signals, is required to realize the circuit's steady state control function. Cell division and intracellular turnover dilute and degrade all internal cell components like transcription factors/toxins and nucleic acids, but AHL signals are only degraded by either environmental or enzymatic degradation. We simulated the effects of degradation on population capping behavior to understand how both kinds of degradation affect the steady state control performance of the *cap and release* system.

We find that AHL degradation is necessary to allow culture growth at all. When k_A is non-zero, but d_A is zero, AHL signals accumulate to high concentrations and activate *ccdB* expression to an extent that the entire population is killed (Fig. 2.9). Increasing d_A allows the establishment of progressively higher population steady states, as AHL no longer accumulates to infinity. At the same time as it increases population steady states, increasing d_A decreases the population's settling time to steady state,

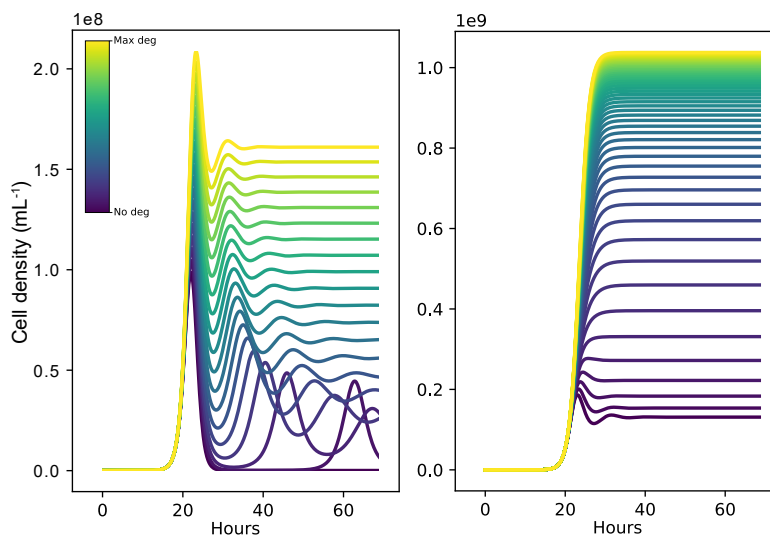


Figure 2.9: Simulating population capping with AHL degradation (LEFT) Simulation of population capping with various rates of passive AHL breakdown, d_a , against k_a of $5 \cdot 10^{-7}$. d_A covers values from 0 to $0.891 \text{ nM} \cdot \text{hr}^{-1}$, the value inferred from data in [52]. (RIGHT) Simulation of population capping subject to various levels of *aiiA* enzyme induction against k_a of $5 \cdot 10^{-7}$; because environmental breakdown is always present, we simulate enzymatic degradation on top of passive environmental breakdown at d_A of $0.891 \text{ nM} \cdot \text{hr}^{-1}$. Settling time is significantly reduced compared to environmental breakdown alone (lowest, purple curve)

demonstrating the trend that faster signal degradation increases population controller speed. Luckily, AHL breakdown will always occur at some rate (meaning d_A is non-zero), but that rate may be too slow in some environments to set population steady states in a reasonable amount of time, necessitating active degradation like we have implemented with *aiiA*. Simulating active enzymatic degradation (increasing d_{ac}) against a background of positive d_A , we see that active enzymatic degradation is able to reduce overshoot and population settling time. AHL degradation trades dynamic range of population capping for controller speed; increasing AHL degradation rate reduces the maximum possible AHL concentration at steady state, setting a lower bound on the population capping performance of the system.

As we can see from the updated model, this new *cap and release* design has many more parameters than the base *pop cap* architecture, each of which will need to be set somewhere in the range of values that allows the circuit to function. To give ourselves the best chance of finding well-performing circuit designs, we chose to build a large pool of circuit variants covering a large amount of parameter space, then screen for improved performance.

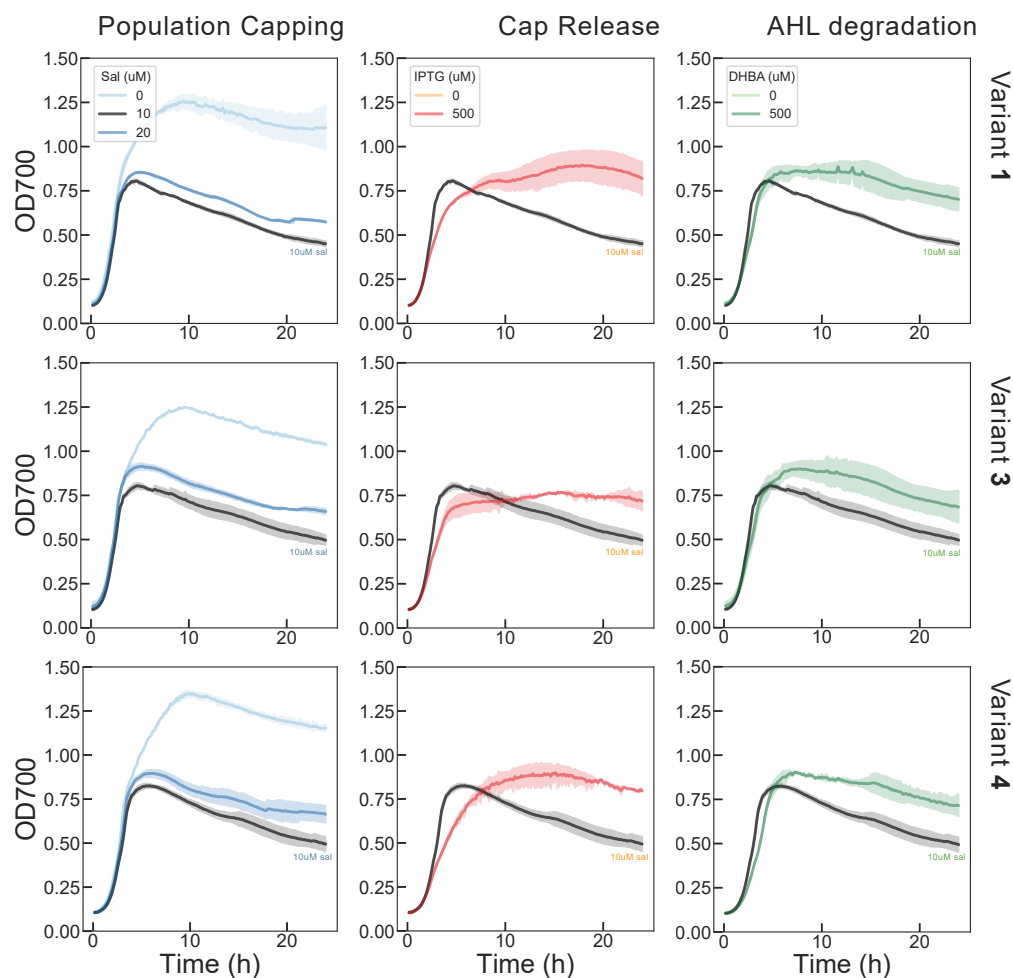


Figure 2.10: Screening *cap* and *release* variants. 3 variants of the *cap* and *release* circuit rebuild exhibiting population capping, cap release and AHL degradation. Curves are the average of 3 replicates, shaded areas represent standard deviation. The maximally capped populations (achieved at 10uM sal in each case) are colored black on each plot to identify density baseline curves that are shared across rows.

The *ccdB* protein is a highly potent toxin and slight overexpression can very easily lead to total population death. As such, the parameter ranges in which this circuit design is actually functional are tight. Previous models and experiments demonstrate that *ccdB* expression rate can be varied to search functional space in this population capping architecture [77]. Using 3G assembly [12], we built the pool of variants with different ribosome binding site (RBS) strengths providing different *ccdB* translation rates to search the widest range of circuit functional space. All other circuit components were designed to be expressed with hardcoded intermediate strength.

Our design goal was a circuit with a large difference in density between capped and uncapped states, the ability to release a population cap, and a density increasing effect

of AHL degradation. We screened the pool of variants by growing each in coarse gradients of population capping inducer, release inducer and degradation inducer (all combinations). Those variants unaffected by the presence of the circuit plasmids (no growth defect at zero inducers) with significant population capping activity, cap release potential and cap interruption by AHL degradation were considered candidate variants for further testing. The screen was conducted in LB medium to optimize this circuit's performance in a more standard bacterial growth medium, rather than the specialized TBK medium used in the original publication of the *pop cap* circuit. The most successful variants demonstrated all three of these behaviors in standard LB medium with significantly increased dynamic range compared to our previous circuit builds (Fig. 2.10).

Each of the tested variants performed very similarly in the screen. Population capping by all three variants (Fig. 2.10, LEFT column) was much more significant than previously demonstrated (capping inducer is now Sal, where it was IPTG before); each variant was capped to an OD700 of ~ 0.5 ($\leq 50\%$ of uncapped density) at 10 μM Sal. Increasing Sal concentration beyond 10 μM does not decrease population cap, instead it appears to cap the populations slightly less strongly. These capped populations also slowly decrease in density after their growth stops at around 5 hours into the experiment. Because maximum population capping was produced by 10 μM Sal, this curve is set as the baseline for visualizing the effects of cap release and AHL degradation (Fig. 2.10, MIDDLE and RIGHT columns).

When *ccdA*-mediated cap release was induced (this time with IPTG), variants 1 and 4 were released most significantly from their caps (Fig. 2.10, MIDDLE column). Cap release also appeared to ameliorate the progressive decline in population density after the arrest of growth at 5 hours. AHL degradation also had the expected steady state density increasing effect on capped cultures, again variants 1 and 4 responded more strongly than did variant 3 (Fig. 2.10, RIGHT column). Degradation did not prevent the slow decline in population density after growth arrest at 5 hours. These results suggest that this slow decline in density is a phenomenon mediated by *ccdB*; only in populations with induction of *ccdB* sequestration is this phenomenon absent.

We chose to make more detailed experiments with variant 4 (Fig. 2.11):

1. Test a very fine gradient of degradation inducer concentrations to visualize effects of degradation on population cap.

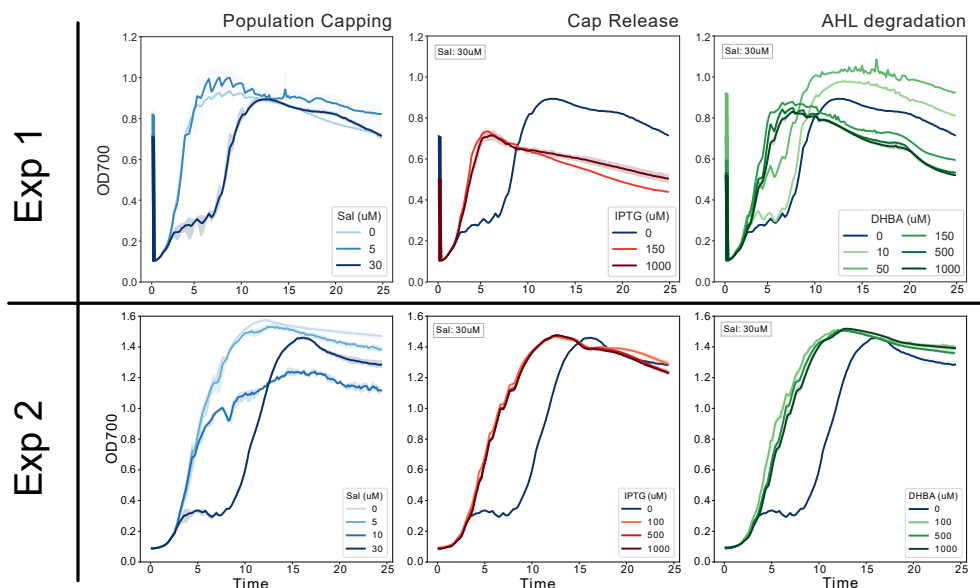


Figure 2.11: Testing *cap* and *release* variant 4 Cultures expressing *Cap* and *release* variant 4 were used in two experiments. The plots presented demonstrate the 3 independent functions of the circuit design, population capping, rescue from capping, and cap interruption with AHL degradation. The curve corresponding to population capping at 30 μ M Sal is colored dark blue in all plots to highlight the baseline from which release and degradation begin.

2. Test finer gradients of *all* component inducers, this time counting CFUs every hour to allow a detailed, dynamic comparison between absorbance-based optical density measurements and viable CFU counts.

Unfortunately, CFU counting for the second experiment is still in progress and the time course comparison between both measurement types is unavailable.

Variant 4's performance differed between each of its experiments (Fig. 2.11). In both experiments with variant 4, 30 μ M Sal produced the most significant population cap, but at 8 hours after the start of *both* experiments, these heavily capped populations exhibited the same cap "escape" behavior previously seen when provoking artificially strong population caps in the base *pop cap* circuit (Fig. 2.3, D-F).

In experiment 1 (Fig. 2.11 TOP), 30 μ M Sal briefly arrested population growth at OD 0.3, but the culture escaped control at 8 hours and grew to match the density of the uncapped population. *ccdA*-mediated release from the 30 μ M Sal cap was incomplete; regardless of *ccdA* induction strength, the population was released to an intermediate density below the uncapped culture's density. AHL degradation produced a variety of different phenotypes: with zero or little degradation against 30 μ M Sal capping, populations were still arrested at low density, then escaped to

high density. With stronger degradation against the 30 μ M Sal cap, populations grew to stable densities below uncapped density; even strong degradation did not allow the cultures to grow to uncapped culture density.

In experiment 2 (Fig. 2.11 BOTTOM), population capping was similar to experiment 1: 30 μ M Sal strongly capped population density, but the culture escaped control after 8 hours. However, in this experiment, only *complete* cap release was observed with increasing induction of *ccdA* and AHL degradation. With any induction of *ccdA* or AHL degradation, the growth arrest produced by 30 μ M Sal was completely ameliorated and the cultures grew as if uncapped.

These two experiments complicate our understanding of *cap and release* circuit function. Before rebuilding the circuit in the form presented in Fig. 2.8, population capping and cap release were reliably produced with their associated inducers, but the effects on population density were small (caps to 75% of uncapped density as measured by OD600, to 30-50% uncapped density as measured by viable cell counts). After building *cap and release* with AHL degradation and screening variants for cap, release and degradation functions, the effects of each function on population density are much more dramatic, but also variable between experiments.

These data demand further experimentation with *cap and release* to test a few hypotheses:

- **Stronger population capping decreases the evolutionary stability of circuit function:**

In experiments 1 and 2, strong population capping arrests growth at a dramatically low density, even when measured using OD700, which overestimates viable cell counts. This growth arrest does not produce a stable population cap; these arrested cultures eventually begin growing again to meet the density of uninduced populations. Less significant inductions of population capping do not demonstrate this "escape" behavior (Fig. 2.10). It is possible that by increasing the population capping power of *cap and release*, we have reached a limit of function at which the growth burden imposed by population capping is so significant that mutants inactivating the circuit are quickly selected and dominate the population. This possible failure mode is not new to synthetic biologists or circuit architectures of this type [64]. Metagenome sequencing of the *cap and release* plasmids in "escaped"

cultures will reveal whether mutation of circuit components is responsible for this phenomenon.

- **Experimental setup alters circuit function:**

The road to performing the variant screen and Experiments 1 and 2 is paved with *cap and release* experiments that failed to demonstrate any kind of population control. The difference between those "failures" and the screen/Experiments 1 and 2 lies in the preparation of the cells for experimentation. We find that cells simultaneously transformed with the *cal* and *pLuxARLccdB* plasmids—a standard co-transformation—never exhibit population control in experiments. Cells sequentially transformed with *cal* plasmid, then *pLuxARLccdB* are more likely to exhibit *cap and release* functions. However, even sequentially transformed cells seem to lose circuit function after extended outgrowth for experimentation. The standard overnight outgrowth before an experiment nearly always renders a *cap and release* cell line incapable of population control.

In the variant screen and Experiments 1 and 2, the cell lines are freshly sequentially transformed with *cal*, then *pLuxARLccdB* plasmids. To avoid overnight culture, these transformants are inoculated into outgrowth medium, then grown only until they reach OD600 ~0.3, then immediately aliquoted into an experiment.

This process minimizes two things: unprotected exposure of cells to ccdB and time under circuit burden. The *cal* plasmid contains the ccdA antitoxin and is expected to "leak" a small amount of ccdA protein even without induction of its expression. Transforming cells with this plasmid first creates an intracellular environment in which normally lethal "leak" of ccdB from the *pLuxARLccdB* plasmid is sequestered by ccdA, allowing cells harboring both plasmids to grow and participate in experiments.

As a population control circuit actuated by a lethal toxin, *cap and release* is designed to impose an extreme burden on cells. The longer this burdensome circuit remains in a cell, the more likely it is to acquire an inactivating mutation. If this mutation inactivates ccdB expression, that mutant is very likely to survive and dominate the population, especially during an experiment during which *non*-mutants are induced to cap their own growth. Overnight growth before an experiment provides a long growth period during which mutations can accumulate and prevent circuit function in a later experiment. Short outgrowth before an experiment hopes to minimize

the possibility of mutating our circuit before it is tested. Experiments comparing outgrowth time to population control function may help us measure how long it takes for inactivating mutations to appear.

It will be critical to continue testing *cap and release* cell lines created and prepared for experimentation with identical procedures to determine how much circuit variability is simply due to stochasticity in circuit function, and how much is due to variation in experiment preparation.

2.3 Discussion

Expanding on the 2004 *pop cap* genetic circuit that imposes a density cap on a population of bacteria using AHL signal feedback and *ccdB* toxin expression, we designed and built the *cap and release* circuit, which adds new population control functions to allow complex population density control and scaling to more complex heterogeneous controlled communities. With its multiple inputs and bidirectional actuators on population density, the *cap and release* circuit can serve as a basic motif for designing more complex multi-strain genetic circuits. One such circuit is the $A=B$ circuit, discussed in the following chapter of this thesis.

In the process of building the *cap and release* circuit, we created modular genetic parts for the *ccdB*, *ccdA* and *aiiA* proteins (available along with all the other parts of this circuit in Addgene Kit 1000000161 "CIDAR MoClo Extension, Volume I").

Two major directions remain to be explored in validating this circuit design. First, the *aiiA* protein is shown to degrade AHL effectively in this circuit, which is predicted to decrease its recovery time after perturbation. Experiments need to be done to verify this model prediction. All presented experiments in this work allow circuit-containing communities to grow to steady state density in a single growth phase without dilution or addition of additional cells. Making this perturbations to a steady system and tracking its recovery by counting viable colonies will be critical to validate *aiiA* as an improvement to the original *pop cap* circuit design.

Secondly, The original population capping circuit was designed to function by exploiting variability in circuit component expression among population members. The authors used *lacZ*-tagged *ccdB* to measure bulk circuit output in the population, but did not measure the *distribution* of *lacZ*-*ccdB* expression among single cells in the population. Where a simple differential equation model of population capping allows a continuous relationship between *ccdB* toxin expression and aggregate population death rate, the reality of this circuit is much noisier and more discrete. Each

individual cell will produce different amounts of *ccdB* toxin in response to Lux AHL due to noisy expression of all its circuit components. Again stochastically, not every cell will die at an identical intracellular concentration of *ccdB*.

To truly understand how this population capping works, we need to investigate the role of noise in circuit function. To learn about the related distributions of *ccdB* expression and cell viability, we have tagged *ccdB* with GFP and plan to use flow cytometry to measure the distribution of GFP-*ccdB* fluorescence along with the distribution of a live/dead cell dye (like the Invitrogen LIVE/DEAD BacLight dye). We suspect that the live cells counted in CFU assays are those on the low end of GFP-*ccdB* expression. These results will clarify the exact mechanisms underlying population capping in this genetic circuit. Stochastic, population level simulation software developed in our laboratory also allows us to model this mechanism and compare data to predictions to assess the validity of our hypothesis [78].

2.4 Materials and Methods

E. coli cell strains

DH5 α Z1 *E. coli* were used to create the *pop cap* strain used in this work. DH5 α Z1 *E. coli* were also used to create the *cap and release* strain containing (*ccdA/ccdB*) toxin sequestration; strain CY027 [79] was used to create the *cap and release* strain containing RNA-level *ccdB* sequestration. Both strains have genome integrations expressing the necessary activator/repressor transcription factors to allow regulated expression of circuit components: DH5 α Z1 has genome integrated expression of LacI and TetR; C027 has genome integrated expression of both RhIR and CinR.

The Marionette Wild (*E. coli* MG1655 base) strain [34] was used to create the rebuilt *cap and release* variants (Fig. 2.4). It contains a genome integrated cassette that expresses 12 different transcription factors allowing gene regulation in response to 12 inducers, including those we use in this work (IPTG, Sal, DHBA and Lux AHL).

DB3.1 *ccdB*-resistant *E. coli* were used to amplify and purify *ccdB* containing *pLuxARLccdB* plasmids. These cells contain the mutant *gyrA462* DNA gyrase, rendering them resistant to *ccdB* toxicity. DB3.1 cells were obtained from the Belgian Co-ordinated Collections of Microorganisms, accession number LMBP 4098. DB3.1 was originally sold by Invitrogen, but has been discontinued as a product.

As mentioned in the text, the method of preparing *cap and release* cell lines is specifically designed to minimize loss of circuit function in the resulting cells.

Whenever a strain must be transformed with plasmids containing the *ccdB* toxin and a toxin sequestration mechanism, the base strain should be transformed first with the plasmid containing the toxin sequestration element. This singly transformed cell line should then be prepared for transformation a second time with the *ccdB* containing plasmid. This process avoids exposing cells to leaky *ccdB* expression without protection with a sequestration element.

Plasmids

The *pop cap* circuit is composed of two plasmids: *pLuxRI2*, *plxuCcdB3* (both from [52])

The *cap and release* circuit with *ccdA/ccdB* sequestration contains 3 plasmids: *pLuxRI2*, *plxuCcdB3* (both from [52]), and *pTetCcdA*.

pTetCcdA was constructed by GoldenGate assembly of (promoter-RBS-CDS-terminator):

pTet - B0033m - *ccdB* - B0015 terminator

into a *pSC101* backbone containing carbenicillin resistance. The *ccdB* coding sequence was taken from the *pOSIP_KO* plasmid [80]

The *cap and release* circuit with RNA-level (RNA-IN/RNA-OUT) toxin sequestration contains 3 plasmids: *pRNAINccdB*, *pRNAOUT* and *pRhII*.

pRNAINccdB was constructed by Gibson assembly of (promoter-RBS-CDS-terminator):

pRhI - RNA-IN module [69] - *ccdB* - B0015 terminator

into a *p15a* backbone containing chloramphenicol resistance.

pRNAOUT was constructed by Gibson assembly of

pCin - RNA-OUT

into a *ColE1* backbone containing kanamycin resistance.

pRhII was constructed by Gibson assembly of:

J23106 promoter - B0034 - *lacI* - B0015 terminator;

pLac - B0034 - *rhII* - B0015 terminator

together into a *pSC101* backbone containing carbenicillin resistance.

Rebuilt *cap and release* variant plasmids with *aiiA* degradase were constructed using the following parts, by the 3G assembly method [12]. The specific constructs are

detailed below in the format (promoter - ribosome binding site - CDS - terminator / ...):

cal:

pTac [34] - BCD8 - ccdA - ECK120033736 /

pCauAM [34] - B0032 - aiiA - L3S2P11 /

pSalAM [34] - B0032 - LuxI - B0015

into plasmid with ColE1 origin of replication, kanamycin resistance.

pluxARLccdB:

pLuxAM [34] - ARL (see link below) - ccdB - B0015

(Link: [ARL ribosome binding site library](#))

into a plasmid with pSC101 origin of replication, chloramphenicol resistance

Unless otherwise noted, all parts used in cloning can be found in the Murray Lab Parts Library (Addgene Kit 1000000161 "CIDAR MoClo Extension, Volume I").

Cell Growth Experiments

Cells containing *pop cap* or *cap and release* were grown from a *freshly transformed* colony (see recommendations under "*E. coli* cell strains") in either LB or TBK medium (10g tryptone, 7g KCl per liter, 100mM MOPS buffer) to an OD600 of 0.3 in medium matching the medium used in the experiment.

These low density outgrowths were then diluted 10x into fresh medium with the appropriate antibiotics (carbenicillin (100 μ g/mL), kanamycin (50 μ g/mL) and chloramphenicol (25 μ g/mL)) and aliquoted in triplicate in 500uL into a square 96 well Matriplate (dot Scientific, MGB096-1-1-LG-L) pre-loaded with chemical inducers. Inducers were added to the 96 well Matriplate before cell suspensions were aliquoted. A Labcyte Echo 525 Liquid Handler was used to aliquot inducers, with the exception of DHBA, into each well of the plate before cell suspensions were added. DHBA is dissolved in ethanol, which is not accurately pipetted by the Echo 525; DHBA was input into plates by hand.

The plate was incubated for the duration of the experiment in a Biotek Synergy H2 incubator/plate reader run by the Gen5 software. Temperature was set to 37°C, shake setting was the maximal rate of *linear* shaking.

OD600/OD700 measurements were taken every 10 minutes. If samples were taken for CFU counting, plates were ejected from the plate reader, 10uL of culture was aliquoted into 30uL of 20% glycerol (15% final glycerol concentration); this glycerol suspension was frozen at -80°C for later colony counting.

Cell Density Quantification

Colony forming units were counted using two methods:

Droplet CFU counting: Cell suspensions were diluted 25,000x into fresh TBK media and aliquoted into a Labcyte Echo 384 well source plate. 50nL drops of this suspension were transferred to regions on a Nunc OmniTray (ThermoFisher: 140156) filled with LB agar containing the appropriate antibiotics. The OmniTray was incubated at 37°C overnight, then colonies were counted. The fraction of droplets spotted on the plate that DID NOT grow colonies was fit to a Poisson distribution to determine λ , which yielded the mean cells/mL.

Plate CFU counting: Cell suspensions were diluted between 10 - 10⁶x into fresh LB medium, then 10uL of this suspension was spread on LB agar petri dishes. These plates were incubated at 37°C overnight, then colonies were counted. The number of colonies grown was multiplied by the dilution factor (and the 4x dilution factor that occurred during sampling) to obtain cells/mL.

Modeling and Simulations

The variables in the presented models are as follows:

C: cell density ($\frac{cell}{mL}$)

T: CcdB concentration (nM)

R: Sequestration device concentration (nM)

A: AHL concentration (nM)

Parameters in the model:

k_c : cell growth rate constant (0.897 hr^{-1}) [52]

C_{max} : carrying capacity for cell growth ($1.16 * 10^9 \text{ ml}^{-1}$) [52]

β : cooperativity of AHL effect ($\beta = 2$)

d_c : cell death rate constant by ccdB ($4 * 10^{-3} \text{ nM}^{-1} \cdot \text{hr}^{-1}$) [52]

k : concentration of AHL to half-maximally active promoter (100 nM) [81]

k_{on} : binding rate of ccdB and sequestration device ($3 \text{ nM}^{-1} \cdot \text{hr}^{-1}$)

g_R : basal production rate of sequestration module; modifiable by experimenter ($0 - 10 \text{ uM} \cdot \text{hr}^{-1}$)

k_T : synthesis rate constant of CcdB ($5 \text{ nM} \cdot \text{hr}^{-1}$) [52]

k_A : synthesis rate constant of AHL ($4.8 \times 10^{-7} \text{ nM} \cdot \text{ml} \cdot \text{hr}^{-1}$) [52]

d_A : decay rate constant of AHL ($0.891 \text{ nM} \cdot \text{hr}^{-1}$) [52]

d_T : decay rate constant of ccdB toxin (2 hr^{-1}) [52]

d_{ac} : per cell AHL degradation rate by aiiA (true value unknown, varied in simulations, $\text{mL} \cdot \text{min}^{-1}$)

Parameter estimates were found in multiple literature sources [52, 58]

2.5 Supplementary Material

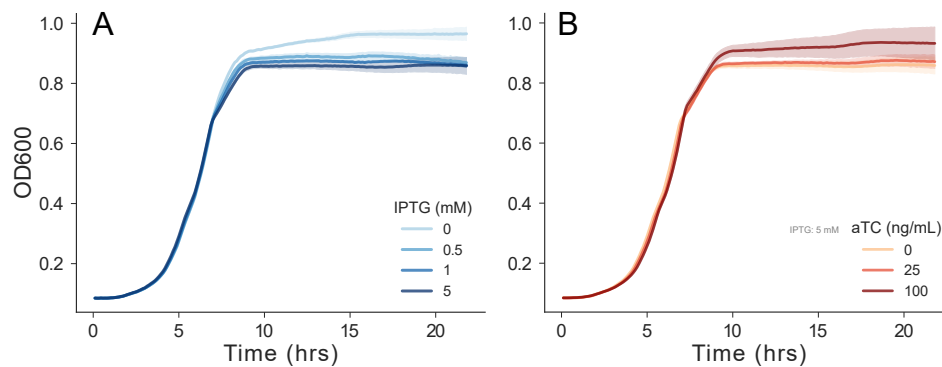


Figure 2.12: Additional testing of *cap* and *release* An additional experiment with *cap* and *release* employing the ccdB/ccdA protein-level sequestration module. At the end of this experiment, samples were taken to measure viable cell counts. Data from this counting is presented in Fig. 2.7

*Chapter 3***COMPOSITION CONTROL IN AN ENGINEERED
MULTI-MEMBER COMMUNITY****3.1 Introduction**

Microbial communities are everywhere and perform critical functions for the health of ecosystems at every scale. When environments change, community species compositions change, but we cannot predict changes or prevent them without greater knowledge of microbial communities and community control technology.

Bioengineers in various fields recognize the importance of microbial community control for different reasons. Genetic circuits in synthetic biology are constrained in their complexity by the burden they impose on cells; increasing the complexity of genetic circuits requires the distribution of circuit burden across a heterogeneous community of microbes [41, 42]. Additionally, genetic circuits operating independently in each cell of a population lose precision due to cell-to-cell variations in the population [43, 44]. Control of community composition and gene expression dynamics are required to create a stable platform for reliable circuit function.

Industrial bioproduction engineers recognize the efficiency and yield gains to be made by distributing production processes across a community of organisms [45, 46]. Systems dividing labor across a community outcompete monoculture only in specific systems optimized for minimal process bottlenecks across the community and ideal productive community composition, necessitating precise, stable control of community composition [47–49].

Ecologists and microbiologists learn more about natural microbial diversity through community control experiments mimicking natural ecologies. Community control deployed in native community environments has the potential to remediate and preserve natural microbial diversity [50, 51].

Acknowledging the growing truth that microbial community composition is integral to important topics like human health and industrial production, synthetic biologists have built circuits to take control of community composition itself.

The processes underlying community composition control are: intercellular signaling communicating population density and composition, information processing to

convert signals into appropriate community control action, and actuation of composition change using regulators of cell growth or death.

Scott *et al* created a two strain community that avoids collapse to a single strain monoculture. Each strain in the community expresses an identically structured, but independent genetic circuit that causes it to go through periodic bursts of growth and lysis. An orthogonal AHL chemical is produced by each strain which induces positive feedback production of more AHL, but also induces expression of the ϕ X174E lysis protein [54]. At a critical concentration of AHL chemical, each strain lyses itself until its density is low and AHL levels decrease. While not implementing a precise form of community composition control, this circuit can prevent the decay of the two-strain coculture to a single strain monoculture over long culture times, even when growth rates or inoculation ratios are greatly mismatched.

Balagaddé *et al* created a circuit producing similar oscillatory growth dynamics, this time linking the member strains together with AHL chemicals, rather than leaving them to grow independently. Their circuit produces the out of phase growth dynamics characteristic of a predator-prey relationship, modeling a natural ecological relationship [58]. The predator strain kills the prey strain by producing an AHL signal that induces expression of *ccdB* toxin in prey, killing them. The prey strain "feeds" the predator strain by producing an orthogonal AHL signal that induces *ccdA* antitoxin in the predator. The predator strain constitutively produces *ccdB*, meaning predator strain growth is always limited by toxin without the prey inducing *ccdA* antitoxin. With the plethora of growth regulatory systems available, there is more than one way to tie predator growth to the prey: an auxotrophic predator strain fed by a metabolite-secreting prey strain could achieve the same goal. This circuit finds new functional space for community control circuits by using a toxin and antitoxin together to both up and downregulate strain growth.

Other circuits maintain cocultures using a genetic circuit only expressed in one strain. Dinh *et al* created a circuit to gradually decrease a strain's growth rate by degrading the early glycolytic enzyme phosphofructokinase A in response to AHL chemical [55]. Grown in coculture with an uncontrolled strain, the circuit-expressing strain will never outcompete its partner strain even if it dominates at inoculation; its growth slows before maximum population density is reached and the partner strain can grow into the community. While this coculture does not have oscillatory dynamics, the coculture composition is not stable. Over time, AHL accumulation will slowly decrease growth rate in the circuit-expressing strain,

eventually the uncontrolled strain will slowly overtake the culture.

Stable community compositions can be achieved using a completely different set of parts. Kerner *et al* created a coculture of auxotrophic *E. coli* whose growth rate and composition can be precisely tuned by the expression of metabolite export proteins [15]. The mutual dependence created by auxotrophy ensures that this community will eventually reach some composition steady state, tunable by the rate of metabolite export from each strain, because each strain requires the presence of the other to survive.

We take a similar mutual dependency approach, but use the *ccdB/ccdA* toxin/antitoxin pair instead. In this circuit, we use our previously reported *cap and release* genetic circuit motif to design a two-member population whose genetic circuit produces population density and composition steady states set by inducer inputs. For its ability to control the composition of the community to a target ratio of A cells to B cells, or $A_{population} = \alpha B_{population}$, we call it the $A=B$ circuit. Like in the *ccdB/ccdA* based synthetic predator prey ecosystem, strain growth in $A=B$ is limited by *ccdB* expression in response to AHL, but in this case, both strains express symmetric circuits that limit their own growth, but rescue the growth limitation of their partner.

Like the cross-feeding circuit published by Kerner *et al*, the $A=B$ design can also be called a "cross-protection mutualism", which has recently been shown to be the best community architecture for establishing stable steady state community composition in two strain communities [82]. The mutual dependence of each strain in our circuit on its partner for protection from toxin expression mimics the metabolic dependence of the strains from Kerner *et al*.

One of the factors limiting the scaling of multi-strain community control circuits to sizes above two strains is the availability of orthogonal signaling molecules. More than two orthogonal AHL signaling systems exist and auxotrophic bacterial strains exist deficient for considerably more orthogonal metabolites. However, signal systems may have significant crosstalk that will limit the design of synthetically controlled communities with membership on the order of native communities

Guided by an analysis of the $A=B$ circuit's sensitivity to its parameters, we detail a screening strategy to search functional parameter space for this genetic circuit. Experimental tests of the circuit as well as models and simulation demonstrate a need for degradation of AHL signals to allow steady state stability and perturbation rejection. By acquiring a genetic part encoding the *aiiA* AHL degradase, we

implement tunable AHL signal degradation and explore its effects on the $A=B$ circuit's performance. Our final implementation of the $A=B$ circuit can successfully regulate the composition of a community, with interesting additional effects on total population density.

3.2 Results

Designing the $A=B$ population control circuit using the *cap and release* motif

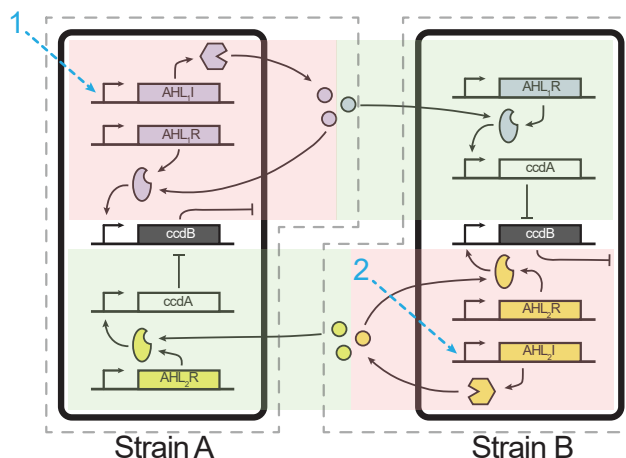


Figure 3.1: The $A=B$ circuit uses a symmetric circuit motif in its two cells to create *cis*-acting negative feedback on each member and *trans*-acting rescues from negative feedback from each member to the other. "1" and "2" indicate genetic components that can be induced by the experimenter using IPTG and salicylate (sal), respectively.

In the $A=B$ circuit, two inducers activate AHL production in each cell, signaling toxin production for each producer and antitoxin production for each partner (Fig.3.1). When AHL production is active, this architecture establishes an interdependence between the two strains where the loss of one strain would lead to the loss of the other due to unchecked toxin production. This interdependence is tunable by the experimenter: changing the level of each inducer pushes the system to new composition steady states (i.e. increasing inducer A produces more AHL_A, reducing the A cell population and increasing B cell population). In the case where both inducers are at maximal levels, the $A=B$ system is an implementation of the "cross-protection mutualism" detailed in Karkaria *et al* [82].

The specific components used in this implementation of $A=B$ are described in Tables 3.1 and 3.2. In general, both strains contain *cap and release* circuit motifs (see Chapter 2). Strain A with negative population feedback driven by the Cin AHL system, release driven by Lux; Strain B with the opposite:

We created an ordinary differential equation model of the $A=B$ system and simulated its composition control function. See Materials and Methods for description of parameters and variables. Subscripts 1 and 2 in the model correspond to the cell strains A and B, respectively.

$$\frac{dC_1}{dt} = k_C \left(1 - \frac{C_1 + C_2}{C_{max}} \right) C_1 - d_c C_1 \frac{T_1}{K_{tox} + T_1} - dC_1 \quad (3.1)$$

$$\frac{dC_2}{dt} = k_C \left(1 - \frac{C_1 + C_2}{C_{max}} \right) C_2 - d_c C_2 \frac{T_2}{K_{tox} + T_2} - dC_2 \quad (3.2)$$

$$\frac{dT_1}{dt} = \beta_{S_1} \left(\frac{S_1^2}{K_{S_1} + S_1^2} \right) + l_{S_1} - k_b A_1 T_1 - d_T T_1 \quad (3.3)$$

$$\frac{dT_2}{dt} = \beta_{S_2} \left(\frac{S_2^2}{K_{S_2} + S_2^2} \right) + l_{S_2} - k_b A_2 T_2 - d_T T_2 \quad (3.4)$$

$$\frac{dA_1}{dt} = \beta_{S_2} \left(\frac{S_2^2}{K_{S_2} + S_2^2} \right) + l_{S_2} - k_b A_1 T_1 - d_T A_1 \quad (3.5)$$

$$\frac{dA_2}{dt} = \beta_{S_1} \left(\frac{S_1^2}{K_{S_1} + S_1^2} \right) + l_{S_1} - k_b A_2 T_2 - d_T A_2 \quad (3.6)$$

$$\frac{dS_1}{dt} = \beta_{Iac} \left(\frac{I^2}{K_{Iac} + I^2} \right) C_1 + l_{Iac} C_1 - d_S S_1 \quad (3.7)$$

$$\frac{dS_2}{dt} = \beta_{sal} \left(\frac{Sal^2}{K_{sal} + Sal^2} \right) C_2 + l_{sal} C_2 - d_S S_2 \quad (3.8)$$

Where C_x (mL^{-1}) represents the cell density of each strain in the population, T_x (nM) represents the average intracellular concentration of ccdB toxin in each strain, A_x (nM) represents the average intracellular concentration of ccdA antitoxin in each strain, and S_x (nM) represents the environmental concentration of each AHL signal (assumed to be equal inside and outside of cells due to free diffusion through cell membranes).

In eqs. 3.1 and 3.2 we model each strain's growth using a logistic model that compares the sum total population density with C_{max} to determine growth rate. Gene expression is never completely "off" when repressed or *not* activated, so in eqs. 3.3 - 3.8 we have included l_x terms to represent leaky expression of proteins (or the leaky synthesis of AHL signals caused by leaky synthase expression in the case of S_1 and S_2). To determine the value of each l_x parameter, we divide the corresponding β_x maximum production rate (describes the maximum production

rate of an inducible promoter) by the reported fold change of that promoter (all values sourced from [34]). All inducer molecule - transcription factor binding events are modeled with Hill equations. We also use a Hill equation to describe the increase in death rate with increasing toxin concentrations. Toxicity is not always modeled this way; sometimes death rate is assumed to be directly proportional to toxin concentration. Both are simplifying assumptions, the biophysical nature of toxicity is different for every toxin; more complicated models may attempt to capture this intricacy.

Table 3.1: Strain A components

<i>Strain A</i>		
Name	Role	Description
CinI	AHL ₁ synthase	An enzyme that synthesizes Cin-type AHL chemicals (3-hydroxy-C14-homoserine lactone, 3-OH-C14-HSL) from S-adenosylmethionine (SAM) (amino donor) and an appropriate acyl–acyl carrier protein (acyl-ACP) (acyl donor). CinI is originally found in <i>Rhizobium etli</i> as part of the Cin AHL system, controlling nitrogen fixation and swarming motility [28, 83]. Cin AHL chemicals can freely diffuse through bacterial membranes, meaning their concentration in a mixed culture environment is equal both inside and outside cells.
CinR	AHL ₁ TF	A transcription factor that binds Cin AHL molecules, dimerizes, then binds as a dimer-AHL complex to the pCin promoter, <i>activating</i> transcription of downstream genes. In Strain A, it activates transcription of ccdB.
LuxR	AHL ₂ TF	A transcription factor that binds Lux AHL molecules, dimerizes, then binds as a dimer-AHL complex to the pLux promoter, <i>activating</i> transcription of downstream genes. In Strain A, it activates transcription of ccdA.
ccdB	toxin	A small 101 amino acid toxin protein expressed natively from the <i>E. coli</i> F plasmid <i>ccd</i> operon. ccdB covalently traps DNA gyrase in an unstable DNA strand-cleaved conformation [60, 61]. Stuck in this state during replication, the genome fragments and the cell dies.
ccdA	antitoxin	When present together with ccdB, ccdA binds ccdB with picomolar affinity [67], sequestering it and blocking its toxic activity. ccdA can bind and inactivate both free ccdB <i>and</i> ccdB already complexed with DNA gyrase; ccdA reverses ccdB/gyrase binding and restores gyrase to normal function.

To visualize the tunable composition control function of $A=B$, we can simulate two types of "virtual experiment". One simulates the growth of $A=B$ cocultures in identical inducer conditions, each starting from a different initial composition; the other simulates coculture growth in varying inducer conditions, starting from

Table 3.2: Strain B components

<i>Strain B</i> - AHL synthase and TFs regulating <i>ccdB</i> and <i>ccdA</i> swapped from Strain A		
Name	Role	Description
LuxI	AHL ₂ synthase	An enzyme that synthesizes Lux-type AHL chemicals (3-oxohexanoyl-homoserine lactone, 3-O-C6-HSL) from S-adenosylmethionine (SAM) (amino donor) and an appropriate acyl–acyl carrier protein (acyl-ACP) (acyl donor) [59]. Lux AHL chemicals can freely diffuse through bacterial membranes, meaning their concentration in a mixed culture environment is equal both inside and outside cells.
CinR	AHL ₁ TF	In Strain B, it activates transcription of <i>ccdA</i> .
LuxR	AHL ₂ TF	In Strain B, it activates transcription of <i>ccdB</i> .

identical initial compositions. These simulations mimic two possible experiments that can be run to test the functions of $A=B$.

In the first simulated experiment (varying initial composition against constant inducer concentrations), we predict the ability of the system to drive cocultures from their initial compositions to the steady state composition encoded in the inducer concentrations. A perfect $A=B$ controller will drive all cocultures to the same final composition, regardless of initial composition.

In the second simulated experiment (constant initial composition with varying inducer concentrations), we predict the range of different composition steady states accessible to the controller, set by the unique combination of inducer concentrations. Ideally, the whole range of steady state compositions from 100% A cells to 0% A cells can be driven by this controller.

AHL signals communicate strain density information around the community and are also the only circuit components not contained inside cells. This means they are not diluted into daughter cells during division and—without components to do so—are not degraded by cellular machinery. Only their passive breakdown in the environment reduces their concentration over time. In each of these simulated experiments we will also explore the role of active cell-mediated AHL signal degradation. In the laboratory, we can implement such degradation using the *aiiA* degradase enzyme, whose expression can be induced in each cell. Without enzymatic AHL degradation, AHLs are assumed to passively degrade in the environment with rate d_S as in eqs. 3.7 and 3.8. To model enzymatic AHL degradation induced in each cell in the system, eqs. 3.7 and 3.8 become 3.9 and 3.10 listed below.

$$\frac{dS_1}{dt} = \beta_{tac} \left(\frac{I^2}{K_{tac} + I^2} \right) C_1 + l_{tac} C_1 - d_{sc} S_1 (C_1 + C_2) - d_S S_1 \quad (3.9)$$

$$\frac{dS_2}{dt} = \beta_{sal} \left(\frac{Sal^2}{K_{sal} + Sal^2} \right) C_2 + l_{sal} C_2 - d_{sc} S_1 (C_1 + C_2) - d_S S_2 \quad (3.10)$$

Where d_{sc} is the per cell AHL degradation rate mediated by *aiiA* enzyme. This value is arbitrarily set by the experimenter by changing the concentration of *aiiA* inducer. The true AHL degradation rate effected by each *aiiA* enzyme is not known, so we make do in simulation by scanning across many values for d_{sc} to observe its effects on the system.

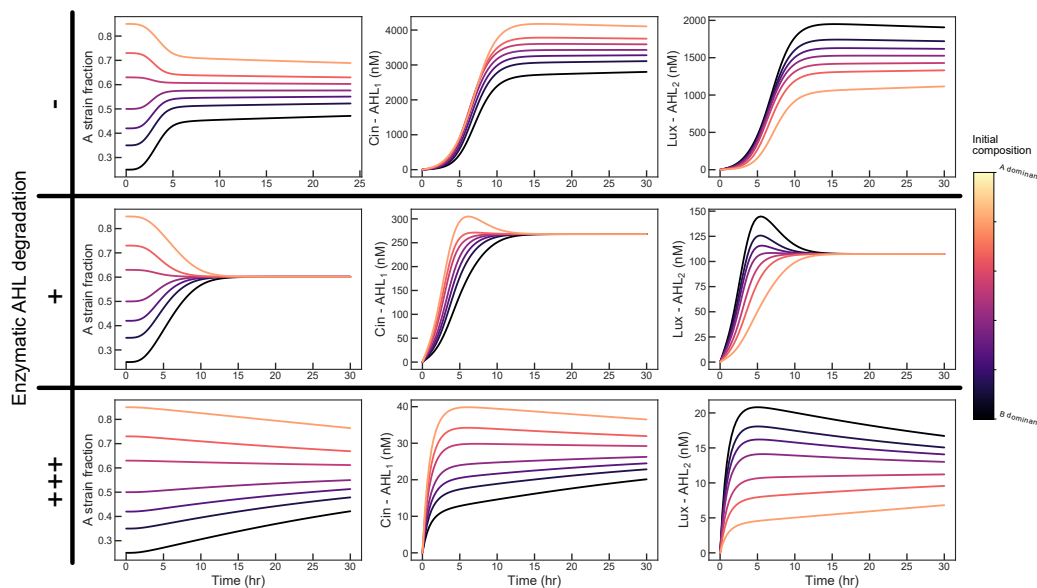


Figure 3.2: $A=B$ sim experiment 1: varying initial compositions The $A=B$ system was simulated starting at compositions varying from A strain dominated to B strain dominated. Per cell enzymatic AHL degradation was either OFF (TOP) or ON (MID) or ON+++ (BOTTOM) to observe the performance effects of increased AHL degradation.

Simulating $A=B$ cocultures starting at varying initial compositions reveals the importance of AHL degradation to composition control performance (Fig. 3.2). Without enzymatic degradation (Fig. 3.2 TOP), the circuit begins to drive the cocultures to a steady state composition, but abruptly loses power, thereafter only very slowly bringing composition under control (steady state achieved at >400 hours). This loss of control performance precludes the establishment of a composition steady state in a realistic experiment (duration on order~days).

Both strains are induced to produce AHL strongly, in theory broadcasting the information necessary for composition control, but perhaps doing so too strongly. While a basal level of passive AHL breakdown is included in the model, it is not sufficient to stabilize AHL concentrations at useful levels against this strong production. Modeling passive AHL breakdown alone, both AHL signals accumulate to concentrations $\sim 10\text{-}20\times$ greater than their binding constants ($K_{S1} = 250nM$ and $K_{S2} = 100nM$ [34, 81]). These concentrations are well into saturating ranges in which changes in AHL concentration do not produce significant changes in gene expression from their associated promoters. As the coculture is growing and AHL signals are accumulating through concentrations near to their binding constants (hours 0-5), the circuit makes an incomplete attempt to drive each coculture to a steady state composition. As the AHLs saturate, the expression rate of actuators *ccdB* and *ccdA* reach their maxima, nearly balancing each other, inhibiting the ability of the circuit to push the cocultures to a steady state composition.

We simulate the enzymatic degradation of AHL in each cell by setting the per cell AHL degradation rate, d_{sc} , to a rate $\sim 100\times$ less than AHL production (Fig. 3.2 TOP). Now, the circuit is able to prevent AHL accumulation, quickly producing steady state AHL levels very close to their binding constants in all cocultures. In these concentration ranges, even the small differences in AHL concentration produced by each coculture are sufficient to functionally alter *ccdB* and *ccdA* expression to achieve a composition steady state.

We simulate extremely strong degradation of AHL by setting d_{sc} $10\times$ higher, and find that *overdegradation* of AHL is possible. At this rate of degradation, AHL signals begin to stabilize at concentrations $\sim 10\times$ lower than their binding constants. At these concentrations, *ccdB* and *ccdA* are not meaningfully activated and the circuit again has unreasonably slow control performance.

It is clearly important that we include the *aiiA* degradase in our laboratory implementation of $A=B$ to control AHL accumulation and coculture composition.

In our second simulated experiment, we start each $A=B$ coculture at the same composition (50% A strain, 50% B strain) and vary the inducer concentrations that direct AHL production from each strain. Intuitively, relatively strong production of AHL from one strain should push the coculture towards a composition dominated by the relatively weakly producing strain. We will again explore the effect of enzymatic AHL degradation.

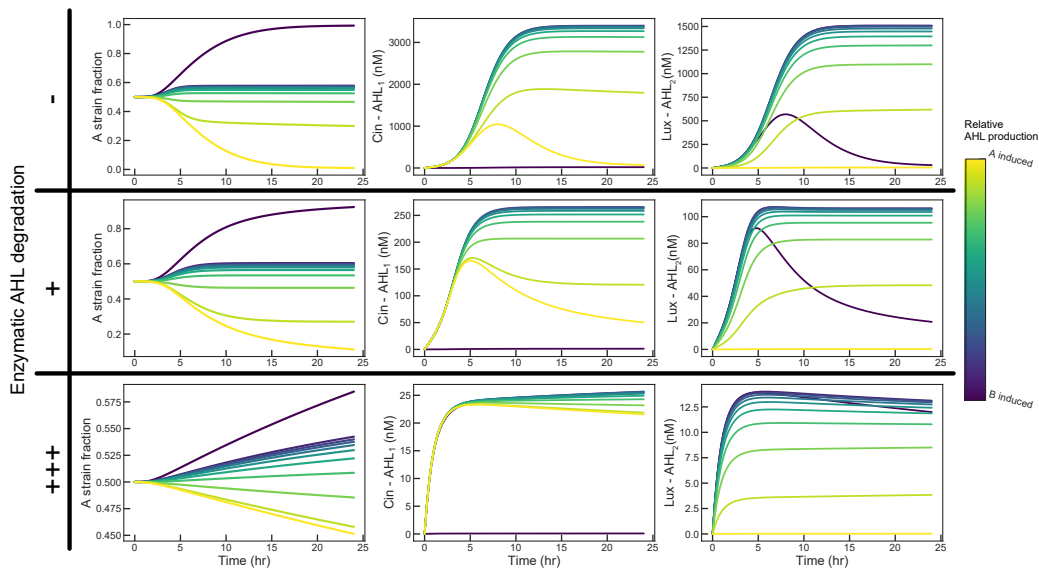


Figure 3.3: $A=B$ sim experiment 2: varying AHL production from each strain The $A=B$ system was simulated starting at a 1:1 strain composition with varying AHL production from each strain. Darker shades represent relatively more AHL production from strain B, lighter shades relatively more from strain A. Per cell enzymatic AHL degradation was either OFF (TOP) or ON (MID) or ON+++ (BOTTOM) to observe the performance effects of increased AHL degradation.

Even without enzymatic AHL degradation (Fig. 3.3 TOP), varying relative AHL production from each strain is capable of setting a variety of different composition steady states that are achieved in a reasonable amount of time. As we expect, progressively stronger AHL production from the A strain (lighter shades) pushes the coculture to a composition dominated by the B strain, and vice versa.

In the extreme cases of AHL production from only one strain (A (bright yellow) or B (dark purple)) the producing strain generates the only AHL in the system and kills itself until it drops out of the coculture. As it drops out, its AHL production wanes until the coculture becomes a monoculture and no AHL is produced at all (Fig. 3.3 TOP - center and right). When AHL production from each strain is approximately equal, balanced coculture compositions are produced.

Without enzymatic degradation, AHLs still accumulate to saturating concentrations by the end of the experiment. As the cocultures are growing, however, AHLs accumulate through concentrations near their binding constants and any imbalance in their accumulation rates still pushes the cocultures to different composition steady states.

With increasing AHL degradation by each cell (Fig. 3.3 MID and BOTTOM),

the same levels of AHL production produce more extreme compositions that are achieved more slowly. These simulations predict that AHL degradation will not affect the range of composition steady states available to the circuit, but will affect the composition produced at a given level of AHL production from each cell. There is still a risk of overdegrading AHL; too much AHL degradation dramatically slows the establishment of different compositions.

These two simulated experiments are models of experiments we can perform in the laboratory to learn whether a real implementation of $A=B$ is functional.

Building the $A=B$ circuit

The $A=B$ circuit is actuated by the *ccdB* toxin, produced by each strain in response to its AHL signal, and sequestered by *ccdA* produced in response to the partner strain's AHL signal. The *ccdB* protein is a highly potent toxin and slight mis-expression can easily lead to total death of one strain (if *ccdB* is too strongly expressed) or the inability to cap a strain's growth at all (if *ccdB* is expressed too weakly). Most parameters in the circuit have a downstream effect on *ccdB* expression, so parameter ranges in which this circuit design is

actually a functional controller are tight. Parameter sensitivity analysis [84, 85] performed with independent models of each cell strain reveals that the steady state density of each strain is sensitive to a few of the parameters in the model: $l_{S_{ccdA}}$ (l_{S_2} in strain A, l_{S_1} in strain B), basal leakiness of *ccdA* expression; $\beta_{S_{ccdB}}$ (β_{S_1} in strain A, β_{S_2} in strain B), maximal *ccdB* expression rate; k_C , cell growth rate; d_C , death rate constant for *ccdB* (*ccdB* potency); d , basal cell death rate (Fig. 3.4). Of all these parameters, only $\beta_{S_{ccdB}}$ (in model as β_{S_1} or β_{S_2}) is modifiable by we the experimenters; the others are constants inherent to the promoters, proteins and cells used.

Thus, to create the functional circuit in the laboratory we chose to screen circuit variants with different ribosome binding site (RBS) strengths driving *ccdB* translation to

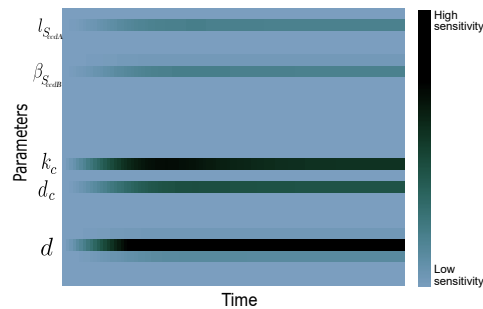


Figure 3.4: Sensitivity analysis of $A=B$ strains reveals the steady state density of each cell strain is sensitive to a few model parameters. Sensitivity analysis performed by the methods described in [84, 85].

search the widest range of circuit functional space. Different RBS sequences change the rate at which *ccdB* mRNA is translated into protein, modifying the maximum rates of *ccdB* expression, β_{S_1} and β_{S_2} .

We used 3G assembly [12] to first assemble plasmids A1 and B1 (Fig. 3.5). These plasmids contain all the invariant parts of each strain’s circuit motif (AHL synthase, *ccdA*). These plasmids were transformed into Marionette Wild *E. coli* [34] to generate the basic chassis of the A and B strains. Note that this circuit assembly process *does not* include the *aiiA* AHL degradase. The resulting cells are not capable of enzymatic AHL degradation.

3G assembly was again used to create sets of A2 and B2 plasmids by assembling a pool of RBS sequences between each plasmid’s AHL inducible promoter and the *ccdB* gene. This process should generate sets of A2 and B2 plasmids with each unique RBS from the pool represented in the set. These plasmid sets were transformed into *ccdB* resistant DB 3.1 *E. coli* to generate single colonies, each containing a unique A2 or B2 plasmid that could be amplified and isolated. A subset of these plasmids were purified and sequenced for use in experimentation. We purified four A2 and B2 plasmids each, then transformed the A1 and B1-containing chassis cells with each of the appropriate 4 A2 or B2 plasmids, generating 4 strain variants each (Fig. 3.5). Their number is drawn from their variant number and clone number (e.g. B42 indicates is was the 2nd clone of the 4th B2 plasmid transformed into B1 containing cells). Strain A is labeled by CFP expression from plasmid A2, strain B is labeled with YFP on plasmid B2.

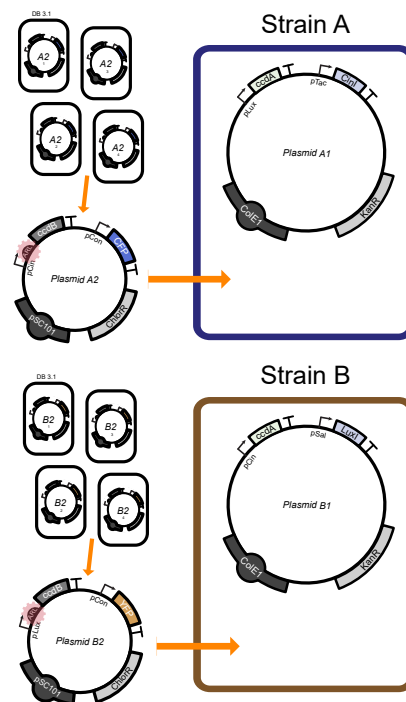


Figure 3.5: Method of generating A and B cell variants

Screening of the different *ccdB* expressing variants of each cell strain had 2 selection phases, a negative selection against variants overexpressing *ccdB* with an overpowered RBS and a functional screen for appropriate community behavior in a simple experiment observing coculture behavior with the circuit “ON”

(both strain inducers (IPTG, Sal) at maximal induction) and “OFF” (no inducers present).

The first phase is complete when viable A and B strain colonies appear after transformation with the A2 and B2 plasmids. Those that grow do not leak *ccdB* expression at a rate that is lethal to cells. In phase two, surviving A and B strain variants are mixed together and grown in both "ON" (1 mM IPTG, 30 μ M sal) and "OFF" (0 IPTG, 0 sal) inducer conditions to check each community's response to maximal AHL production and zero AHL production. Communities that collapse to monoculture in either induction condition were passed over as candidates for further testing.

We know from the coculture of non-circuit-containing control bacteria that a coculture growing without any genetic circuit-based population control will maintain its initial composition over a growth phase (Fig. 3.10). We know from simulation that approximately equal AHL production from each strain in coculture should lead to the establishment of mixed composition at steady state, not a monoculture. Thus, our screen seeks to identify cocultures made of A and B cell variants that express *ccdB* at rates that will produce mixed compositions with full induction of A and B cell AHL production.

A note about the Marionette cell line used to generate the A and B strain variants: It contains a genome integrated cassette expressing 12 transcription factors whose responses to their inducers are completely characterized. From the data presented

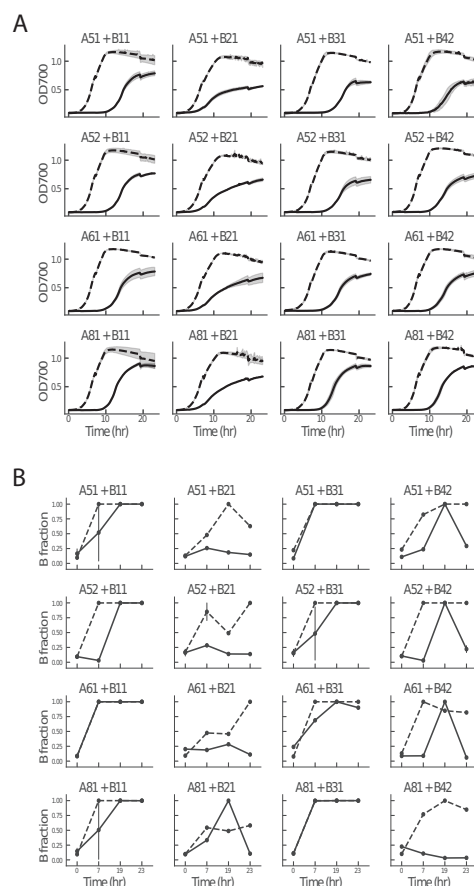


Figure 3.6: A=B screening results Mixtures of variants of each cell type scan parameter space, demonstrating that total density control is much more robust to parameter changes than composition control. Induced mixtures of cells are drawn as solid lines, uninduced mixtures are dashed. (A) Total community density measured by OD700 (B) Calculation of B strain fraction in the community from flow cytometry.

in the supplement of Meyer *et al.* [34], we knew what concentrations of IPTG and sal to use to achieve maximal circuit induction (1 mM IPTG, 30 μ M sal).

During community growth, total density was measured as OD700 in an incubator/plate reader. At four time points, samples were taken from each community, and analyzed with a flow cytometer. To separate bacteria from noise and dust in the flow cytometer, we stained each culture sample with ThermoFisher Syto 62 dye (catalog # S11344), which diffuses into cells (both live and dead) and stains nucleic acids with red fluorescence. Only the cytometry events with strong red fluorescence were passed through for determining community composition. Strain A's CFP expression was weak, providing little resolution between CFP⁺ A cells and CFP⁻ B cells. Instead we made our community composition analysis using the YFP channel, assuming YFP⁺ cells were B cells and YFP⁻ cells were A cells. A Gaussian mixture model was fit to the YFP channel cytometry data and used to assign events to either the narrow YFP⁻ or wide YFP⁺ peaks. See Materials and Methods for a detailed description of cytometry gating strategies, data analysis and community composition computation.

Composition control was variable across the screened co-cultures (Fig. 3.6 B). Cocultures containing B11 and B31 did not appear to achieve different compositions in different inducer conditions, rather they nearly immediately collapsed to A cell monocultures in both inducer conditions. Cocultures containing B21 and B42 maintained mixed compositions that performed similarly in response to inducers, regardless of A strain variant. In general, the B strain variant seemed to determine the behavior of the coculture. Cocultures of interest included all those with variants B21 and B42. The strain variants in these cocultures were considered candidate functional strains and saved for more detailed testing.

Interestingly, where neither of our two simulated experiments predicted significant alterations in steady state population density due to circuit action (Fig. 3.11), a population density control phenotype was observed in all cocultures tested (Fig. 3.6 A). Every induced coculture's density was capped to 75-50% of its uninduced final density; again, the B strain seemed to determine the specific population capping dynamics observed. These results suggests that *ccdB* expression is outstripping *ccdA* expression when AHLs are produced in these cocultures.

Altogether the screening method we used was not as predictive or helpful as expected. The low time resolution and poor separation of CFP⁺ and CFP⁻ A cells may have limited our ability to detect interesting composition control behaviors. The results

presented in the next section did not match the data generated in our screen. It is possible that the strains chosen for testing were simply lucky picks from the screening process or that the flow cytometry screen did not return accurate results.

Testing the $A=B$ circuit—varying AHL production

With our saved strains, we hoped to demonstrate *tunable* population density and composition steady states by testing intermediate inducer concentrations between the binary "ON" and "OFF" used in the screening process. This experiment is a version of simulated experiment 2 in which we varied AHL production from each strain. We expect induction of AHL production from each strain to effect changes from the initial composition (Fig. 3.3). The effect is predicted to be observable even though these strains lack the ability to enzymatically degrade AHL.

We mixed the indicated cell strains together 1:1, then grew them in a set of 4 inducer conditions over which both inducer concentrations increased together. The cultures were grown for 18 hours, then diluted 1:10 in identical inducer concentrations to observe whether the initial steady states are maintained through another growth cycle. Every 10 minutes, we measured OD700, YFP and CFP in each culture. At 5 time points throughout the experiment, we also took samples of each coculture to determine viable cell counts (Fig. 3.7 A-B, *Right*)

We concurrently grew various control cultures to help estimate coculture composition from CFP and YFP fluorescence values. The control cultures were simply monocultures of each strain tested—monoculture A61, monoculture B21, monoculture B42—grown from the same starting density as the mixtures in the same inducer concentrations. For these control monocultures, fluorescence was divided by OD700 at every time point to create a reference fluorescence/OD value that indicated how many fluorescence units to expect per OD unit for a culture composed entirely of CFP⁺ B42 cells or YFP⁺ A61 cells etc. Fluorescence/OD units were computed for each experimental coculture and compared to the same units from the control monocultures to estimate what fraction of that coculture was one cell strain or the other. The method is not completely precise, but provides very highly time resolve estimates of coculture composition. This method does not *directly* measure coculture composition, instead it computes two separate estimates of strain A/B population fraction by comparing coculture fluorescent output to the output from two independent A or B strain monocultures. This is why both blue (A strain) and yellow (B strain) population fraction estimates are plotted in (Fig. 3.7 B *Left*),

because the estimate of A strain population fraction does not imply B strain fraction and vice versa. Because cocultures are composed of *only* blue - A or yellow - B cells and viable cell counting directly visualizes and quantifies both strains, A cell fraction implies B cell fraction ($1 - A_{frac}$). As a result, only A fraction is displayed for clarity.

Where AHL degradation is not required for setting different composition steady states by varying AHL production from each strain, AHL degradation is required for rejecting perturbations to composition steady states (Fig. 3.12). The dilution of the tested cocultures does not explicitly perturb composition, but does perturb population density. Because the strains in these cocultures cannot degrade AHL, we do not expect them to reject any perturbations to composition produced by dilution.

Population density of both cocultures was capped at or below OD700 1.0 during the first 18 hour growth phase in all inducer conditions (Fig. 3.7 A *Left*). The lowest inducer concentrations (IPTG 100 μ M, Sal 5 μ M) produced the strongest cap on steady state density, where the densities produced by the other induction conditions were not distinguishable from that of the uninduced condition. This trend was common to both cocultures. In the second growth phase after the 1:10 dilution, density control appeared to be lost; both cocultures grew past their initial density caps to the carrying capacity of the vessel (OD700 1.4).

Viable cell counts revealed different total population density dynamics between the two cocultures ((Fig. 3.7 A *Right*) and Table 3.3). In the first growth phase, A61+B21 grew to densities on order 10^6 cells/mL, the uninduced coculture reached a density $\sim 2x$ greater than the induced cocultures. In the second growth phase, A61+B21 in each inducer condition reached a density $\sim 10x$ greater than its first phase steady state—density control was lost. Where OD700 did not detect significant differences in total population density at the end of the second growth phase in A61+B21, in any of the inducer conditions, viable cell counts revealed significant continuing effects of inducer on total population density. Generally, increasing inducer concentrations produced lower total density.

A61+B42 responded very differently after dilution. In the first growth phase, A61+B42 grew to densities on order 10^6 cells/mL without large differences between inducer conditions. However, at the end of the second growth phase, induced A61+B42 did not exceed its first phase density steady states to the great degree A61+B21 did. Uninduced A61+B42 grew past its first phase density by $\sim 50x$, but the induced cocultures grew to densities within 1-3x their first phase densities—

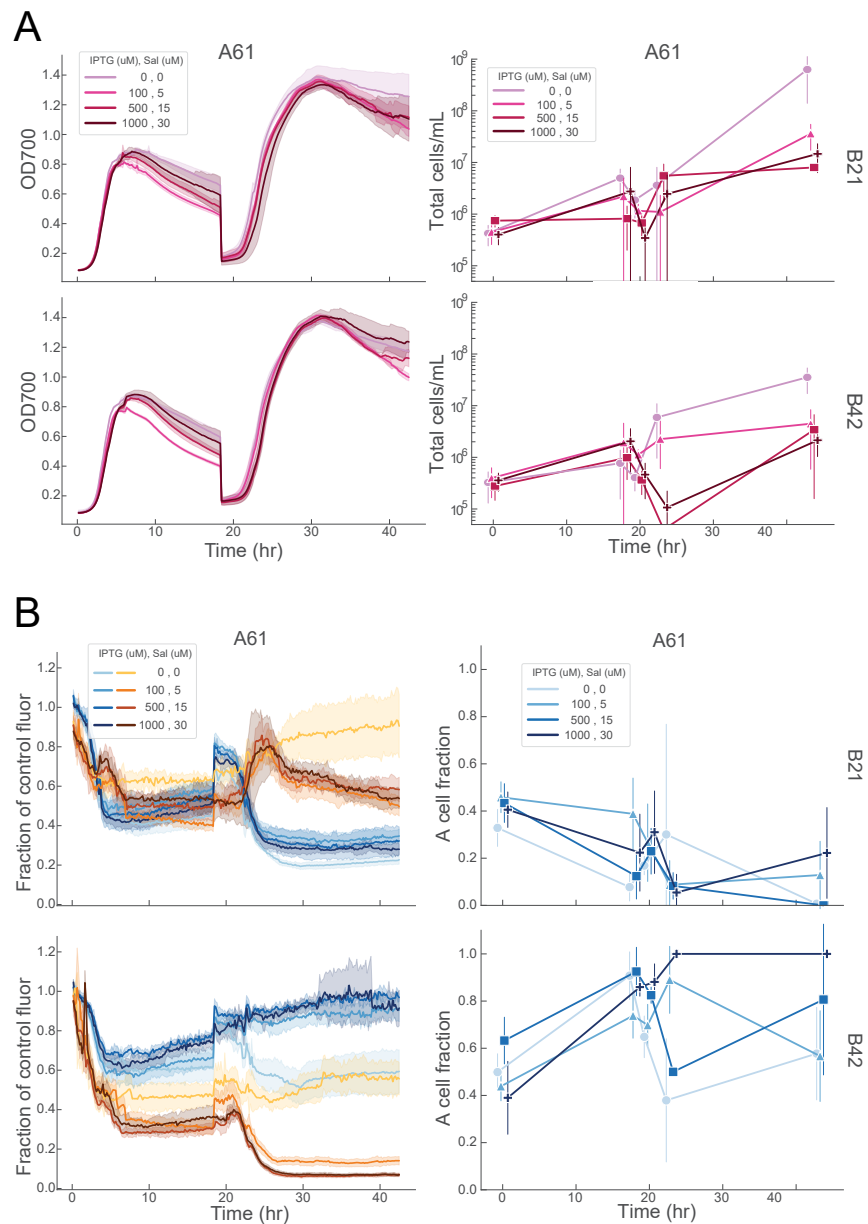


Figure 3.7: Tuning population density and composition with perturbation. Two cocultures composed of A and B cell variants A61, B21, B42 in all AB combinations were grown in increasing inducer concentrations. (A) Total population density measured using (Left) OD700 and (Right) viable cell counts. (B) Coculture composition analysis (Left) Two independent estimates of A and B population fraction from fluorescence measurements (Right) Population composition determined from viable cell counts using fluorescent strain labels. Because cocultures are composed of *only* blue - A or yellow - B cells and viable cell counting directly visualizes and quantifies both strains, A cell fraction implies B cell fraction ($1 - A_{frac}$). As a result, only A fraction is displayed.

density control may have been maintained through the perturbation.

<i>A61 + B21</i>		
IPTG, Sal	Density steady state 1 - 18 hr	Density state 2 - 43 hr
0 uM, 0uM	$4.89 \cdot 10^6$ cell/mL	$6.2 \cdot 10^8$ cell/mL
100 uM, 5 uM	$2.2 \cdot 10^6$	$3.6 \cdot 10^7$
500 uM, 15 uM	$8.0 \cdot 10^5$	$8.0 \cdot 10^6$
1000 uM, 30 uM	$2.7 \cdot 10^6$	$1.4 \cdot 10^7$
<i>A61 + B42</i>		
IPTG, Sal	Density steady state 1 - 18 hr	Density state 2 - 43 hr
0 uM, 0uM	$7.7 \cdot 10^5$ cell/mL	$3.5 \cdot 10^7$ cell/mL
100 uM, 5 uM	$1.9 \cdot 10^6$	$4.4 \cdot 10^6$
500 uM, 15 uM	$9.8 \cdot 10^5$	$3.4 \cdot 10^6$
1000 uM, 30 uM	$2.0 \cdot 10^6$	$2.1 \cdot 10^6$

Table 3.3: Coculture total viable cell counts

Each coculture was pushed to a different composition in response to increasing inducer concentrations (Fig. 3.7 B). Uninduced A61+B21 decayed quickly to B strain monoculture. Composition estimates from YFP and CFP data do not indicate this movement towards B strain dominance until after the dilution at 18 hours, though viable cell counts demonstrate this trend during the entire experiment. Induced A61+B21 behave similarly, cocultures in each induction condition decay to B strain monoculture with similar dynamics to the uninduced coculture.

Uninduced A61+B42 maintained its starting 1:1 population composition throughout the experiment according to both fluorescence-based composition estimates and viable cell counts. This is expected from an unregulated mixture of non-interacting cells (Fig. 3.10). Increasing inducer concentrations consistently pushed A61+B42 towards A strain dominance. Fluorescence measurements indicated nearly complete dominance of the A strain at the end of the experiment, regardless of inducer concentration, while viable cell counts suggest a possible dependence of final A strain population fraction on strength of induction. The large variance in viable cell counts may artificially produce this apparent relationship between final composition and inducer concentrations; more counts need be taken in the future to increase our confidence in composition measurements.

Adding AHL degradation to $A=B$

Using cocultures without the ability to actively degrade AHL, we expect AHL signals to accumulate into saturating concentrations, blunting composition control.

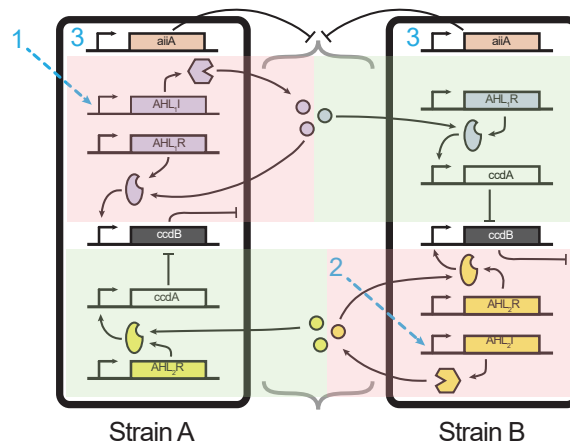


Figure 3.8: AHL degradation in the A=B circuit. (A) The *aiiA* degradase is added to both A and B strains under control of the pCau DHBA responsive promoter. It is placed on plasmids A1 and B1 as part of the invariant chassis of the A and B strains. (Inducer 1 = IPTG, AHL₁ = Cin AHL (3-hydroxy-C14-HSL), inducer 2 = sodium salicylate, AHL₂ = Lux AHL (3-O-C6-HSL), inducer 3 = 3,4-dihydroxybenzoic acid (DHBA)).

We considered two options for controlling AHL accumulation in our system: either physically dilute the coculture during an experiment to remove AHL—at the cost of regular perturbations of the system from steady state—or add active AHL degradation to the circuit.

Active AHL degradation is provided by the *Bacillus thuringiensis* gene *aiiA*, encoding a lactonase that promiscuously degrades AHL signals. Various *aiiA* DNA coding sequences can be found across microbiology [75] and synthetic biology literature [20, 86], but we found the originally deposited sequence (GenBank: AF196486.1) to work most reliably in our system [18]. We added *aiiA* expressing sequences to the A1 and B1 plasmids that form the invariant chassis for the A and B strains, both controlled by the pCau promoter induced by DHBA, so enzymatic AHL degradation could be induced from all cells in a coculture with one inducer (Fig. 3.8). Since AHLs diffuse across cell membranes, *aiiA* enzymes made inside cells will deplete AHLs from the total environment.

We combined *both* physical and enzymatic methods of AHL removal in one experiment to learn how they affect population control by the A=B circuit. We grew the A61+B42 coculture for 8 hours in a few inducer conditions: no induction, maximal A strain induction (1 mM IPTG), maximal B strain induction (30 uM Sal), maximal induction of both strains (1 mM IPTG, 30 uM Sal), max induction of both strains with *aiiA* induction (1 mM IPTG, 30 uM Sal, 1 mM DHBA). This experiment is again modeled after simulated experiment 2 in which cocultures at the same

starting composition are grown in different inducer concentrations to set different composition steady states.

Every hour each coculture was diluted 1:2. Before each dilution, samples of the coculture were removed for precise quantification by counting viable cells.

As demonstrated in (Fig. 3.7) an incubator/plate reader can provide very high resolution estimates of total population density and composition if appropriate control cultures are grown alongside experimental cocultures, but the estimates are only approximate. Flow cytometry may estimate community composition more exactly, but sacrifices time resolution and accuracy in total population density estimation. Viable cell counting is the gold standard method for measuring viable cell counts; combined with fluorescent imaging it can provide the most exact estimates of both total population density and composition.

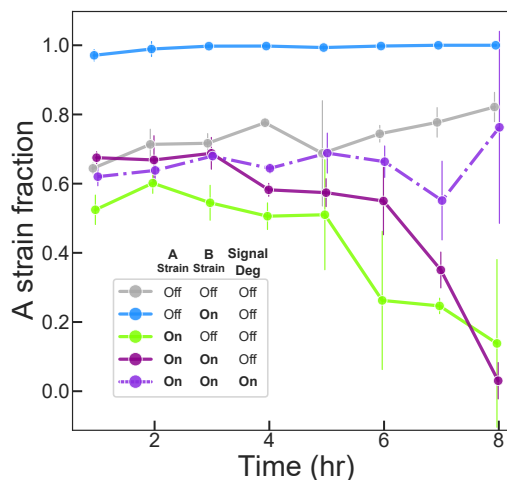


Figure 3.9: Setting composition steady states with $A=B$. A61 and B42 strains were mixed in a 1:1 ratio and grown in the indicated conditions. A strain ON = 1 mM IPTG alone; B strain ON = 30 μ M Sal alone; both strain ON = 1 mM IPTG, 30 μ M Sal; both ON with deg = 1 mM IPTG, 30 μ M Sal, 1 mM DHBA

Because this experiment is regularly diluted, steady state population density is never achieved (Fig. 3.13), but community composition—the characteristic whose control is predicted to be most affected by AHL degradation—can be observed precisely by counting viable colony forming units of each cell strain just before each dilution.

First, the experiment clearly shows that lopsided induction of A or B cells causes the expected shift towards monoculture composition (e.g. A strain induction causes A cell death and B cell monoculture), but with different time scales. B strain induction almost immediately causes the culture to become dominated by A cells, but A strain induction only slowly decays towards B cell dominance. In our experiment testing the A61+B42 coculture's response to parallel increasing inducers, we found it decays to A strain dominance with induction. Here we demonstrate that other composition steady states are possible with different inducer concentrations.

We find regular dilution of AHL signal (and cells) is not sufficient to prevent a coculture's runaway towards monoculture. Even with maximal induction of both A and B strains, the population still slowly decays towards B strain monoculture. The coculture is clearly not stable compared to the control uninduced culture, which, as expected, maintains a stable composition throughout the experiment despite the regular dilutions.

In our previous experiment, the opposite trend was observed, maximal induction of A and B strains produced a shift towards A strain monoculture. The previous experiment was only allowed to grow through 2 complete growth cycles, where the cocultures in this experiment were regularly diluted to allow constant growth. It is possible that with more growth cycles, an A strain dominated A61+B42 coculture would eventually decay to B strain dominance as well.

When both A and B strains are maximally induced, *and* *aiiA* is induced, the coculture behaves as if no AHL is present at all, like in the control coculture. The results suggest that we may have entered the regime of *overdegradation* of AHL in which strong *aiiA* expression causes the population to degrade AHL signals faster than it produces them, blocking all $A=B$ circuit effects on population composition. Further experimentation with intermediate levels of *aiiA* expression seems likely to allow customizable rates of AHL degradation in arbitrary environments.

3.3 Discussion

Using the *cap and release* population control motif, we created an engineered two-strain bacterial community capable of regulating both its composition and total population density to desired steady states. Toxin produced *in-cis* and antitoxin produced *in-trans* sequester each other to implement a pseudo-integral controller in the most stable circuit architecture for controlling community composition.

To search this system's large, multidimensional parameter space to find functional circuits, we created pools of strain variants and screened their mixtures, finding population density regulation to be a much more robust behavior to parameter variation, while composition control was rarer to find.

Experiments and model exploration revealed the critical need for degradation of the AHL signals that transfer information around the circuit. Saturation of AHL signals leads to very slow establishment of composition steady states incomplete rejection of perturbations to composition in simulation.

Periodic physical removal of AHL signals via dilution was insufficient to solve the

problem of AHL saturation; only strong expression of the *aiiA* lactonase enzyme could remove AHL at an appropriate rate.

This work is a basic demonstration of multi-strain community control using our circuit motif. With 3 inducers and a need to explore responses to perturbation, there is a lot of experimental space to cover to fully characterize this $A=B$ circuit. Future work will explore all the various combinations of strain inducers and AHL degradation inducer to appropriately map the functional ranges available to this system. Additional experiments that perturb composition steady states are also necessary to verify the hypothesis that strong AHL degradation is critical to composition perturbation rejection by this circuit.

This successful use of the *cap and release* motif to make a functioning two-strain control circuit is exciting proof of the modularity of the motif. The $A=B$ circuit is just one of many multi-strain circuit architectures *cap and release* makes available. We hope it provides a useful building block for bacterial community engineering work.

3.4 Materials and Methods

E. coli cell strains

The base *E. coli* strain used is the "Marionette Wild" strain from Meyer *et. al.* [34]. This cell strain was used to generate the A and B strain variants (Fig. 3.6) that yielded the chosen variants A61, B21 and B41, used in the experiments presented in Figures 3.7 and 3.9.

DB3.1 *ccdB*-resistant *E. coli* were used to amplify and purify *ccdB* containing A2 and B2 plasmids. These cells contain the mutant *gyrA462* DNA gyrase, rendering them resistant to *ccdB* toxicity. DB3.1 cells were obtained from the [Belgian Coordinated Collections of Microorganisms](#), accession number LMBP 4098. DB3.1 was originally sold by Invitrogen, but has been discontinued as a product.

The method of preparing $A=B$ cell lines is specifically designed to minimize loss of circuit function in the resulting cells. Whenever a strain must be transformed with plasmids containing the *ccdB* toxin and *ccdA*, the base strain should be transformed first with the plasmid containing *ccdA*. This singly transformed cell line should then be prepared for transformation a second time with the *ccdB* containing plasmid. This process avoids exposing cells to leaky *ccdB* expression without protection by *ccdA*.

Plasmids and plasmid construction

Each cell line contains 2 plasmids A/B 1 and A/B 2, described below. All plasmids were assembled using the method detailed in *Halleran et al.* [12]. All inducible promoter sequences are taken from *Meyer et al.* [34] to make use of the optimized expression characteristics between the Marionette transcription factors and their associated evolved promoters. All parts are sourced from the Murray Lab parts library (Addgene Kit 1000000161 "CIDAR MoClo Extension, Volume I").

A1 and B1 plasmids contain a *ccdA* expression unit and an AHL synthase. They replicate using a low-copy ColE1 origin and express kanamycin resistance. The specific constructs are detailed below in the format (promoter - ribosome binding site - CDS - terminator / ...)

plasmid A1:

pLuxB - BCD8 - *ccdA* - L3S3P11

pTac - B0034 - CinI - ECK120029600

plasmid B1:

pCin - BCD8 - *ccdA* - L3S3P11(modified)

pSalTTC - B0034 - LuxI - ECK120029600

A2 and B2 plasmids contain a *ccdB* expression unit and a constitutively expressed fluorescent tag. They replicate using a low-copy pSC101 origin and express chloramphenicol resistance. These plasmids were assembled using a pool of ribosome binding sites (*ARL*), the Anderson RBS pool ([link](#)), such that cells transformed with the plasmid assembly each contain a different RBS. These unique plasmid variants were initially transformed into DB3.1 *E. coli* to allow amplification of the *ccdB* containing plasmids without risk of mutation, purified and sequenced, then transformed into Marionette Wild cells containing the appropriate A2 or B2 plasmid.

plasmid A2:

pCin - *ARL* - *ccdB* - B0015 /

J23100 - BCD6 - CFP - L3S3P11

plasmid B2:

pLuxB - *ARL* - *ccdB* - B0015 /

J23100 - BCD6 - sfYFP - L3S3P11

Cell growth experiments

Screening for functioning A and B cell variants

A and B strain variants were grown from *freshly transformed* colonies (see note about preparation in "*E coli* cell strains" in LB medium to OD600 0.3

These low density outgrowths were then mixed in all possible combinations in a 1:5 A:B ratio into fresh LB media with half-strength kanamycin ($25\mu\text{g}/\text{mL}$) and chloramphenicol ($12.5\mu\text{g}/\text{mL}$) and aliquoted in triplicate in $500\mu\text{L}$ into a square 96 well Matriplate (dot Scientific, MGB096-1-1-LG-L) pre-loaded with chemical inducers. A Labcyte Echo 525 Liquid Handler was used to aliquot inducers into each well of the plate before cell suspensions were added. Induced/"ON" mixtures were induced with 1mM IPTG and $30\mu\text{M}$ Sal, while uninduced/"OFF" mixtures received no inducers.

The plate was incubated for 23 hours in a Biotek Synergy H2 incubator/plate reader at 37°C with maximum linear shaking while OD600 and fluorescence measurements were taken every 10 minutes.

At hours 0, 7, 19, 23, $10\mu\text{L}$ of mixed culture in each well was sampled into 15% glycerol and frozen at -80°C for community quantification by flow cytometry

A note on strain numbers: strain A61 was not the 61st A strain tested, not was B42 the 42nd. 4 variants of both A and B strains were generated by transforming 4 unique A2 and B2 plasmids into cells already containing A1 and B1. 2 presumably identical colonies were taken from each of these transformations, for a total of 8 A and B strain variants each. Not all of these 8 variants grew up overnight for use in screening, leaving us with the 4 A and B strain variants presented here. 2 presumed identical clones of each A and B cell variant were taken for experimentation in case one clone failed to outgrow, or one clone had lost population control capacity by the time of the experiment.

A=B community induction with dilution

An A cell and a B cell variant were separately grown to OD 0.3 from a *freshly transformed* plate of cells containing both A/B1 and A/B2 plasmids (e.g. A1 plasmid + A2 plasmid version 61)

These low density outgrowths were mixed in all possible combinations into fresh LB media (half-strength kanamycin ($25\mu\text{g}/\text{mL}$) and chloramphenicol ($12.5\mu\text{g}/\text{mL}$)) in a 1:1 A:B ratio.

Mixtures were aliquoted in triplicate in 500 μ L into a square 96 well Matriplate containing inducers pre-pipetted into the plate using the Labcyte Echo. The plate was incubated for 18 hours in a Biotek Synergy H2 incubator/plate reader at 37°C with maximum linear shaking while OD600 and fluorescence measurements were taken every 10 minutes. At 18 hours, the plate was removed from the incubator, 90% of the contents of each well was removed, the Labcyte Echo 525 was used to pipet new inducer at each well's original inducer concentration, and fresh LB medium was added up to 500 μ L, yielding a 10x culture dilution into identical inducer conditions.

At hours 0, 18, 18 post-dilution, 25 and 43.5, the mixed culture in each well was sampled into 15% glycerol and frozen at -80°C for colony counting.

*A=B coculture with regular dilutions and *aiiA* degradation*

The A61 strain and B42 strain were separately grown to OD 0.3 from a *freshly transformed* plate of cells containing both A/B1 and A/B2 plasmids (e.g. A1 plasmid + A2 plasmid version 61).

These low density outgrowths were then mixed into fresh LB media (half-strength kanamycin (25 μ g/mL) and chloramphenicol (12.5 μ g/mL)) in all possible combinations in a 1:1 A:B ratio.

Mixtures were aliquoted in triplicate in 500 μ L into a square 96 well Matriplate containing inducers pre-pipetted into the plate using the Labcyte Echo 525. DHBA inducer was added manually to each well since it is dissolved in ethanol and is not pipetted accurately by the Echo.

The plate was incubated for 8 hours in a Biotek Synergy H2 incubator/plate reader at 37°C with maximal linear shaking while OD600 and fluorescence measurements were taken every 10 minutes. Every hour, the plate was removed from the incubator, half of the contents of each well were removed, and fresh LB medium with identical inducer concentrations was added up to 500 μ L, yielding a 2x culture dilution into identical inducer conditions. Before each dilution the culture in each well was sampled into 15% glycerol and frozen at -80°C for colony counting.

Density and Composition quantification

Flow cytometry Frozen cell samples were diluted 30x into PBS buffer containing Syto 62 nuclear stain (Thermo S11344) and incubated on ice for 30 minutes. These samples were then analyzed on a Miltenyi MACSQuant flow cytometer using the mKate/APC channel to detect Syto labeled cells from detector noise, GFP channel

to detect YFP and the CFP channel to detect CFP. FCS files were unpacked to pandas dataframes using the *fcsparser* [87] python package.

The *scikit learn* package *GaussianMixture* was used to train a double-peaked GMM model on the YFP channel of each culture’s dataset. This package automatically assigns data points to the peaks in the model, allowing us to classify each cytometry event as a YFP⁺ event or YFP⁻ event.

Colony counting Frozen cell samples were diluted 4 times to final dilutions between $10^x - 10^4x$ into fresh LB media, then $10\mu\text{L}$ of each diluted suspension was spread on LB agar petri dishes. These plates were incubated at 37°C overnight, then colonies were counted. The number of colonies grown was multiplied by the dilution factor to obtain cells/mL.

Modeling and simulations

Mathematical model

The description of the model species and the model parameters are given in Tables (3.4, ??) respectively. Note that the subscripts 1 and 2 in the model correspond to the cell strains A and B respectively. Parameter guesses for the inducers, the signals, and the promoter strengths were taken from [34].

Table 3.4: Model species

Species	Description
C_1	Cell type 1 (C_1) population count
C_2	Cell type 2 (C_2) population count
T_1	Average toxin (ccdB) con. in C_1 population
T_2	Average toxin (ccdB) con. in C_2 population
A_1	Average anti-toxin (ccdA) con. in C_1 population
A_2	Average anti-toxin (ccdA) con. in C_2 population
S_1	Signal 1 (S_1), Lux con. in environment
S_2	Signal 2 (S_2), Cin con. in environment

Simulations

All simulations of the ODE model were performed using the Python SciPy library [88].

3.5 Supplementary Material

Table 3.5: Model parameters

Parameter	Description	units	value
k_C	cell growth rate	hr^{-1}	0.897
C_{max}	carrying capacity	mL^{-1}	1.16e9
d_c	death rate constant ccdB	$mL \times hr^{-1}$	0.4
k_{tox}	binding constant of ccdB	nM	1
β_{tac}	Max transcription rate, pTac	$nM \times hr^{-1}$	4.8e-06
l_{tac}	leak rate, pTac	$nM \times hr^{-1}$	$\beta_{tac} / 320$
k_{tac}	activation constant, pTac	uM	190
d_s	Environmental degradation constant of AHL	hr^{-1}	0.891
d_{sc}	Enzymatic AHL degradation constant	$mL \times hr^{-1}$	(-) 0; (+) 1e-8; (+++) 1e-7
β_{sal}	Max transcription rate, pSal	$nM \times hr^{-1}$	3e-06
l_{sal}	leak rate, pSal	$nM \times hr^{-1}$	$\beta_{sal} / 760$
k_{sal}	activation constant, pSal	uM	29
β_{S1}	Max transcription rate, pCin	$nM \times hr^{-1}$	5
l_{S1}	leak rate, pCin	$nM \times hr^{-1}$	$\beta_{S1} / 340$
k_{S1}	activation constant, pCin	nM	250
k_{on}	ccdA/ccdB binding rate	$nM^{-1} hr^{-1}$	300
d_t	protein degradation rate	hr^{-1}	2
β_{S2}	Max transcription rate, pLux	$nM \times hr^{-1}$	5
l_{S2}	leak rate, pLux	$nM \times hr^{-1}$	$\beta_{S2} / 480$
k_{S2}	activation constant, pLux	nM	100
I	IPTG inducer concentration	uM	0-1000
Sal	Sal inducer concentration	uM	0-30

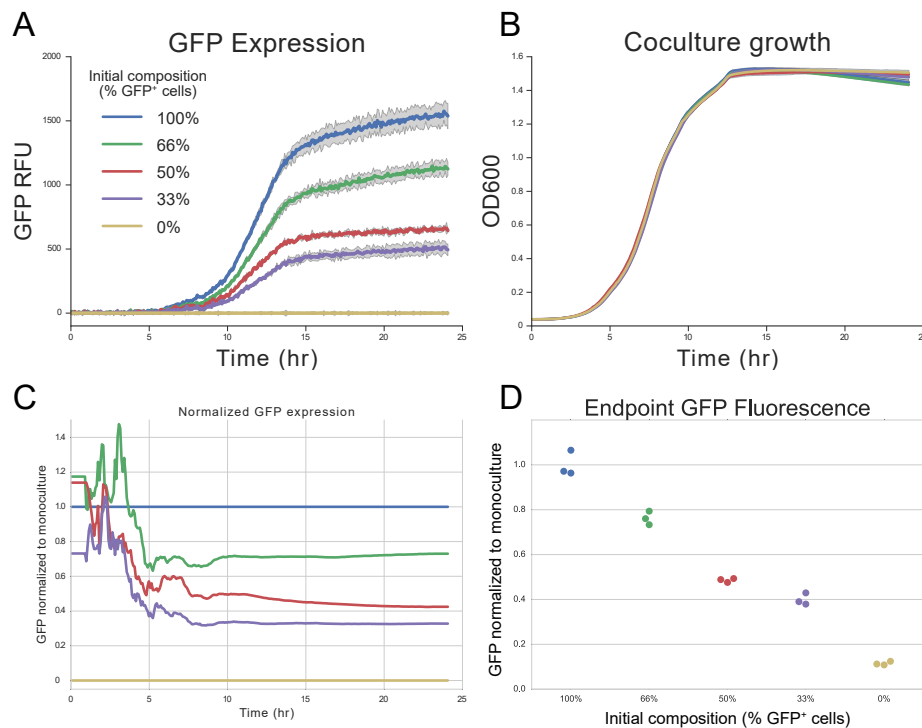


Figure 3.10: Open loop coculture growth *E. coli* labeled with either GFP or RFP were mixed in the indicated compositions, then allowed to grow over a growth cycle. Over the course of this growth, the cocultures maintained their initial compositions, as computed using GFP fluorescence normalized to the monoculture GFP⁺ condition. (A) GFP fluorescence units, background GFP fluorescence from monoculture RFP⁺ condition subtracted from all values. (B) Growth curves of each culture measured by OD600. (C) GFP values normalized at each time point to the monoculture GFP⁺ condition. Estimates composition over time. (D) Endpoint GFP values normalized to the monoculture GFP⁺ condition. Initial seeding composition appears to be maintained.

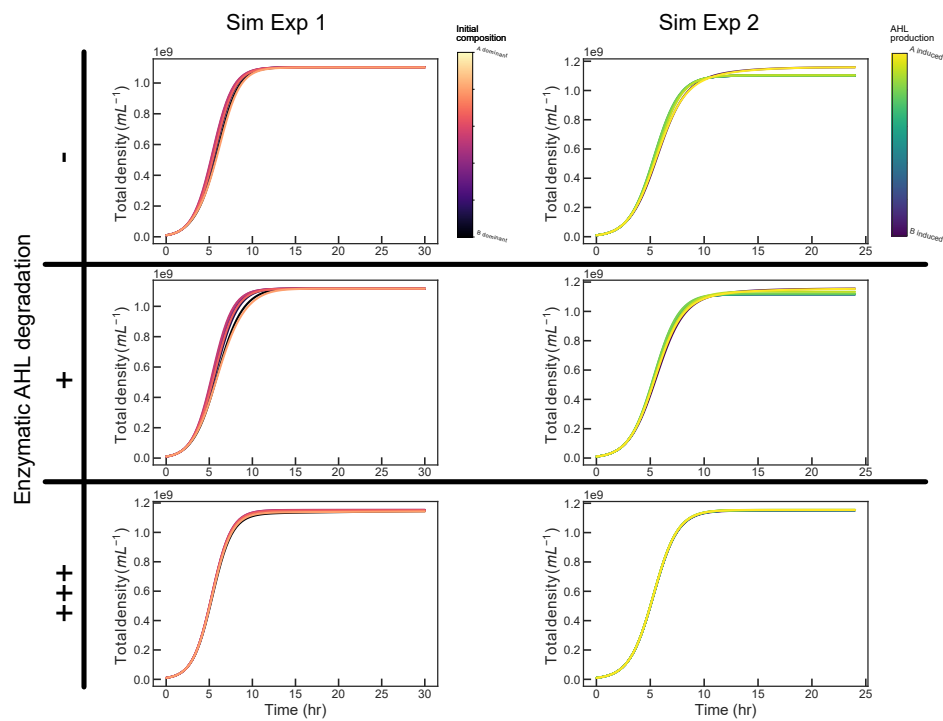


Figure 3.11: $A=B$ Total population dynamics in simulated experiments For both simulated experiments (1: varying coculture initial composition, constant strong AHL production from each strain; 2: constant 1:1 initial composition, varying AHL production rates), total population dynamics do not vary significantly in response to AHL degradation rate, initial composition, or AHL production rates from both strains.

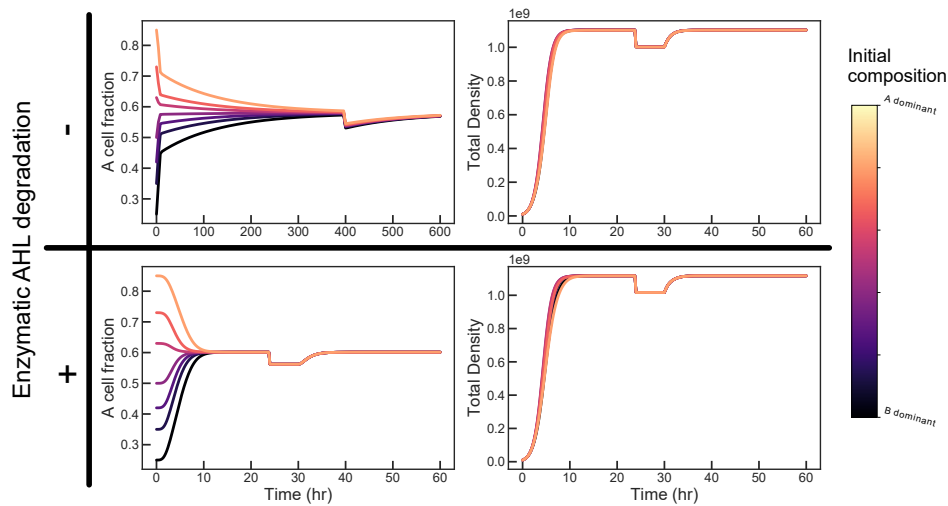


Figure 3.12: Effect of AHL degradation on perturbation rejection While AHL degradation does not appear to be required to reject disturbances in population density steady state, strong AHL degradation is required to allow the $A=B$ system to respond to perturbations on reasonable timescales. The timescale on the simulation of population composition without AHL degradation is greatly extended to allow the system to achieve steady state (approx. 400 hours), so the slow response to composition perturbation (approx. 200 hours) is more clear.

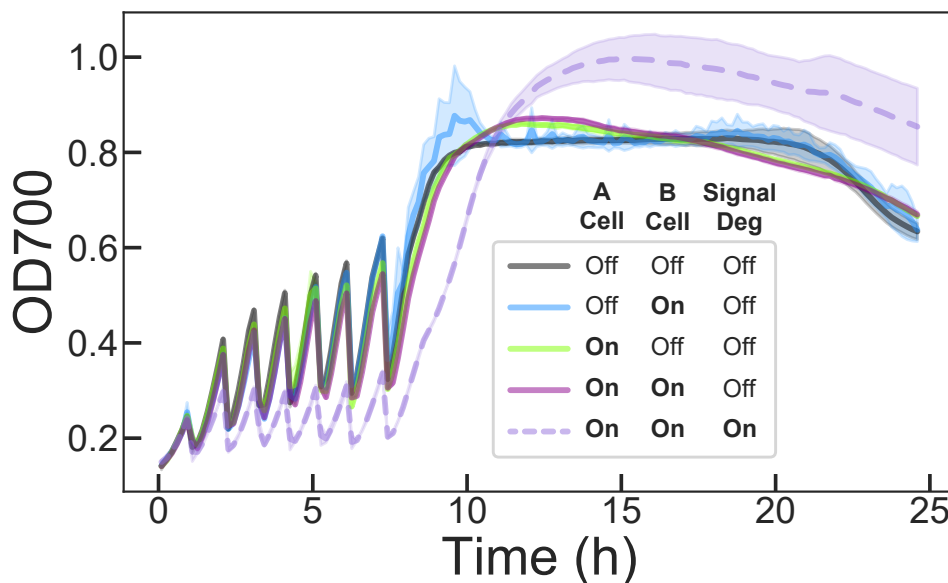


Figure 3.13: Population density dynamics in a regularly diluted $A=B$ experiment Every hour, the A61+B42 strain coculture was diluted 1:2 with fresh medium containing identical inducer concentrations. Population steady state is never achieved, but composition is allowed to progress to steady state through many cycles of log phase growth.

*Chapter 4*COLICIN TOXINS AS MULTI-FUNCTIONAL TOOLS FOR
BACTERIAL POPULATION CONTROL

This chapter is based heavily on work done in collaboration with Leah Keiser (at the time undergraduate at Northwestern University, now graduate student in Chemical Engineering at UC Berkeley). The project direction and experimental designs were decided by RM and LK together; all experiments and data analysis were performed by LK with advice provided by RM.

4.1 Introduction

Bacteriocins are bacterial protein exotoxins that target bacteria of similar species. Since their discovery in 1925 in *E. coli* [89], bacteriocins have been found to be produced by a great diversity of bacterial species both Gram-positive and Gram-negative, each specifically toxic to members of its own or closely related species. As the original bacteriocin, **colicin**, was named for the *E. coli* that produce it, so the convention has been adopted to name bacteriocins for the producing species (Pyocins from *Pseudomonas*, klebicins from *Klebsiella* etc.). The colicins have been studied extensively in antibiotic research, bacterial membrane physiology and ecology [90]. Through this work, we have learned they have attractive structural properties for engineering and exploration of protein design; we rely on the wealth of structural and mechanistic literature concerning colicins in our exploration of their utility in genetic circuit design and investigation of their domain modularity.

Restriction mapping, deletion and recombination of various colicin plasmids revealed a conserved operon structure, plasmid type, and domain structure (cXa) across colicins [90, 91]. Colicin proteins are nearly all composed of 3 functional domains in a conserved order from N to C terminus. The N-terminal T (translocation) domain mediates secondary receptor binding and transfer of the protein through the outer membrane, periplasmic space and inner membrane; the central R (receptor binding) domain binds a specific primary membrane protein on target cells; and the C-terminal C (cytotoxic) domain is the active killing domain. Colicins can be grouped into a number of categories by cell surface receptor specificity, membrane transport mechanism, or cytotoxic mechanism Table 4.1).

Colicin	Receptor	Translocation System	Toxic Activity	Colicin Group
E2, E7, E8, E9	BtuB	OmpF, TolABQR	DNase	A
E3, E6	BtuB	OmpF, TolABQR	RNase	A
DF13	IutA	TolAQR	RNase	A
E1	BtuB	TolCAQ	Membrane pore formation	A
A	BtuB	OmpF, TolABQR	Membrane pore formation	A
N	OmpF	OmpF, TolAQ	Membrane pore formation	A
K	Tsx	OmpFA, TolABQR	Membrane pore formation	A
Col5	Tsx	TolC, TonB, ExbBD	Membrane pore formation	B
Col10	Tsx	TolC, TonB, ExbBD	Membrane pore formation	B
Ia, Ib	Cir	TonB, ExbBD	Membrane pore formation	B
B	FepA	TonB, ExbBD	Membrane pore formation	B
D	FepA	TonB, ExbBD	Inhibit protein synthesis	B
M	FhuA	TonB, ExbBD	Inhibit synthesis of murein and LPS	B

Table 4.1: Colicin functional groups

Colicins are produced inside immune producer bacteria, exported/released into the extracellular environment, then internalized by target cells that die unless they themselves are immune (Fig. 4.1, TOP). This toxin life cycle begins at production from the colicin operon in a producer cell harboring the colicin plasmid (usually pColX, X as the colicin identifier). Colicin operons encode the toxic colicin gene, usually *cXa* for colicin X (identifier) activity; the specific immunity protein, either *cXi* or *immX*; and the release/lysis protein *cXI* that lyses producers to release colicin into the environment. With few exceptions, the operon is organized in the order *cXa-cXi-cXI*. *cXa* transcription is regulated by an SOS/stress responsive promoter; *cxi* is usually weakly constitutively produced by a separate promoter—though sometimes additionally produced as *cXa* read-through; *cXI* is usually only transcribed as read-through of the *cXi* gene [92]. This regulatory strategy supports 2 goals: producing a stoichiometric excess of antitoxin over toxin, and stochastic, low-copy production of lysis protein—which kills the producer, releasing the toxin—when the operon is active. When these regulatory goals are met, producer cells actively making toxin will not poison themselves and only a fraction of them will lyse, ensuring toxin release into the environment without complete destruction of all producer cells.

Released toxin stays complexed with its immunity protein in the extracellular environment. The toxin-immunity complex binds to a receiver cell at a specific membrane protein, generally one involved in an fitness-determining cell process (Table 4.1), with its receptor-binding domain. Bound to the cell surface at the primary receptor, the long receptor binding (R) domain serves as an an-

chor around which the rest of the colicin turns [93]. This swivel action allows the anchored colicin to "search" membrane space around the primary receptor for a secondary receptor that will bind the translocation (T) domain and initiate transmembrane transport. Transmembrane transport is a complex process involving partial to complete toxin unfolding [94], unbinding of the immunity protein [95], import through an outer membrane pore protein, transit of the periplasmic space, and penetration of the inner membrane (Fig. 4.1 BOTTOM).

This transport process is facilitated by the Tol and/or Ton family of periplasmic proteins that use the energy of the transmembrane proton gradient to move colicins [90]. Depending on the toxic mechanism of the colicin's C domain, the final cytotoxic step of the colicin life cycle is different. Membrane pore forming toxins insert themselves into the inner membrane of the receiver cell

and create pores that destroy normal ion gradients, killing the receiver. Nuclease C domains must fully enter the cytoplasm of the

receiver to access their substrate. Nuclease colicins are partially transported through the inner membrane by the FtsH protein, exposing the C domain to the cytoplasm. FtsH then cleaves the C domain from the rest of the colicin at a specific linker sequence, releasing just the C domain into the cytoplasm to find its target[96].

Studies of recombinant colicin plasmids not only helped map colicin domain boundaries and determine domain functions, but also discovered that resulting recombinant hybrid colicins (e.g. a T domain from colicin A, R domain from colicin E1, C domain from colicin A) can still function as exotoxins, and furthermore that each domain in a hybrid colicin can confer its native activity to the hybrid, despite being

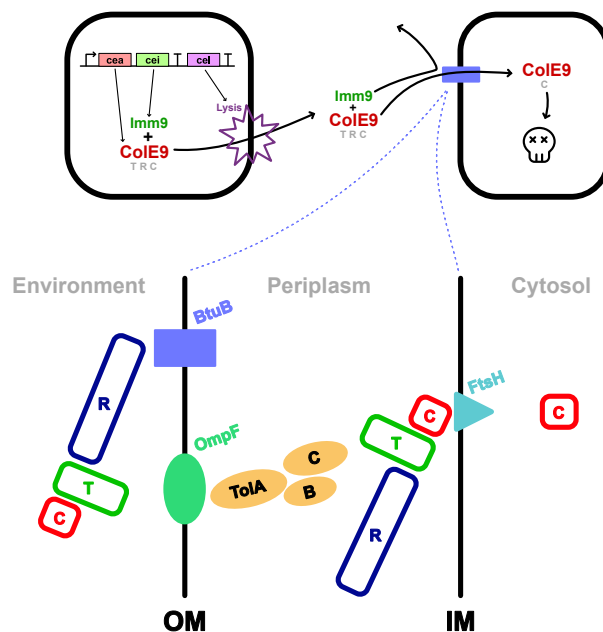


Figure 4.1: Diagram of colE9 activity. C represents cytotoxic domain, T translocation domain, R receptor binding domain. OM and IM stand for outer membrane and inner membrane, respectively.

removed from its original neighboring domain context [97]. Not every hybrid colicin is perfectly functional, however; some are less efficient killers and others do not work at all, suggesting that some domains are variably dependent on the presence of the—or perhaps one of a set of—compatible neighboring domains. The space of hybrid colicins is not fully explored and the extent to which domains across the diversity of colicins are modular—on a spectrum from functionally independent of their neighbors to dependent on their neighbor(s)—is not completely known.

This apparent toxin domain modularity along with DNA technology to delete or change target cell surface proteins makes the colicin system a potentially powerful tool for designing or altering microbial community systems. In the introduction, we discussed the required functions for creating genetic circuits that control communities of bacteria:

1. Send information between cells in the community
2. Process and respond to information signals from the community (or environment/experimenter)
3. Regulate the number of cells of any type in the community

Bacteriocins can perform all three functions; they transmit themselves between cells, have unique high-affinity sequestering antitoxin proteins, and are toxins to receiver cells. They may also help minimize one of the most pervasive problems in synthetic biology: mutation. The DNA sequence of bacteriocins is just as susceptible to mutation as any other DNA sequence, but their mechanism of action makes it difficult for bacteria to gain a fitness advantage by their mutation. In the *pop cap*, *cap and release* and *A=B* circuits, the *ccdB* actuator places lethal burden on cells in the circuit, creating a large selective pressure for inactivating mutations in circuit components. Before too long, communities continuously running these circuits will eventually be overrun by mutated cells no longer participating in circuit action, an outcome we and others regularly observe [64].

Bacteriocins act *in-trans*, at a distance, meaning bacteriocin expression is not lethal to the producer, but to another cell. Producers do not gain a significant fitness advantage by inactivating the bacteriocin and target cells are actually penalized for mutations that immunize them against incoming bacteriocins (most bacteriocins parasitize physiologically important cell processes whose loss/alteration decreases

growth rate). While lysis proteins or costly non-toxic proteins in a circuit are certainly targets for mutation by a producer, the selective advantage to their mutation is significantly less than the advantage gained by inactivating a lethal toxin like *ccdB*. Evolution of greater fitness is inherent to biology and difficult to accommodate in engineering; bacteriocins do not solve this problem, but it is possible that using the colicins in place of AHL signals and traditional toxins may improve long-term population control circuit integrity.

Bacteriocins are increasingly represented in recent work engineering bacterial communities. Non-*E. coli* bacteriocins like nisin and lactococcin A [56, 57] have been used as actuators in genetic circuits for population control. Despite the great diversity of bacteriocin systems, synthetic biologists are limited by the lack of well-understood, orthogonal "parts" that allow their use on a larger scale. The E-type colicins are as useful for population control as nisin or lactococcin, but are not adequately characterized to bring them into popular usage. The apparent modularity in E-type colicin domains makes the E-type colicin family especially attractive for characterization and investigation as a protein engineering chassis. We present the beginnings of a characterization of the E type colicins and an exploration of modularity in their domains.

4.2 Results

Creating independent parts from the colicin E2 operon

There are nine E-type colicins (E1 - E9), all of which are BtuB-binding proteins with varying toxic mechanisms of action. The plasmids and operons from which these colicins are expressed are very similar in regulation and structure. To begin characterization of this colicin family, we focus on the relatively well-studied colicin E2. The colicin E2 operon is,

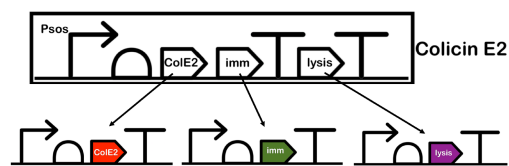


Figure 4.2: Basic structure of the ColE2 operon. Separating the parts of the operon allows us to investigate them independently in standard synthetic biology workflows.

like many native operons, denser and more complicated than the simple, engineered sequences we tend to create in synthetic biology. In our genetic engineering work, we usually create sequences composed of: a promoter that initiates transcription, a ribosome binding site (RBS) that initiates translation of the mRNA transcript, the coding sequence of a gene of choice, and a transcription terminator—in order, with

this sequence structure repeated for every gene in a system. The colicin E2 operon is not so simply structured; it expresses 3 different proteins co-transcriptionally, that is, it uses a single promoter to produce one mRNA transcript that can be translated into 3 different proteins (Fig. 4.2) [92].

Accessing the coding sequences for the activity protein (colE2a), immunity protein (imm2) and lysis protein (colE2I, hereafter just "lysis protein") was made simple by the generous provision of the ColE2-P9 plasmid by Benjamin Kerr's laboratory at University of Washington, and the complete annotated sequence of said plasmid deposited by the Madeleine Opitz lab at Ludwig-Maximilians-Universität München. The Opitz lab also provided their pMO3 plasmid, in which all the toxic genes of the colicin operon (colE2a and lysis proteins) are replaced with fluorescent reporters that allow measurement of operon output across the different sections of its sequence.

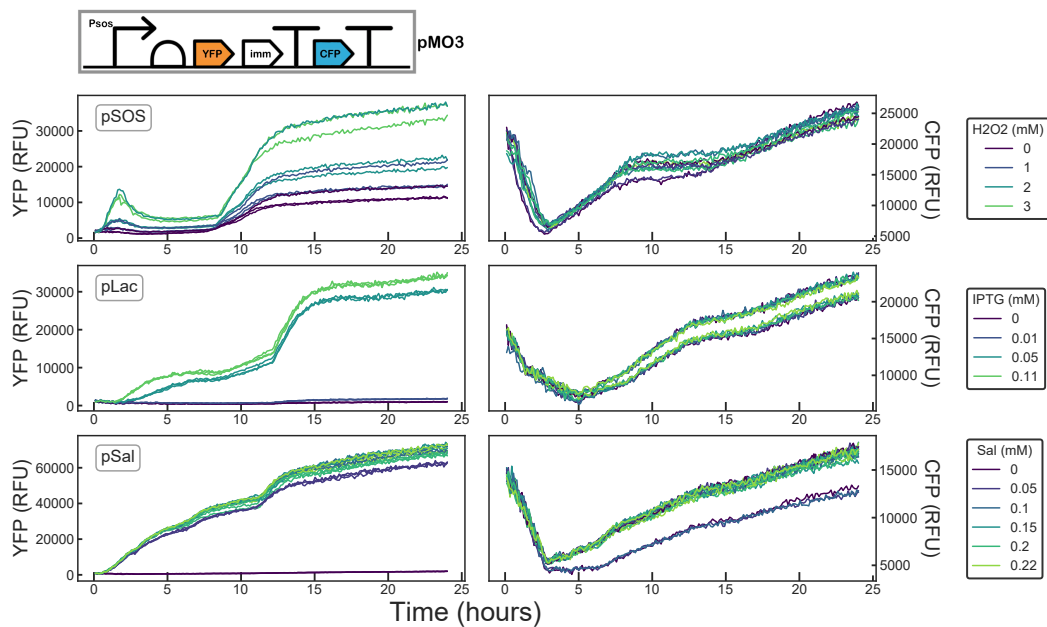


Figure 4.3: Comparing output from alternative colE2 operon promoters The pMO3 pSOS promoter was replaced with the pLac and pSal inducible promoters. Expression from each was driven by different concentrations of inducer chemicals. (LEFT) Raw YFP signal from each recombinant pMO3 operon. (RIGHT) Raw CFP signal from each operon. At the beginning of the CFP traces, we see a rapid drop from a high starting value, this may be an artifact from the incubator/plate reader used or the breakdown of residual CFP left over from the end of culture outgrowth for experimentation.

Replicating colicin E2 operon regulation with synthetic parts

The Madeleine Opitz lab has done extensive work with pMO3 to understand the strength and dynamics of native colicin E2 expression [92, 98].

To help integrate colicin expression into genetic circuit designs, we replaced the native promoter element of the *colE2* operon with well-characterized, optimized inducible promoters to gain more predictable control of operon expression.

The *colE2* plasmid can be found for purchase in the *E. coli* strain BZB1011; we chose to use the Marionette Wild *E. coli* strain [34], popular in synthetic biology for its built-in expression of various transcription factor proteins. We take advantage of this strain's expression of LacI and NahR in our replacement of the pSOS promoter.

In situ on the pMO3 plasmid, we replaced the native pSOS (stress-induced) promoter driving the pMO3 operon with orthogonal, small molecule controlled promoters pLac and pSal, induced by IPTG and salicylate respectively. These recombinant operons, as well as the native pSOS-regulated pMO3, were induced with their appropriate inducers (pSOS was treated with hydrogen peroxide to create oxidative stress) to learn what levels of the inducers IPTG/sal were required to achieve fluorescent output similar to the native operon (Fig. 4.3).

We found the pLac promoter to express the *colE2a* reporter, YFP, to very similar endpoint levels as the maximally activated pSOS promoter ($\sim 3 \cdot 10^4$ YFP RFU), while pSal seemed to strongly overexpress YFP compared to pSOS ($\sim 6 \cdot 10^4$ YFP RFU). YFP expression from pSOS briefly pulsed in the first 3 hours, then increased slowly until 9 hours, at which point expression grew dramatically to levels set by the hydrogen peroxide stress inducer concen-

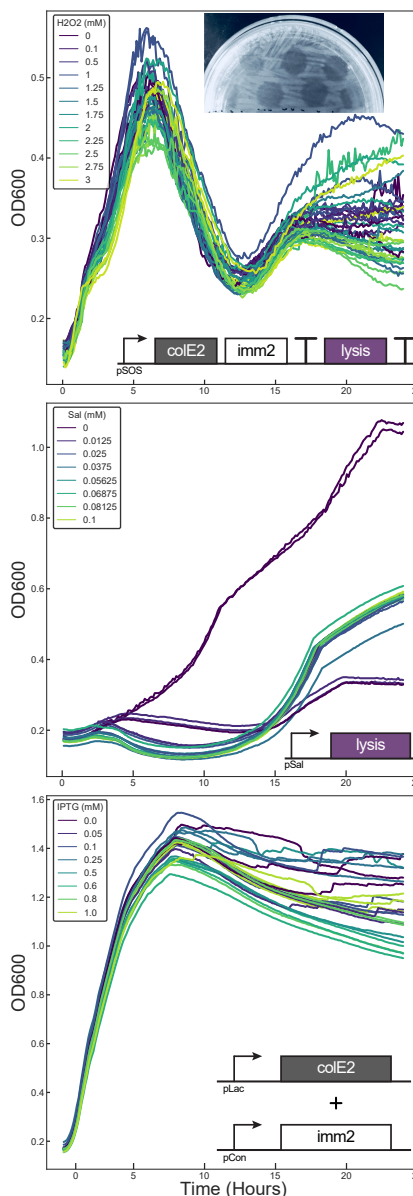


Figure 4.4: Effects of *colE2* operon parts (*Top*) Effect of full *colE2* operon on population density. Inset shows zones of clearing caused by *colE2a* treatment of sensitive cells. (*Middle*) Induction of the *colE2* lysis protein. (*Bottom*) Induction of *colE2* toxin against constitutive *imm2* expression.

tration. The pLac promoter showed similar YFP expression dynamics, with YFP signal increasing slowly until 12 hours, then dramatically increasing to its maximum, which was not greatly modified by IPTG inducer concentration. The pSal promoter did not demonstrate these expression dynamics, driving nearly constant YFP expression over the course of the experiment. Both pSal and pLac were significantly less leaky than pSOS, staying neatly "off" when uninduced. While maximal YFP expression was similar between pSOS and pLac, pLac did not achieve intermediate YFP expression values, even with a gradient of IPTG inducer.

Similarly, the pLac promoter produced the most comparable level of lysis gene reporter (CFP) to the native pSOS promoter, although in this case, the pSal promoter *underexpressed* compared to pSOS. CFP dynamics were nearly identical from all three operons. A greater dynamic range of CFP expression was possible through induction of the pLac and pSal driven operons. The CFP reporter was significantly leakier than the YFP reporter in the pLac and pSal designs, though this is very likely due to read through from the accessory constitutive pCei promoter—normally found within the colE2 gene sequence—retained in pMO3 [92, 98].

These data indicate that pLac is an appropriate promoter choice to enable inducible expression of colE2 operon genes to appropriate levels without requiring cell-stressing inducers. It is especially important that any synthetic regulatory elements used to drive colE2a or lysis protein expression have very low leak. The colE2a and lysis proteins are both potent toxins that can severely inhibit producer populations with only weak expression.

Techniques to measure colicin E2 action

We tested two techniques to visualize the growth inhibiting effects of colE2 operon expression on producer populations and sensitive receiver populations. Cells expressing the entire colE2 operon, the lysis protein alone, or colE2a + imm2 were grown in an incubator/plate reader and optical density was measured over time to observe the dynamic effects on population density produced by the expressed proteins. We also released colE2a from a culture containing the native colE2 plasmid using chloroform and dropped the released colicin onto a lawn of healthy target cells to observe regions of growth inhibition in the target cells due to colicin toxicity (method described in [99]).

Both techniques were capable of reporting the expected growth inhibitory activity (or protective activity in the case of imm2) in these tests. The native colicin E2 plasmid

caused dramatic alteration of normal logistic bacterial growth (Fig. 4.4 *TOP*). After 5 hours of growth the density of all populations containing the native plasmid was suddenly cut in half (OD600 0.5 to 0.25) regardless of hydrogen peroxide stressor concentration, followed by a recovery to a widely variable steady state only slightly affected by stressor concentration. In our induction of the pMO3 plasmid, the CFP lysis protein reporter only began to show expression just before 5 hours of growth. It seems likely that the sudden population density reduction we observe here is due to lysis protein expression. At the end of the experiment, cultures growing in the highest concentrations of hydrogen peroxide had recovered to the lowest densities. While it is clear that the colicin operon dramatically alters growth dynamics, it is not known whether these different end point densities are caused by the physiologic effects of hydrogen peroxide, or colicin operon action.

In these growth curves we can appreciate the precise regulation of the colE2 operon's proteins: the entire population was not destroyed by operon expression, even with increasing induction of oxidative stress. Imm2 protein is produced in a sufficient amount to protect the producer cells from complete destruction by colE2a and transcriptional read-through of the colE2a-imm2 terminator allows just enough lysis protein expression to kill a portion of the population that will release colE2a into the environment.

Historically, colicin has been released from colicinogenic cultures by treatment with chloroform, which disrupts bacterial membranes, allowing the release of colicin from an entire culture [99]. Because chloroform is volatile, allowing a chloroform treated culture to sit or shake for a short amount of time should remove the chloroform from the culture by evaporation. When working with colicinogenic colonies on agar plates, the plate can be placed above a chloroform bath, surrounding it with chloroform gas, releasing colicin from colonies.

We treated a culture of colE2 expressing cells with 10% chloroform, then filtered the treated culture through an 0.22 μ M sterile filter to remove cells and debris. The cell-free colicin-containing medium was spotted onto a lawn of sensitive cells. Obvious zones of inhibition were reliably produced by colicinogenic culture medium on mats of sensitive bacteria (Fig. 4.4 *TOP*).

Independent expression of lysis protein slowed growth significantly but did not outright destroy the culture at any induction level (Fig. 4.4, *MIDDLE*). There appeared to be a zone in the induction range that produced the strongest attenuation of growth, but only transiently. All cells induced to express lysis protein seemed

to recover from its expression, perhaps completely; the cells intermediately induced seemed to be growing towards high density by the end of the experiment. Despite the low leakiness of the pSal promoter used to express lysis protein, uninduced cells still showed a dramatic alteration in their growth curve; even tiny amounts of lysis protein can disrupt cell growth. It is possible that even leaky lysis protein expression from pSal may outproduce the native operon; the colE2 operon is structured to express only the barest hint of lysis protein, our synthetic constructs may not be able to express lysis protein so weakly without introducing impediments to expression into the expression construct (e.g. terminators, similar to native colE2 operon structure).

We were also able to observe the inhibition of colE2a toxicity by imm2 (Fig. 4.4, *BOTTOM*). Strongly expressed imm2 was sufficient to prevent alteration of cell growth even when colE2a was induced strongly. Late in the growth curve, we begin to see possible decreases in cell density due to colE2a expression, despite the presence of imm2. A longer experiment would be necessary to see if this trend becomes significant. Additional experiments with constructs expressing colE2a alone are necessary to confirm that imm2 is indeed preventing alteration of cell growth by colE2a; without demonstrating growth defects due to colE2a, we cannot clearly demonstrate imm2's protective effects. The severe toxicity of colE2a, however, makes it difficult to acquire a colE2a expressing construct; further efforts are required to create a colE2a construct that is non-toxic until the toxin is induced.

Building a colicin E2 based population feedback circuit

We attempted to build a genetic circuit for feedback control of population density using colicin E2. We have not created expression constructs capable of independently expressing colE2a, imm2 and lysis proteins at native levels, so we decided to replace the pSOS promoter driving the entire native colE2 operon with one that fit into our circuit design.

A YFP labeled activator strain can be induced to produce Cin AHL signal. A colicinogenic strain contains the colE2 operon regulated by the pCin promoter (Fig. 4.5 TOP). Intuitively, when the activator strain is induced to send its signal into the environment, the the colicinogenic strain is induced to produce colE2a that will kill activator cells. This creates a closed loop feedback circuit to regulate the growth of activator strain.

Tests of this circuit suggested the circuit components were functional, but that the circuit design was not optimized for lasting dynamic control. The density of the

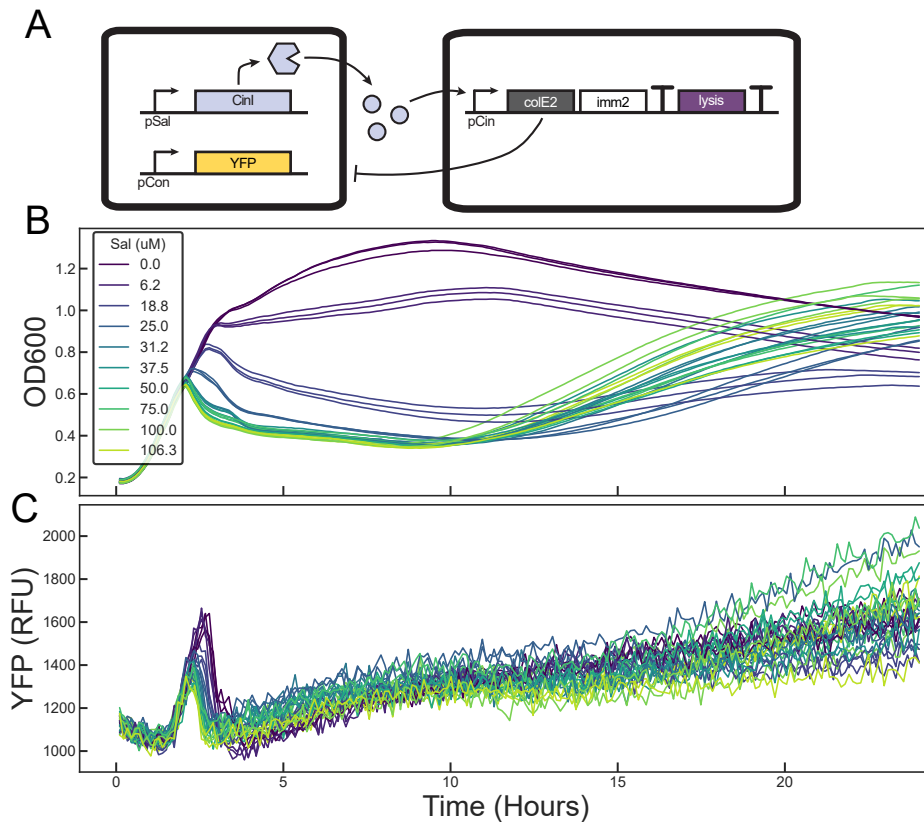


Figure 4.5: Creating a genetic circuit using the ColE2 operon A signal sender cell (YFP⁺) can be induced to produce an AHL signal that will activate a recombinant colE2 operon, which should release colE2a toxin into the environment and inhibit sender cell growth.

coculture was regulated by the inducer of Cin AHL synthesis, but YFP measurements indicated that the activator strain population was quickly annihilated by strong negative feedback due either to overproduction of Cin AHL or overactivation of the colE2a production from the pCin promoter in the colicinogenic strain, both of which would result in the release of a high concentration of colE2a, high enough to be uniformly toxic to all activator cells. We believe the observed density control behavior was caused by lysis protein regulation of the colicinogenic strain's density, rather than any true control action by the circuit. The most strongly induced cocultures have growth curves that resemble the curves produced by the native, pSOS-regulated colE2 operon (Fig. 4.4, *TOP*), supporting the hypothesis that this circuit's recorded behavior was mostly due to colicin operon effects rather than circuit feedback.

4.3 Future Work

The E-type family of colicins bind to the BtuB vitamin B12 receptor, but use different membrane transport and cytotoxic mechanisms (Table 4.1). E-type colicin domains have been recombined successfully among themselves or with domains from colicin A and colicin Ia to explore the structure of colicin plasmids and to clarify the mechanism of colicin toxicity to sensitive cells [97, 100, 101]. These studies uncovered important information about colicin physiology and are important proofs of the concept of colicin modularity, but from a protein design perspective, left a lot of the functional capacity of hybrid colicins unexplored.

Jakes *et al* [101] created a hybrid colicin with the T and C domains of colicin Ia and the R domain of colicin E3, removing each one of those domains from their normal neighboring domain context. That this hybrid was even partially functional is an amazing demonstration of domain modularity. That said, the hybrid produced did not dramatically expand the set of functions available to BtuB binding colicins. Toxic domains with nuclease (DNA and RNA) and membrane pore forming mechanisms are already represented among the BtuB binding E-type colicins; this hybrid added another orthogonal membrane pore forming toxic domain to the BtuB binding colicin set.

Most toxic domains of bacteriocins are specifically paired with only one immunity protein, so having multiple DNAses or membrane pore forming toxic domains received through only one membrane receptor "channel" is not redundant. However, not every cell expresses every membrane receptor and complex strain targeting in community regulation is enabled by having a full complement of toxic domains available through each membrane receptor channel.

We believe a very similar project to that published by Jakes *et al* would be important to increase functional diversity among the colicins. Where Jakes *et al* replaced the R domain of colicin Ia with the R domain of colicin E3, replacing the colicin Ia C domain with domains from the E-type colicins would add new toxic mechanisms to the set of Cir-binding colicins and open that Cir-binding "channel" for population control design goals.

Jakes *et al* split the colIa protein into its 3 domains at these boundaries: T domain from AA positions 0-249, R domain from AA 250-407, C domain from AA 408-626. We propose retaining colIa AA 0-407 and fusing to this the reported toxic domains of colE3 (AA 450-551 [102]), colE9 (AA 453-580 [103]) and colE1 (AA 332-522 [104]). Because producers must be immune to the toxic effects of their colicin,

the immIa protein must also be swapped to imm3/9/1 to allow hybrid producer cells to grow.

We also propose the creation of an intercellular protein shuttle, using the binding and membrane transport functions of colicins to transmit a protein of choice between cells. By replacing the toxic C domain of a colicin with a protein of interest, the bacteriocin "chassis" composed of the T and R domains might convey this protein of interest from a producer cell into the cytosol of a target cell. An intercellular protein shuttle like this could be a way to transmit dense, peptide information through communities of bacteria.

We made initial attempts to design such a shuttle by replacing the colE9 C domain with the small complementing LacZ α fragment, hoping to transfer the small fragment to a receiver strain expressing the larger Δ LacZ fragment. We reasoned that the smaller the payload protein, the less likely it would be to interfere with the membrane transfer process mediated by the T and R colicin domains. Complementation would allow receiver cells to hydrolyze the X-Gal substrate. We could measure the resulting change in color from colorless to blue in a plate reader or by microscopy.

ColE9 was chosen for modification due to the specific mechanism of its toxicity. ColE9 has a nuclease (DNAse) type toxic domain, which must be released into the cytoplasm of the cell to access its substrate. We imagine the utility of a protein shuttle lies in its ability to send a protein of interest to interact with the cytoplasm of the receiver cell, easiest achieved with a payload released into the cytoplasm. Nuclease toxic domains are released into the receiver cell cytoplasm by the inner membrane protein FtsH, which cleaves the toxic domain from the rest of the colicin protein at a specific linker site that is conserved across the E-type nuclease colicins [96]. We retained this linker site in our shuttle protein in hopes that FtsH would still recognize and release our payload protein into the receiver cell.

We could only attempt very preliminary experiments which did not demonstrate complementation in target bacteria, but the reason why remains to be determined. While colicin domains may be modular, it is possible that each domain should at least be a *colicin* domain, even if they are not from the *same* colicin. Replacing the payload cytotoxic domain with a different protein or appending an additional payload to the cytotoxic domain might disrupt the interplay between domains and their target proteins under this hypothesis. More careful testing of these types of modified colicins can tell us if this is true. Perhaps more informed rational designs or a directed evolution strategy can generate a successful protein shuttle device.

4.4 Discussion

Bacteriocins are powerful multi-functional proteins that play roles in normal microbial ecology that we are still discovering. For their ability to transmit themselves between cells and regulate the density of target strains, they are finding increased use in modern engineering of microbial communities. Separating the various proteins of the *E. coli* colicin operon from their native regulatory context is an important step towards the use of colicins in bespoke microbial community engineering. Our preliminary characterization of the colE2 activity, immunity and lysis proteins provide basic guidelines for their use in synthetic circuits, but more quantitative studies are required before we understand the perfect parameters for their use alongside other well-understood genetic circuit components.

Past and present investigations of colicin plasmid and protein structure revealed well-defined, conserved operon structure and protein domain boundaries. These same studies also generated functional hybrid proteins composed of domains from multiple different colicin proteins, suggesting a surprising tolerance to modification and potential reconfigurable modularity in domain structure. We propose a number of hybrid colicins whose success would expand the range of toxic mechanisms available through different cell surface receptors, opening valuable orthogonal avenues to bacterial community design.

The extent to which colicins tolerate recombination or modification is not fully known, but the success of hybrid proteins suggests an exceedingly versatile chassis for innovation, perhaps even beyond the normal functions of colicins. By replacing the toxic domain of colicin E2 with a non-colicin protein payload, we attempted to create an intercellular protein shuttle based on the receptor binding and transmembrane transport functions of the T and R colicin domains. While we did not demonstrate successful protein transfer, we hope to continue this protein design work.

4.5 Materials and Methods

E. coli cell strains

The base *E. coli* strain used to generate the cell lines used in this work is the "Marionette Wild" strain from Meyer *et. al.* [34].

The ColE2 plasmid was provided to us in BZB1011 *E. coli* by the Kerr lab at University of Washington. The plasmid was subsequently purified and transformed into Marionette.

Plasmids and plasmid generation

ColE2-P9 was provided by the Kerr lab at University of Washington

pMO3 was provided by the Optiz lab at Ludwig-Maximilians-Universität München.

All colE2 operon components were isolated by PCR and cloned into the standard Murray lab part vectors (see Addgene Kit #1000000161 "CIDAR MoClo Extension, Volume I") using either GoldenGate or Gibson assembly.

The plasmids we generated are structured as follows:

pSal & pLac driving pMO3 operon

pMO3 from the ribosome binding site to the final terminator was amplified by PCR with appropriate extensions to allow GoldenGate assembly of the pSal or pLac upstream. This recombinant pMO3 operon with promoter replaced was assembled by GoldenGate assembly into a backbone with p15a origin and kanamycin resistance.

Plasmid expressing lysis protein

pSalAM - BCD8 - lysis protein - B0015

assembled into a backbone with pSC101 origin and chloramphenicol resistance

Plasmids expressing colE2a and imm2

The cell line concurrently expressing colE2a and imm2 contains two plasmids:

pLac - BCD8 - colE2a - L3S2P55

assembled into a backbone with p15a origin and kanamycin resistance

J23100 - BCD2 - imm2 - B0015

assembled into a backbone with high copy ColE1 origin and carbenicillin resistance.

Feedback circuit plasmids

CinI producer cells

pSal - BCD8 - CinI - B0015

J23106 - B0033 - YFP - L3S3P11

both assembled into a backbone with high copy ColE1 origin and kanamycin resistance

Colicinogenic cells

The ColE2 operon from the ribosome binding site to the final terminator was amplified by PCR with appropriate extensions to allow GoldenGate assembly of the pCin promoter upstream. This recombinant ColE2 operon with promoter replaced was assembled by GoldenGate assembly into a backbone with pSC101 origin and kanamycin resistance.

Cell growth experiments

For all growth experiments, the experimental cell strain was picked from a freshly transformed colony directly into 50mL of LB medium containing the appropriate antibiotics.

This suspension was mixed well, then aliquoted in triplicate in 500 μ L into a square 96 well Matriplate containing inducers pipetted into the plate using the Labcyte Echo.

Plates were incubated for 24 hours in a Biotek Synergy H2 incubator/plate reader at 37° with maximal linear shaking while OD600 and fluorescence measurements were taken every 10 minutes.

Bacterial lawn inhibition by colicinogenic cultures

The bacterial strain used to create the sensitive lawn is DH5 α -Z1.

BZB1011 *E. coli* carrying the ColE2 plasmid were grown in 5mL of LB medium overnight. Chloroform release of colicin was performed as describe in [99]; chloroform was added to culture to a final concentration of 10%. Chloroform treated culture was allowed to shake at 37°C for 10 minutes. Chloroform released culture was passed through a 0.22 μ M filter to remove cells. 1 μ L of this colicin containing cell-free medium was dropped onto a freshly seeded, but dry, lawn of DH5 α -Z1 *E. coli*. This lawn was grown overnight at 37°C and imaged the next day.

CONCLUDING REMARKS AND LESSONS LEARNED

5.1 Working with burdensome genetic circuits

After years working with the *pop cap*, *cap and release*, and $A=B$ circuits, it is no longer a surprise to me that relatively few projects have been published in the space of explicit bacterial population control. It is extremely difficult—and at some level a matter of luck—to generate bacteria that contain functional versions of a population control circuit, and again difficult to prepare these bacteria for experiments in which they must demonstrate their population control circuit functions.

Genetic circuits that burden bacteria work against evolution by natural selection and are quickly lost [64], overtaken by mutants that reduce circuit burden. In a sense, population control circuits like ours are the *ultimate* burdensome circuit in that they are designed to burden cells *to death* when performing their control functions. Consequently, the threat of circuit mutation is around every corner and demands very precise, mutation-aware experimental procedures. Much of our experimentation with population control circuits resulted in "failed" experiments in which a cell line designed to perform some population control function would not demonstrate that function, presumably because it had acquired an inactivating mutation along the way to the experiment. Experiments like these do not generate quantitative data that help us make progress on lines of inquiry, but rather send us back to the drawing board, where we must grasp at possible reasons for their "failure" and hope to address these reasons with some tweak to the experiment preparation.

For experimenters working with highly burdensome genetic circuits, especially those incorporating lethal toxins, we suggest making tweaks to minimize two things: intensity of circuit burden and duration of growth under burden.

The stronger the fitness penalty imposed by a genetic circuit, the more quickly a population of bacteria expressing that circuit will be overtaken by unburdened mutants. In our case of toxin containing genetic circuits, direct addition of toxin-expressing DNA to cells is *guaranteed* to result in some amount of toxin expression in cells due to leaky expression from that DNA. Due to the potency of the most bacterial toxins, even this very weak expression represents a strong fitness penalty that predisposes that population of cells to takeover by mutant bacteria that have

inactivated the toxin. If possible, minimize the intensity of that fitness penalty by expressing an antitoxin in the cells *before* toxin-expressing DNA is ever introduced.

In preparing our cell lines for experimentation, we changed the conventional practice of two plasmid co-transformation into two plasmid transformation by *sequential* single plasmid transformation. In most cases, concurrent co-transformation of toxin and antitoxin containing plasmids would not generate functional cell lines; somehow all resultant colonies from this transformation were without the desired functions. Instead, first transforming antitoxin expressing plasmid, then transforming toxin expressing plasmid into that singly transformed cell line would yield the desired results. We hypothesize that the antitoxin-expressing DNA, arriving first, produces enough antitoxin to sequester any toxin basally expressed off the plasmid that arrives second, minimizing the burden of that toxin.

The second quantity to minimize is the duration of time a cell line is allowed to grow containing a burdensome genetic circuit. Even cell lines prepared carefully by transforming antotoxin and toxin-containing plasmids in the right order are subject to loss of function. The standard practice in preparing bacterial cells for experimentation is an overnight outgrowth to high density followed by dilution to low density for experimentation. We find that this overnight growth step gives our cell lines entirely too much time to acquire inactivating mutations; cell lines grown overnight *usually* do not demonstrate the desired circuit functions. We specify "*usually*" because the acquisition of mutations is not a deterministic process; some overnight cultures may acquire mutations early during outgrowth and lose function, some may not. We would expect the distribution of functional vs non-functional overnight cultures to follow that outlines in Luria and Delbrück's famous experiment [105].

Thus, in our preparations for experimentation, we minimize outgrowth duration. Instead of overnight outgrowth to densities around OD600 2-3, we only briefly outgrow cells from fresh transformations for a few hours to around OD600 0.3. The combination of correct transformation order and minimal outgrowth helped us reliably set up experiments that demonstrated *some* circuit behavior, though the reproducibility of each dataset remains to be seen.

Minimizing these two quantities, burden intensity and duration of growth under burden, precludes normal storage conventions for bacterial cell strains. Generating glycerol stocks of genetic circuit containing bacteria requires too much growth under circuit burden to ensure the stocked cell line will be functional. Instead, store

plasmids and freshly transform cell lines before each experiment.

5.2 Choosing appropriate measurements

Determining characteristics of bacterial cocultures can be done using a number of different measurement methods. In our work, we used optical measurements made by an incubator/plate reader, flow cytometry measurements and viable cell counting to measure our two coculture quantities of interest: total population size and coculture composition.

Optical measurements can be taken with the highest time resolution thanks to laboratory robots like incubator/plate readers that can culture cells and take optical measurements at the same time. This time resolution is incredibly valuable when working with systems that are expected to show characteristic dynamics. However, optical measurements sacrifice accuracy for time resolution. In our experiments, we found that optical density measurements severely misrepresent the total size of a population that is undergoing active cell death due to toxin expression. Additionally, determining the composition of a coculture of cells, even if they are distinctly labeled with fluorescent markers, is also inaccurate.

In theory, the most accurate way to measure the composition of a coculture is to perform flow cytometry. Flow cytometry is a technique designed to resolve different populations of label-expressing cells and as such, should be the perfect tool for determining coculture composition. It turns out this is generally true. We were able to make confident measurements of coculture composition using flow cytometry, but the trade off of accuracy vs time resolution is again true with this technique. Measuring cocultures with flow cytometry requires periodic sampling of the coculture and lengthy preparation for the cytometry process. This greatly limits the realistic time resolution possible with this technique. Additionally, flow cytometers are operating at the limit of their particle size resolution when measuring bacteria, meaning dust, debris and noise are often easily confused for a bacterium during cytometry. This makes estimates of total population size very inaccurate.

The gold standard technique for determining total population size is CFU counting: estimating viable cell density by counting colonies of bacteria on agar plates. This technique again requires sampling and preparation, limiting time resolution, but this time the trade of time resolution for measurement accuracy may be worth it. Combining CFU counting with fluorescent imaging allows the measurement of labeled subpopulation densities and thus, the composition of a coculture. The high

accuracy of population size and composition measurement makes this technique desirable for experiments where accuracy matters.

Taken together, methods like high throughput screening, which we use extensively in our work generating population control circuits, may be better conducted using easy to acquire, but inaccurate measurements like optical density or fluorescence measurement. Later, during more detailed testing, CFU counting would be the preferred measurement type. In our particular work, we do not believe flow cytometry is a viable measurement type and suggest CFU counting as an alternative.

BIBLIOGRAPHY

- [1] Jack A Gilbert et al. “Current understanding of the human microbiome”. In: *Nature medicine* 24.4 (2018), pp. 392–400.
- [2] Aea Hector et al. “Plant diversity and productivity experiments in European grasslands”. In: *science* 286.5442 (1999), pp. 1123–1127.
- [3] Pierre-Alain Maron et al. “High Microbial Diversity Promotes Soil Ecosystem Functioning”. In: *Applied and Environmental Microbiology* 84.9 (2018). Ed. by Harold L. Drake. ISSN: 0099-2240. DOI: 10.1128/AEM.02738-17. eprint: <https://aem.asm.org/content/84/9/e02738-17.full.pdf>. URL: <https://aem.asm.org/content/84/9/e02738-17>.
- [4] Peter J Turnbaugh et al. “An obesity-associated gut microbiome with increased capacity for energy harvest”. In: *nature* 444.7122 (2006), pp. 1027–1031.
- [5] Jack A Gilbert et al. “Microbiome-wide association studies link dynamic microbial consortia to disease”. In: *Nature* 535.7610 (July 2016), pp. 94–103. ISSN: 0028-0836. DOI: 10.1038/nature18850. URL: <https://doi.org/10.1038/nature18850>.
- [6] June L Round and Sarkis K Mazmanian. “The gut microbiota shapes intestinal immune responses during health and disease”. In: *Nature reviews immunology* 9.5 (2009), pp. 313–323.
- [7] Kary B. Mullis et al. *Process for amplifying, detecting, and/or cloning nucleic acid sequences using a thermostable enzyme*. US Patent 4965188A. May 1987. URL: <https://patents.google.com/patent/US4965188>.
- [8] Daniel G Gibson et al. “Enzymatic assembly of DNA molecules up to several hundred kilobases”. In: *Nature methods* 6.5 (2009), pp. 343–345.
- [9] Carola Engler, Romy Kandzia, and Sylvestre Marillonnet. “A One Pot, One Step, Precision Cloning Method with High Throughput Capability”. In: *PLOS ONE* 3.11 (Nov. 2008), pp. 1–7. DOI: 10.1371/journal.pone.0003647. URL: <https://doi.org/10.1371/journal.pone.0003647>.
- [10] Frederick Sanger, Steven Nicklen, and Alan R Coulson. “DNA sequencing with chain-terminating inhibitors”. In: *Proceedings of the national academy of sciences* 74.12 (1977), pp. 5463–5467.
- [11] Addgene. *Bacterial Transformation*. 2021. URL: <https://www.addgene.org/protocols/bacterial-transformation/> (visited on 03/20/2021).

- [12] Andrew D. Halleran, Anandh Swaminathan, and Richard M. Murray. “Single Day Construction of Multigene Circuits with 3G Assembly”. In: *ACS Synthetic Biology* 7.5 (2018). PMID: 29715010, pp. 1477–1480. DOI: 10.1021/acssynbio.8b00060. eprint: <https://doi.org/10.1021/acssynbio.8b00060>. URL: <https://doi.org/10.1021/acssynbio.8b00060>.
- [13] Michael B Elowitz and Stanislas Leibler. “A synthetic oscillatory network of transcriptional regulators”. In: *Nature* 403.6767 (2000), pp. 335–338.
- [14] Timothy S Gardner, Charles R Cantor, and James J Collins. “Construction of a genetic toggle switch in *Escherichia coli*”. In: *Nature* 403.6767 (2000), pp. 339–342.
- [15] Alissa Kerner et al. “A Programmable *Escherichia coli* Consortium via Tunable Symbiosis”. In: *PLOS ONE* 7.3 (Mar. 2012), pp. 1–10. DOI: 10.1371/journal.pone.0034032. URL: <https://doi.org/10.1371/journal.pone.0034032>.
- [16] Israel Castillo-Juárez et al. “Role of quorum sensing in bacterial infections”. In: *World Journal of Clinical Cases: WJCC* 3.7 (2015), p. 575.
- [17] Kai Papenfort and Bonnie L Bassler. “Quorum sensing signal–response systems in Gram-negative bacteria”. In: *Nature Reviews Microbiology* 14.9 (2016), p. 576.
- [18] Yi-Hu Dong et al. “AiiA, an enzyme that inactivates the acylhomoserine lactone quorum-sensing signal and attenuates the virulence of *Erwinia carotovora*”. In: *Proceedings of the National Academy of Sciences* 97.7 (2000), pp. 3526–3531. ISSN: 0027-8424. DOI: 10.1073/pnas.97.7.3526. eprint: <https://www.pnas.org/content/97/7/3526.full.pdf>. URL: <https://www.pnas.org/content/97/7/3526>.
- [19] Jared R. Leadbetter and E. P. Greenberg. “Metabolism of Acyl-Homoserine Lactone Quorum-Sensing Signals by *Variovorax paradoxus*”. In: *Journal of Bacteriology* 182.24 (2000), pp. 6921–6926. ISSN: 0021-9193. DOI: 10.1128/JB.182.24.6921-6926.2000. eprint: <https://jb.asm.org/content/182/24/6921.full.pdf>. URL: <https://jb.asm.org/content/182/24/6921>.
- [20] Tal Danino et al. “A synchronized quorum of genetic clocks”. In: *Nature* 463.7279 (2010), pp. 326–330.
- [21] Chen-Yu Tsao et al. “Autonomous induction of recombinant proteins by minimally rewiring native quorum sensing regulon of *E. coli*”. In: *Metabolic engineering* 12.3 (2010), pp. 291–297.
- [22] Arthur Prindle et al. “Rapid and tunable post-translational coupling of genetic circuits”. In: *Nature* 508.7496 (2014), pp. 387–391.

- [23] Seok Hoon Hong et al. “Synthetic quorum-sensing circuit to control consortial biofilm formation and dispersal in a microfluidic device”. In: *Nature communications* 3.1 (2012), pp. 1–8.
- [24] Andrew D. Halleran and Richard M. Murray. “Cell-Free and In Vivo Characterization of Lux, Las, and Rpa Quorum Activation Systems in *E. coli*”. In: *ACS Synthetic Biology* 7.2 (2018). PMID: 29120612, pp. 752–755. DOI: 10.1021/acssynbio.7b00376. eprint: <https://doi.org/10.1021/acssynbio.7b00376>. URL: <https://doi.org/10.1021/acssynbio.7b00376>.
- [25] Spencer R Scott and Jeff Hasty. “Quorum sensing communication modules for microbial consortia”. In: *ACS synthetic biology* 5.9 (2016), pp. 969–977.
- [26] Nicolas Kylilis et al. “Tools for engineering coordinated system behaviour in synthetic microbial consortia”. In: *Nature communications* 9.1 (2018), pp. 1–9.
- [27] Kenneth H. Nealson, Terry Platt, and J. Woodland Hastings. “Cellular Control of the Synthesis and Activity of the Bacterial Luminescent System”. In: *Journal of Bacteriology* 104.1 (1970), pp. 313–322. ISSN: 0021-9193. eprint: <https://jb.asm.org/content/104/1/313.full.pdf>. URL: <https://jb.asm.org/content/104/1/313>.
- [28] Ruth Daniels et al. “The cin quorum sensing locus of *Rhizobium etli* CN-PAF512 affects growth and symbiotic nitrogen fixation”. In: *Journal of Biological Chemistry* 277.1 (2002), pp. 462–468.
- [29] Shaobin Guo and Richard M Murray. “Construction of incoherent feed-forward loop circuits in a cell-free system and in cells”. In: *ACS synthetic biology* 8.3 (2019), pp. 606–610.
- [30] Tae Seok Moon et al. “Genetic programs constructed from layered logic gates in single cells”. In: *Nature* 491.7423 (2012), pp. 249–253.
- [31] Victoria Hsiao et al. “A population-based temporal logic gate for timing and recording chemical events”. In: *Molecular systems biology* 12.5 (2016), p. 869.
- [32] Victoria Hsiao et al. “Design and implementation of a biomolecular concentration tracker”. In: *ACS synthetic biology* 4.2 (2015), pp. 150–161.
- [33] François St-Pierre et al. “One-step cloning and chromosomal integration of DNA”. In: *ACS synthetic biology* 2.9 (2013), pp. 537–541.
- [34] Adam J Meyer et al. “*Escherichia coli* “Marionette” strains with 12 highly optimized small-molecule sensors”. In: *Nature chemical biology* 15.2 (2019), pp. 196–204.
- [35] Laurence Van Melderen and Manuel Saavedra De Bast. “Bacterial toxin–antitoxin systems: more than selfish entities?” In: *PLoS Genet* 5.3 (2009), e1000437.

- [36] Nathan Fraikin, Frédéric Goormaghtigh, and Laurence Van Melderen. “Type II toxin-antitoxin systems: evolution and revolutions”. In: *Journal of bacteriology* 202.7 (2020).
- [37] Jérôme Izard et al. “A synthetic growth switch based on controlled expression of RNA polymerase”. In: *Molecular systems biology* 11.11 (2015), p. 840.
- [38] Andreas Miliadis-Argeitis et al. “Automated optogenetic feedback control for precise and robust regulation of gene expression and cell growth”. In: *Nature communications* 7.1 (2016), pp. 1–11.
- [39] Bernard R Glick. “Metabolic load and heterologous gene expression”. In: *Biotechnology advances* 13.2 (1995), pp. 247–261.
- [40] Bruce A Hesselbach and Dai Nakada. ““Host shutoff” function of bacteriophage T7: involvement of T7 gene 2 and gene 0.7 in the inactivation of Escherichia coli RNA polymerase”. In: *Journal of Virology* 24.3 (1977), pp. 736–745.
- [41] Hao Song et al. “Programming microbial population dynamics by engineered cell–cell communication”. In: *Biotechnology journal* 6.7 (2011), pp. 837–849.
- [42] Behzad D Karkaria et al. “From microbial communities to distributed computing systems”. In: *Frontiers in Bioengineering and Biotechnology* 8 (2020), p. 834.
- [43] Carolyn Zhang, Ryan Tsoi, and Lingchong You. “Addressing biological uncertainties in engineering gene circuits”. In: *Integrative biology* 8.4 (2016), pp. 456–464.
- [44] William H Mather et al. “Translational cross talk in gene networks”. In: *Biophysical journal* 104.11 (2013), pp. 2564–2572.
- [45] Ryan Tsoi et al. “Metabolic division of labor in microbial systems”. In: *Proceedings of the National Academy of Sciences* 115.10 (2018), pp. 2526–2531.
- [46] Gang Wu et al. “Metabolic burden: cornerstones in synthetic biology and metabolic engineering applications”. In: *Trends in biotechnology* 34.8 (2016), pp. 652–664.
- [47] J Andrew Jones et al. “Complete biosynthesis of anthocyanins using E. coli polycultures”. In: *MBio* 8.3 (2017).
- [48] Haoran Zhang and Gregory Stephanopoulos. “Co-culture engineering for microbial biosynthesis of 3-amino-benzoic acid in Escherichia coli”. In: *Biotechnology journal* 11.7 (2016), pp. 981–987.

- [49] J Andrew Jones et al. “Experimental and computational optimization of an *Escherichia coli* co-culture for the efficient production of flavonoids”. In: *Metabolic engineering* 35 (2016), pp. 55–63.
- [50] Gino Vrancken et al. “Synthetic ecology of the human gut microbiota”. In: *Nature Reviews Microbiology* 17.12 (2019), pp. 754–763.
- [51] Sami Ben Said and Dani Or. “Synthetic microbial ecology: engineering habitats for modular consortia”. In: *Frontiers in microbiology* 8 (2017), p. 1125.
- [52] Lingchong You et al. “Programmed population control by cell–cell communication and regulated killing”. In: *Nature* 428.6985 (2004), pp. 868–871.
- [53] Tim Miyashiro and Edward G Ruby. “Shedding light on bioluminescence regulation in *Vibrio fischeri*”. In: *Molecular microbiology* 84.5 (2012), pp. 795–806.
- [54] Spencer R Scott et al. “A stabilized microbial ecosystem of self-limiting bacteria using synthetic quorum-regulated lysis”. In: *Nature microbiology* 2.8 (2017), p. 17083.
- [55] Christina V Dinh, Xingyu Chen, and Kristala LJ Prather. “Development of a quorum-sensing based circuit for control of coculture population composition in a naringenin production system”. In: *ACS synthetic biology* 9.3 (2020), pp. 590–597.
- [56] Feng Liu et al. “Synthetic, context-dependent microbial consortium of predator and prey”. In: *ACS synthetic biology* 8.8 (2019), pp. 1713–1722.
- [57] Wentao Kong et al. “Designing microbial consortia with defined social interactions”. In: *Nature Chemical Biology* 14.8 (2018), pp. 821–829.
- [58] Frederick K Balagaddé et al. “A synthetic *Escherichia coli* predator–prey ecosystem”. In: *Molecular systems biology* 4.1 (2008), p. 187.
- [59] Matthew R Parsek et al. “Acyl homoserine-lactone quorum-sensing signal generation”. In: *Proceedings of the National Academy of Sciences* 96.8 (1999), pp. 4360–4365.
- [60] Philippe Bernard et al. “The F plasmid CcdB protein induces efficient ATP-dependent DNA cleavage by gyrase”. In: *Journal of molecular biology* 234.3 (1993), pp. 534–541.
- [61] Katherine E Scheirer and N Patrick Higgins. “The DNA cleavage reaction of DNA gyrase: comparison of stable ternary complexes formed with enoxacin and CcdB protein”. In: *Journal of Biological Chemistry* 272.43 (1997), pp. 27202–27209.

- [62] Kendall Morgan. *Plasmids 101: Origin of Replication*. 2021. URL: <https://blog.addgene.org/plasmid-101-origin-of-replication> (visited on 04/21/2021).
- [63] Qiagen. *How do I know if my plasmid is a high- or low copy number type?* 2021. URL: <https://www.qiagen.com/us/resources/faq?id=1f42840e-fbd7-4734-b0cd-e17372a9e5a4&lang=en> (visited on 04/21/2021).
- [64] Frederick K Balagaddé et al. “Long-term monitoring of bacteria undergoing programmed population control in a microchemostat”. In: *Science* 309.5731 (2005), pp. 137–140.
- [65] Nilesh K Aghera et al. “Mechanism of CcdA-mediated rejuvenation of DNA Gyrase”. In: *Structure* 28.5 (2020), pp. 562–572.
- [66] Alexandra Vandervelde et al. “Molecular mechanism governing ratio-dependent transcription regulation in the *ccdAB* operon”. In: *Nucleic acids research* 45.6 (2017), pp. 2937–2950.
- [67] Natalie De Jonge et al. “Rejuvenation of CcdB-poisoned gyrase by an intrinsically disordered protein domain”. In: *Molecular cell* 35.2 (2009), pp. 154–163.
- [68] Matthew R Parsek et al. “Acyl homoserine-lactone quorum-sensing signal generation”. In: *Proceedings of the National Academy of Sciences* 96.8 (1999), pp. 4360–4365.
- [69] Chang C Liu et al. “An adaptor from translational to transcriptional control enables predictable assembly of complex regulation”. In: *Nature methods* 9.11 (2012), pp. 1088–1094.
- [70] Laurence Van Melderen, Philippe Bernard, and Martine Couturier. “Lon-dependent proteolysis of CcdA is the key control for activation of CcdB in plasmid-free segregant bacteria”. In: *Molecular microbiology* 11.6 (1994), pp. 1151–1157.
- [71] Ron Milo and Rob Phillips. *How Fast Do RNAs and Proteins Degrade?* 2021. URL: <http://book.bionumbers.org/how-fast-do-rnas-and-proteins-degrade/> (visited on 05/03/2021).
- [72] Ania-Ariadna Baetica et al. “Design Guidelines For Sequestration Feedback Networks”. In: *bioRxiv* (2018). DOI: 10.1101/455493. eprint: <https://www.biorxiv.org/content/early/2018/10/30/455493.full.pdf>. URL: <https://www.biorxiv.org/content/early/2018/10/30/455493>.
- [73] Corentin Briat and Mustafa Khammash. “Perfect adaptation and optimal equilibrium productivity in a simple microbial biofuel metabolic pathway using dynamic integral control”. In: *ACS synthetic biology* 7.2 (2018), pp. 419–431.

- [74] Yili Qian and Domitilla Del Vecchio. “Realizing ‘integral control’ in living cells: how to overcome leaky integration due to dilution?” In: *Journal of The Royal Society Interface* 15.139 (2018), p. 20170902.
- [75] Dali Liu et al. “Mechanism of the quorum-quenching lactonase (AiiA) from *Bacillus thuringiensis*. 1. Product-bound structures”. In: *Biochemistry* 47.29 (2008), pp. 7706–7714.
- [76] Su-Jin Park et al. “The role of AiiA, a quorum-quenching enzyme from *Bacillus thuringiensis*, on the rhizosphere competence”. In: *Journal of microbiology and biotechnology* 18.9 (2008), pp. 1518–1521.
- [77] Zhaoshou Wang et al. “Artificially constructed quorum-sensing circuits are used for subtle control of bacterial population density”. In: *PLoS One* 9.8 (2014), e104578.
- [78] Anandh Swaminathan et al. “Fast and flexible simulation and parameter estimation for synthetic biology using bioscrape”. In: *bioRxiv* (2019). DOI: 10.1101/121152. eprint: <https://www.biorxiv.org/content/early/2019/03/25/121152.full.pdf>. URL: <https://www.biorxiv.org/content/early/2019/03/25/121152>.
- [79] Ye Chen et al. “Emergent genetic oscillations in a synthetic microbial consortium”. In: *Science* 349.6251 (2015), pp. 986–989.
- [80] François St-Pierre et al. “One-step cloning and chromosomal integration of DNA”. In: *ACS synthetic biology* 2.9 (2013), pp. 537–541.
- [81] ML Urbanowski, CP Lostroh, and EP Greenberg. “Reversible acyl-homoserine lactone binding to purified *Vibrio fischeri* LuxR protein”. In: *Journal of bacteriology* 186.3 (2004), pp. 631–637.
- [82] Behzad D Karkaria, Alex JH Fedorec, and Chris P Barnes. “Automated design of synthetic microbial communities”. In: *Nature communications* 12.1 (2021), pp. 1–12.
- [83] Kristien Braeken et al. “Genetic determinants of swarming in *Rhizobium etli*”. In: *Microbial ecology* 55.1 (2008), pp. 54–64.
- [84] Chelsea Y Hu et al. “Engineering a functional small RNA negative autoregulation network with model-guided design”. In: *ACS synthetic biology* 7.6 (2018), pp. 1507–1518.
- [85] Chelsea Y Hu, Jeffrey D Varner, and Julius B Lucks. “Generating effective models and parameters for RNA genetic circuits”. In: *ACS synthetic biology* 4.8 (2015), pp. 914–926.
- [86] Brendan M Ryback et al. “Design and analysis of a tunable synchronized oscillator”. In: *Journal of biological engineering* 7.1 (2013), pp. 1–10.
- [87] Eugene Yurtsev. *FCSParser : Python package for reading fcs files*. [Online; accessed April 30 2019].

- [88] Eric Jones, Travis Oliphant, Pearu Peterson, et al. *SciPy: Open source scientific tools for Python*. [Online; accessed April 30 2019].
- [89] André Gratia. “Sur un remarquable exemple d’antagonisme entre deux souches de colibacille”. In: *C. R. Soc Biol* 93 (1925), pp. 1040–1042.
- [90] Eric Cascales et al. “Colicin biology”. In: *Microbiology and molecular biology reviews* 71.1 (2007), pp. 158–229.
- [91] Robert J Watson, Thierry Vernet, and Louis P Visentin. “Relationships of the Col plasmids E2, E3, E4, E5, E6, and E7: restriction mapping and colicin gene fusions”. In: *Plasmid* 13.3 (1985), pp. 205–210.
- [92] Andreas Mader et al. “Amount of colicin release in *Escherichia coli* is regulated by lysis gene expression of the colicin E2 operon”. In: *PloS one* 10.3 (2015), e0119124.
- [93] Stanislav D Zakharov et al. “The colicin E3 outer membrane translocon: immunity protein release allows interaction of the cytotoxic domain with OmpF porin”. In: *Biochemistry* 45.34 (2006), pp. 10199–10207.
- [94] Hélène Bénédicti et al. “Colicin A unfolds during its translocation in *Escherichia coli* cells and spans the whole cell envelope when its pore has formed.” In: *The EMBO journal* 11.2 (1992), pp. 441–447.
- [95] Mireille Vankemmelbeke et al. “Immunity protein release from a cell-bound nuclease colicin complex requires global conformational rearrangement”. In: *MicrobiologyOpen* 2.5 (2013), pp. 853–861.
- [96] Liliana Mora and Miklos de Zamaroczy. “In vivo processing of DNase colicins E2 and E7 is required for their import into the cytoplasm of target cells”. In: *PLoS One* 9.5 (2014), e96549.
- [97] Hélène Benedetti et al. “Individual domains of colicins confer specificity in colicin uptake, in pore-properties and in immunity requirement”. In: *Journal of molecular biology* 217.3 (1991), pp. 429–439.
- [98] Alexandra Götz et al. “CsrA and its regulators control the time-point of ColicinE2 release in *Escherichia coli*”. In: *Scientific reports* 8.1 (2018), pp. 1–12.
- [99] Harvey R Herschman and Donald R Helinski. “Purification and characterization of colicin E2 and colicin E3”. In: *Journal of Biological Chemistry* 242.22 (1967), pp. 5360–5368.
- [100] Robert J Watson, Thierry Vernet, and Louis P Visentin. “Relationships of the Col plasmids E2, E3, E4, E5, E6, and E7: restriction mapping and colicin gene fusions”. In: *Plasmid* 13.3 (1985), pp. 205–210.
- [101] Karen S Jakes and Alan Finkelstein. “The colicin Ia receptor, Cir, is also the translocator for colicin Ia”. In: *Molecular microbiology* 75.3 (2010), pp. 567–578.

- [102] Sandriyana Soelaiman et al. “Crystal structure of colicin E3: implications for cell entry and ribosome inactivation”. In: *Molecular cell* 8.5 (2001), pp. 1053–1062.
- [103] Alexander Klein et al. “Structural and biophysical analysis of nuclease protein antibiotics”. In: *Biochemical Journal* 473.18 (2016), pp. 2799–2812.
- [104] Patricia Elkins et al. “A mechanism for toxin insertion into membranes is suggested by the crystal structure of the channel-forming domain of colicin E1”. In: *Structure* 5.3 (1997), pp. 443–458.
- [105] Salvador E Luria and Max Delbrück. “Mutations of bacteria from virus sensitivity to virus resistance”. In: *Genetics* 28.6 (1943), p. 491.